Alma Mater Studiorum · Università di Bologna

Scuola di Scienze
Dipartimento di Fisica e Astronomia
Corso di Laurea Magistrale in Fisica

Quantum Fisher Information for bilinear-biquadratic model

Relatore:
Prof.ssa Elisa Ercolessi

Presentata da:
Federico Dell'Anna

Anno Accademico 2018/2019

Abstract

In this thesis we show how the Quantum Fisher Information is effective to detect the multipartite structure of entanglement in the topological phases for a certain spin-1 system: the bilinear-biquadratic model. We provide the analytical form of QFI by using string operators. In particular we are interested in the shape of the density of QFI (f_Q) because it provides directly a measure of entanglement for the ground state of a system. Indeed, performing numerical calculations moving from the Haldane phase to the dimer one, we really find a different behavior of f_Q also in the phase transition point. Furthermore we confirm that valence-bound picture is the exact representation for the ground state of AKLT point where the entanglement is maximum while it can be considered a good approximation for the dimer phase.

Abstract

In questo lavoro di tesi mostriamo come la Quantum Fisher Information riesce a rilevare la struttura multipartita dell'entanglement nella fasi topologiche del modello bilineare-biquadratico. Determiniamo la forma analitica della QFI attraverso l'uso di operatori di stringa. In particolare siamo interessati all'andamento della densità della QFI (f_Q) poichè fornisce una diretta misura dell'entanglement per lo stato fondamentale di un sistema. Infatti, effettuando calcoli numerici, troviamo, passando dalla fase di Haldane a quella dimer, un diverso andamento di f_Q anche nel punto di transizione di fase. Inoltre confermiamo che la "valence-bond representation" è l'esatta rappresentazione per lo stato fondamentale del punto AKLT dove l'entanglement è massimo mentre può essere considerata una buona approssimazione per la fase dimer.

Contents

1 Beyond Landau's paradigm: the topological order **13**

1.1 Landau's paradigm 13

1.2 Topological order 17

1.2.1 Quantum Hall Effect 18

1.3 Local Unitary and Stochastic transformations 21

1.4 Symmetry Protected Topological order 24

1.5 Adiabatic equivalence and topological invariants 25

1.5.1 The Bloch theorem and Berry phase 26

1.5.2 Su-Schrieffer-Heeger model 29

2 MPS representation and bilinear-biquadratic model **33**

2.1 MPS representation 33

2.1.1 Product state 36

2.1.2 Greenberger–Horne–Zeilinger state 36

2.1.3 W state 37

2.1.4 Majumdar–Ghosh model 38

2.2 Bilinear-biquadratic model 39

2.3 On-site unitary transformation and Projective Representation 41

2.4 MPS representation of AKTL and dimer states 45

2.4.1 AKTL state 45

2.4.2 Dimer state 48

2.5 Characterization of the phases by their projective representation 50

2.6 New non-local order parameters 53

3 Entanglement and the Quantum Fisher Information **57**

3.1 Information and correlation in classical probability theory 58

3.1.1 Correlation fuctions 60

3.1.2 Mutual Information 61

3.2 Quantum Entanglement 64

3.2.1 Bipartite quantum system and Shmidt decomposition 66
3.2.2 Tripartite quantum system 68
3.3 Fisher Information 70
3.3.1 Classical Fisher Information 70
3.3.2 Quantum Fisher Information 71
3.3.3 An Upper Bound for Quantum Fisher Information 72
3.3.4 Uncertainty Relations from Quantum Fisher Information 73
3.4 Entanglement criterion derived from F_Q 74
3.4.1 Theorem 3: F_Q^{k+1} criterion. 75

4 Evaluation of the QFI by NLOP **79**
4.1 Multipartite entanglement in topological quantum phases 79
4.2 String order parameters 81
4.3 Quantum Fisher Information for string operators 83
4.4 Numerical evaluation of QFI by using string order operator 85
4.4.1 Haldane phase 86
4.4.2 Phase transition $\beta = 1$ 89
4.4.3 Dimer phase 89

A Proofs of Theorems 1 and 2. **95**
A.0.1 Theorem 1 95
A.0.2 Theorem 2 97

B ITensor library and numerical code **99**
B.0.1 Numerical code 100

Introduction

In this thesis we will show how it is possible to use Quantum Fisher Information in order to detect multipartite structure of entanglament in the bilinear-biquadratic model.
After decades of development, quantum information science and technology have now come to their golden age. Quantum information processing offers the secure and high rate information transmission, fast computational solution of certain important problems, which are at the heart of the modern information technology. It also provides new angles, tools and methods which help in understanding other fields of science, among which one important area is the link to modern topological matter physics.
Topological matter is an ever-growing field of condensed matter physics which, from a theoretical point of view, offers a variety of intersections of different branches of theoretical physics. The novelty of this field is the discovery of phase transitions without any kind of spontaneous symmetry breaking, especially in low-dimensional systems. In fact, for a long time, people believed that all phases of matter were described by Landau's symmetry-breaking theory, and the transitions between those phases were described by the change of symmetry-breaking orders. However, after the discovery of fractional quantum Hall effect, it was realized in 1989 that the fractional quantum Hall states contain a new type of order (named topological order) which is beyond Landau symmetry breaking theory. Therefore, it was made necessary to investigate which were the key properties that truly distinguish one state from another. An important hint came from topology, a branch of mathematics concerned with the classification of geometrical objects, like manifolds and surfaces. Roughly, two states are in the same topological phase if one can be slowly deformed into the other, by changing its parameters, without going through any phase transitions. What quantum information science brings is the theoretic understanding of correlation, and a new concept called 'entanglement', which is a pure quantum correlation that has no classical counterpart. Such input from quantum information science led to a recent realization that the new topological order in some strongly correlated systems is strictly related to the pattern of many-body entanglement. The study of topological order and the related new quantum phases is actually a study of patterns of entanglement and its multipartite structure. The non-trivial patterns of en-

tanglement is the root of many highly novel phenomena in topologically ordered phases (such as fractional quantum Hall states and spin liquid states), which include fractional charge, fractional statistics, protected gapless boundary excitations, emergence of gauge theory and Fermi statistics from purely bosonic systems ect. The literature, during the years, has mostly focused on bipartite entanglement but recently, several studies have been done on certain spins systems (such as Ising [37], XY [38] models) by using the Quantum Fisher Information calculated by using local order parameters in order to show multipartite entanglement (ME). However, it has been emphasized that this approach, based on local operators, fails to detect ME at topological QPTs [37]. For this task, methods based on the QFI generally require the extension of entanglement criteria for non-local operators. Indeed, recently, Pezzè et al [25] really used nonlocal operators to calculate the QFI for a paradigmatic model showing topological phases: the Kitaev chain of spinless fermions in a lattice with variable-range pairing.
The QFI is a quantum generalization of the classical Fisher information which allows us to understand the 'degree' of entanglement in which the ground state of a system is. In particular, by its properties, it is possible to show that QFI has to satisfy an upper limit condition [32]. The violation of this limit represents a criterion to detect k-partite entangled states.
This work focuses on a particular $SU(2)$-symmetric class of spin-1 models, that is the bilinear-biquadratic model which is of particular interest given that it provides for two massive phases, i.e. the topological Haldane phase and the trivial dimer phase. These topological phases, like the Haldane phase, are massive and have short-range order, that is exponentially decaying correlation functions and consequently the conventional order parameters which were widely used to detect and distinguish different symmetry-breaking orders are insensitive to this new kind of topological order. Nevertheless it was noticed that the Haldane phase have a hidden string order detected by a different type of order parameters, i.e. non-local order parameters, given by the expectation value of some non-local operator. These non-local order parameters can distinguish the various topological phases or signal the presence of trivial topological order.
The present thesis is structured as follows:

- In Chapter 1 we give an introduction to some basic notion used in topological matter. We start from the failure of Landau's paradigm and move onto quantum Hall effect which can be seen as a first example to describe topological order. Then, we will give a classification of topological phases. At the end of the chapter we will present topological invariants that can be used to distinguish topological phases (in particular we will discuss the SSH model as example). Other ways to distinguish

them, such as by using non-local order parameters, will be treated in the next chapters.

- In Chapter 2 we introduce Matrix Product State representation for the bilinear-biquadratic model. Indeed, we will use here the matrix product state representation of the AKLT state, as representative of the Haldane phase, and of the dimer state, as representative of the dimer phase, in order to analytically evaluate new non-local order parameters which can characterize and detect the two massive phases of the bilinear-biquadratic model.

- In Chapter 3 we discuss correlation and entanglement in many-body systems. We start from introducing the concepts of independence and correlation in probability theory, which leads to understanding of the concepts of entropy and mutual information, which are of vital importance in modern information theory. Following up all that, we move into looking at the theory of Ficher Information, from both classical and quantum point of view. In particular, in order to understand the role that the Quantum Ficher Information plays in quantum scenario, we will provide a criterion that allows us to detect k-partite entanglement.

- In Chapter 4 we provide the analytical form of QFI by using string operators. In particular we are interested to the shape of the density of QFI (f_Q) because it provides directly a measure of entanglement for the ground state of a system. Then, performing numerical calculations, moving from the Haldane phase to the dimer one, we find a different behavior of f_Q also in the phase transition point. Furthermore we confirm that valence-bound picture is the exact representation for the ground state of AKLT point where the entanglement is maximum while it can be regarded a good approximation for the dimer phase.

Chapter 1

Beyond Landau's paradigm: the topological order

1.1 Landau's paradigm

Even though all matter is made by relatively few types of particles, it can have many different properties and macroscopical behaviors. These rich properties of materials come from the rich ways in which the particles are organized. For example, the liquid phase is characterized by a random distribution of the particles that can be placed at an arbitrary distance from each other, so we say that there is a continuous translation symmetry. In a crystal, by contrast, the particles show a precise structure: they organize in a lattice with a clear geometry and fixed distances, so we say that there is only discrete translation symmetry. When a system passes from the liquid phase to the crystal one (thus when a phase transition happens), its symmetry is changing, in particular it reduces the continuous translation symmetry into a discrete one. Liquid and crystal are just two examples. It can be shown that different orders (i.e. ways of organization of the particles) correspond to different symmetries so when the material undergoes a phase transition, a symmetry is broken. This way for understanding the phenomena of phase transitions is known as Landau's paradigm or Landau's symmetry-breaking theory. Landau's paradigm is a very successful theory and for a long time physicists believed that all the possible state of matter (and consequently all possible phase transitions) could be described by it. The traditional way to see how the Landau's symmetry-breaking works is to consider a simple example: the classic Ising model.
The classic Ising model has the following Hamiltonian:

$$H = -J \sum_{<ij>} \sigma_i \sigma_j - B \sum_i \sigma_i \tag{1.1}$$

where: the spin σ_i are bulean variables so that they can assume the values of ± 1; the sum is over the near neighbours; B is a magnetic field oriented in one of the two opposite directions of the spins. This model well describes the paramagnetic-ferromagnetic transition. Let us switch off the magnetic field. We know that for a canonical ensemble the system evolves in a way that minimizes its free energy:

$$F = E - TS \tag{1.2}$$

Intuitively there are two competitors that want to establish their own type of order: the principle of minimal energy, that wins at low temperature, tends to orient all spins in a direction (ferromagntic phase) and the principle of maximum entropy, that wins at high temperature, tends to direct the spins accidentally (paramagnetic phase).
Then we can characterize these two states by introducing an order parameter (i.e. average magnetizzation) that is zero in the paramagnetic phase and different from zero in the ferromagnetic one.
Now let us deal with the quantum case. Before introducing a specific model, it is important to clarify some peculiar concepts related to the quantum systems (with large size L, in particular $L \to \infty$ in the thermodynamic limit): dimensionality, locality, correlation and gap.
Quantum systems usually live in a space of fixed dimension. For example: a sodium crystal is composed by ions froming a three-dimensional lattice, graphene sheet is made of carbon atoms in two dimensions, nanowires are effectively one-dimension and so on...
Systems in the same dimension can have different geometry or topology: in one dimension the sysyem can be in a closed ring with no boundary or in an open chain with two end points; in two dimensions the system can be in a disc with a one-dimensional boundary or in a sphere or torus with no boundary but with different topology. Another important property of the systems, that usually is examined, is the locality: particles can interact with each other only with a finite number of them and only if they are within certain distance (finite range). Then the total Hamiltonian of the system is a sum of such local interaction terms:

$$H = \sum_i H_i \tag{1.3}$$

In the thermodynamic limit, an important property of H is related to the gap. The system is called gapped if, as $L \to \infty$, the ground state degeneracy is upper-bounded by a finite integer number and the gap Δ between the ground states and the first excited state of H is lower-bounded by a finite positive number.

In a quantum many-body system, the correlation is usually defined between local

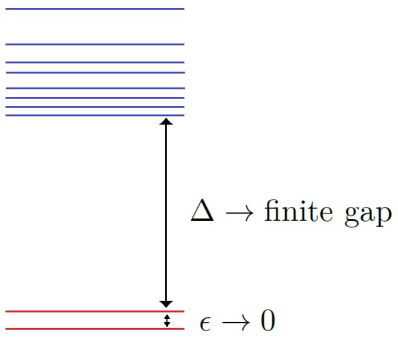

Figure 1.1: The energy spectrum for a gapped quantum system: the gap Δ which separates the ground states (in red) to the others (in blue) remains finite in the thermodynamic limit. Conversely the energy splitting ϵ goes to zero in same limit.

operators as:

$$C^{O_1O_2}(r) = \langle O_1O_2\rangle - \langle O_1\rangle\langle O_2\rangle \tag{1.4}$$

The behavior of the correlation function when $r \to \infty$ is an important indicator of the physical properties of the system. In particular:

1. for a gapped system with a unique ground state, all correlation functions decay exponentially with r, that is:

$$C(r) \sim e^{-\frac{r}{\xi}} \tag{1.5}$$

   where ξ is the correlation length of the system. Therefore, a gapped quantum system with non-degenerate ground state has a finite ξ.

2. for a gapless system, the correlation function dacays polynomially with r:

$$C(r) \sim \frac{1}{r^\beta} \qquad with \qquad \beta > 0 \tag{1.6}$$

   Such systems are said to have infinite correlation lengths ξ.

Let us consider the quantum case. It's important to stress that the classical phase transition emerge by varying the temperature instead quantum phase transitions emerge by varying the Hamiltonian's parameters. Indeed quantum phases of the matter are phases of the matter at zero temperature, so they correspond to the ground states of the quantum Hamiltonians.
Let us consider now the transverse-field Ising model on a 1-dimensional chain which has the following Hamiltonian:

$$H = -J\sum_{i=1}^{L} Z_iZ_{i+1} - B\sum_{i=1}^{L} X_i \tag{1.7}$$

where X_i, Y_i, Z_i are the Pauli's matrices on the i-th site

$$X = \begin{pmatrix} 0 & 1 \\ 1 & 0 \end{pmatrix} \qquad Y = \begin{pmatrix} 0 & -i \\ i & 0 \end{pmatrix} \qquad Z = \begin{pmatrix} 1 & 0 \\ 0 & -1 \end{pmatrix} \tag{1.8}$$

It is a gapped system as long as $J \neq B$. If $|J| < |B|$, the ground state is nondegenerate, in particular when $B = 0$ there is a set of basis states that span it:

$$|0\rangle^{\otimes L} = |00\cdots0\rangle \qquad and \qquad |1\rangle^{\otimes L} = |11\cdots1\rangle \tag{1.9}$$

where $|0\rangle$ and $|1\rangle$ are a basis of eigenvalues of Z, so this unique ground state has a finite correlation length. When $J = 0$ the ground state becomes:

$$|+\rangle^{\otimes L} = \left(\frac{1}{\sqrt{2}}|0\rangle + \frac{1}{\sqrt{2}}|1\rangle\right)^{\otimes L} \tag{1.10}$$

and it has correlation length $\xi = 0$. Finally, when $|J| > |B|$ the ground state is twofold degenerate.

Now let us set $J = 1$. We can also write the ground state of the system by using a variational parameter. Let us choose our trial wave function as:

$$|\Psi\rangle = \otimes_i[\cos(\Phi/2)\,|0\rangle_i + \sin(\Phi/2)\,|1\rangle_i] \tag{1.11}$$

Then average energy per site is given by:

$$\begin{aligned} \epsilon(\Phi) &= \frac{\langle\Psi_\Phi|\,H\,|\Psi_\Phi\rangle}{N} = \\ &= -[cos(\Phi/2)^2 - sin(\Phi/2)^2]^2 - 2Bcos(\Phi/2)sin(\Phi/2) \end{aligned} \tag{1.12}$$

In the Fig 1.2 we can see how the shape of $\epsilon(\Phi)$ varies for different values of B and we note a symmetry-breaking transition at about B=1. For $B > 1$ the energy has a minimum in $\Phi = \pi/2$, where the ground state does not break the spin-flip symmetry $\Phi \to \Phi - \pi$. For $B < 1$ the energy has two minimum points placed at $\Phi = \pi/2 \pm \Delta\Phi$ that correspond to two degenerate ground states:($|\Psi_{\pi-\Delta\Phi}\rangle$ and $\langle\Psi_{\pi+\Delta\Phi}|$, each of them does break the spin-flip symmetry.

The presence of such a near two-fold degeneracy is a very important feature. In fact, we know that symmetry group $\mathbb{Z}_2$ has only a single irreducible rappresentation then it cannot give rise to two-fold degeneracy. On the other hand, if we explicitly break the symmetry by adding $B_z \sum_i Z_i$ to the Hamiltonian, the degeneracy will vanish. We conclude that the symmetry protects the degeneracy of the ground states even if they don't belong to its representation. In this sense we can say that a quantum system with a finite symmetry group is in a symmetry-breaking phase if and only if it has "robust" nearly

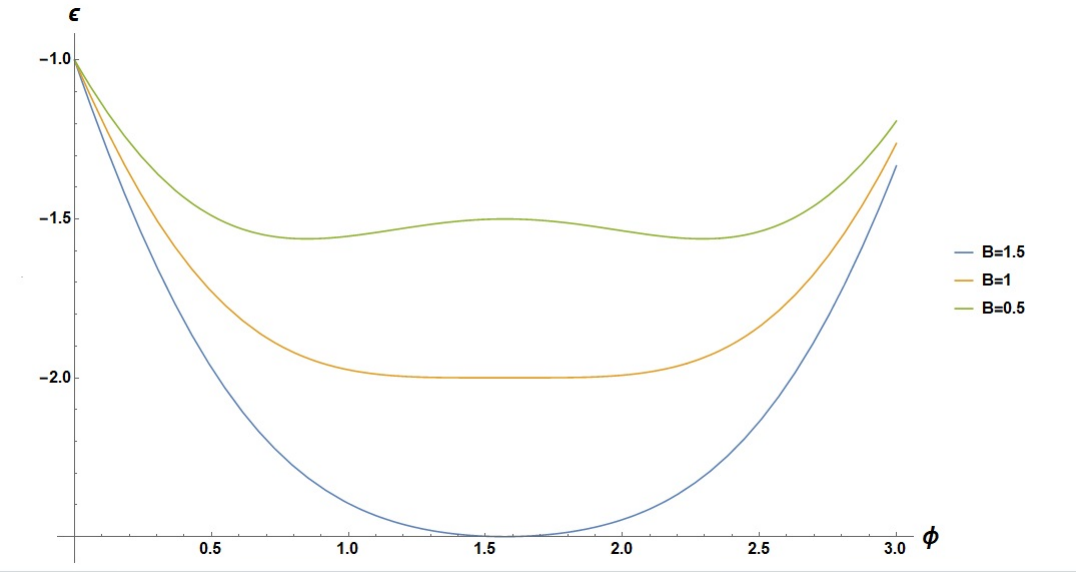

Figure 1.2: Shapes of ϵ for different values of B

degenerate ground states that belong at least two different irreducible representations of the symmetry group where "robust" means that the degeneracy remains after any perturbations that preserve the symmetry.
Actually, the true ground state, in quantum theory, is:

$$|\Psi_+\rangle = \frac{|\Psi_{\pi-\Delta\Phi}\rangle + \langle\Psi_{\pi+\Delta\Phi}|}{2} \tag{1.13}$$

that doesn't break any symmetry and shows a GHZ-type of quantum entanglement that will be better explained in the next chapters.
From Landau's symmetry-breaking theory, it emerges that we can use group theory to classify symmetry-breaking phases: all we need is a pair of mathematical objects (G_H, G_Φ), where G_H is the symmetry group of the Hamiltonian and G_Φ is the symmetry group of the ground state. In our case, for example, the transverse-field Ising model is labeled by $(\mathbb{Z}_2, 1)$.

1.2 Topological order

Starting from the 1980s of the last century, evidence began to emerge in support of the fact that Landau's symmetry-breaknig theory cannot describe all possible phases of matter. In fact, the chiral spin state was introduced to explain hight-temperature superconductivity [2, 3] and it was quickly realized that there are many different chiral spin states having the same symmetry [4]: the pair (G_H, G_Φ) alone was not enough to distinguish different chiral spin states. This means that a new kind of order must

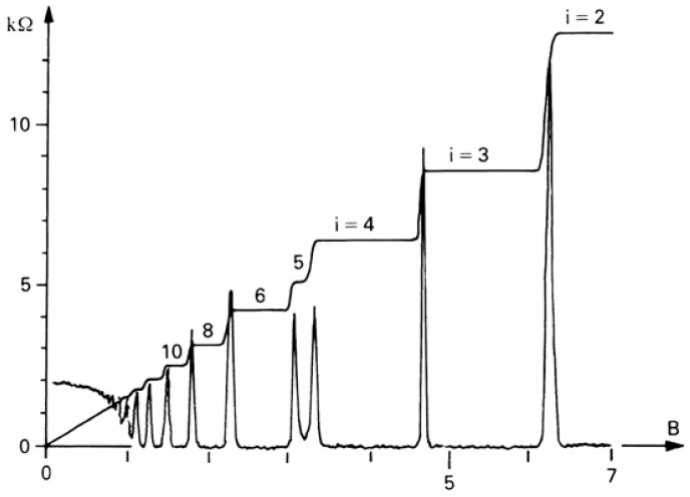

Figure 1.3: Integer quantum Hall effect (figure taken from [10])

exist that is beyond the usual Landau's paradigm. It was named "topological order" [5]. Historically, an important role was played by the discovery of integer and fractional quantum Hall effect.

1.2.1 Quantum Hall Effect

In 1980 von Klitzing, using samples prepared by Dorda and Pepper [1], performed experiments exploring the quantum regime of Hall Effect. Both the Hall resistivity ρ_{xy} and the longitudinal resistivity ρ_{xx} exhibit interesting behaviour. As we can see in the figure 1.3, the Hall resistivity exhibits a plateau trend in different ranges of magnetic field at different heights. On these plateaus, the resistivity takes the value:

$$\rho_{xy} = \frac{2\pi\hbar}{e^2}\frac{1}{\nu} \tag{1.14}$$

whereas the centre of each of these plateaus occurs when the magnetic field takes the value:

$$B = \frac{2\pi\hbar}{e}\frac{n}{\nu} = \frac{n}{\nu}\Phi \tag{1.15}$$

where n is the electron density, Φ is known as the quantum flux and the value of ν is measured to be an integer to an extraordinary accuracy.
Also ρ_{xx} shows unexpected behaviour: it vanishes when ρ_{xy} is on the plateau and spikes when ρ_{xx} jumps to the next plateau. Usually, when a system has $\rho_{xx} = 0$ it is regarded as a perfect conductor. The exact form of conductivities is [10]:

$$\sigma_{xx} = \frac{\rho_{xx}}{\rho_{xx}^2 + \rho_{xy}^2} \qquad and \qquad \sigma_{xy} = -\frac{\rho_{xy}}{\rho_{xx}^2 + \rho_{xy}^2} \tag{1.16}$$

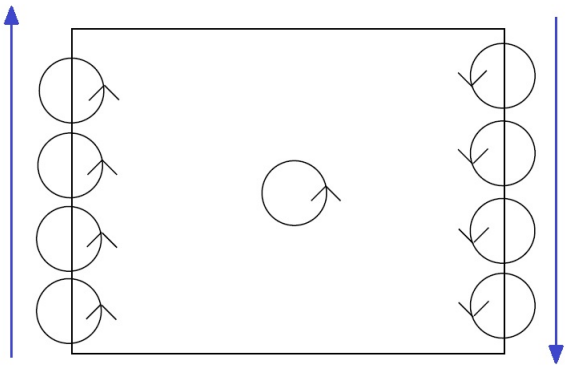

Figure 1.4: The skipping motion along the borders of the system gives rise to chiral particles which can move only in one direction

If $\rho_{xy} = 0$ then $\sigma_{xx} = \frac{1}{\rho_{xx}}$, however if $\rho_{xy} \neq 0$ we have:

$$\rho_{xx} = 0 \qquad \Rightarrow \qquad \sigma_{xx} = 0 \tag{1.17}$$

so the system has to be regarded as a perfect conductor. How could this be possible? In this situation the current is flowing perpendicular to the applied electric field so $\mathbf{E}\cdot\mathbf{J} = 0$. Recalling the $\mathbf{E}\cdot\mathbf{J}$ is the work done in accelerating charges, the fact that this vanishes means that we have a steady current flowing without doing any work and, correspondingly, without any dissipation. On the other hand $\sigma_{xx} = 0$ is telling us that no is current flowing in the longitudinal direction just like an insulator.

Another interesting aspect of the QHE is the edge modes, that can be understood classically too. Consider particles on a xy plane which, subjected to a magnetic field, are moving in circles. For a fixed direction of the magnetic field, all the particles turn in a specific direction, for example anti-clockwise. Near the edge of the sample, the orbits must collide with the boundary. As all motion is anti-clockwise, the only option for these particles is to bounce back. The result is a skipping motion in which the particles move along the one-dimensional boundary (see the Fig.1.4). Particles move in one direction on left side of the sample, and in the opposite direction on the other side of the sample. This ensures that the net current, in the absence of an electric field, vanishes.

We can also see how the edge modes emerge in the quantum theory. The edge of the sample is modelled by a potential (function only of x) which rises steeply so as to confine the particles in the x-direction. The Hamiltonian will be:

$$H = \frac{1}{2m}\left(p_x^2 + (p_y + eBx)^2\right) + V(x) \tag{1.18}$$

Without the potential, we know [10]that the wavefunctions are Gaussian of width $l_B = \sqrt{\frac{\hbar}{eB}}$. Furthermore, we assume that the potential is smooth over distance scales l_B, then,

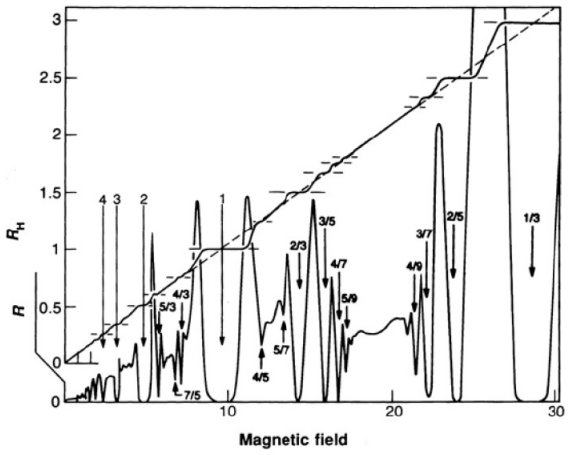

Figure 1.5: The fractional quantum Hall effect (figure taken from [10])

for each state, we can expand the potential around its location x:

$$V(x) \approx V(x_0) + V'(x - x_0) \qquad with \qquad V' = \frac{dV}{dx} \tag{1.19}$$

where we have neglected the quadratic term. The result is a drift velocity in the y-direction now given by:

$$v_y = -\frac{1}{eB}\frac{dV}{dx} \tag{1.20}$$

Each wavefunction, labelled by momentum k, sits at a different x position, $x = -kl_B$ and has a different drift velocity. In particular, the modes at each edge travel in opposite directions: $v_y > 0$ on the left and $v_y < 0$ on the right. This agrees with the classical result of skipping orbits.

Fractional Quantum Hall states (FQH) were discovered in 1982 before the introduction of the concept of topological order. They are gapped ground states of 2D electrons in a strong magnetic field, characterized by an electric field (in the transverse direction) induced by a current density:

$$E_y = R_H J_x \qquad with \qquad R_H = \frac{p}{q}\frac{h}{e^2}, \qquad p, q \in \mathbb{N} \tag{1.21}$$

Different quantized R_H (that is various values of p and q correspond to different FQH states. The integer quantum Hall effect can be understood using free electrons. In contrast, to explain the fractional quantum Hall, we need to take interactions between electrons into account. This makes the problem much harder (see Fig 1.5) than integer quantum Hall. For these results, the 1998 Nobel prize was awarded to Tsui, Störmer and Laughlin.

Just like chiral states, they cannot be described by Landau's theory but must contain a new kind of order. FQH states were not the first experimentally discovered

topologically ordered states. The first were superconductors, ironically the Landau's symmetry-breaking theory was developed to describe them despite the fact they are not symmetry-breaking states but topologically ordered ones.
Just as zero viscosity and magnetization define, respectively, the concept of superfluid and ferromagnetic orders, we need to use some new probes to define the concept of topological order: in the late '80s, it was conjectured that it can be completely characterized by using only two topological proprieties:

1. Topoligical ground state degeneracies on closed spaces of various topologies.
2. Non abelian geometric phases of those degenerate ground states from deforming spaces [5].

The first point is a phenomenon of quantum many-body systems in the large size limit. It has the following features:

a) The topological degeneracy is not exact: the low energy ground states have a small energy splitting. It becomes exact when the system size becomes infinity.

b) The topological degeneracy is robust against any local perturbation.

c) The topological degeneracy for a given system is different for different topological spaces.

We usually could attribute degeneracy to symmetry; however, for the point b) topological degeneracy is robust against any local perturbation that can break all the symmetries, so it is not due to symmetry: its presence is a surprising phenomenon and implies the existence of a new kind of quantum phase.

1.3 Local Unitary and Stochastic transformations

After the discovery of topological order, it took us more than 20 years to really understand its microscopic nature: it is due to long-range entanglement, and different patterns of long-range entanglement give rise to different topological orders.
Let us start to consider the classical view of phase transitions in which for a given system we can calculate some macroscopic quantities such as density, magnetization, viscosity. Changing smoothly the parameters of our system (temperature, magnetic field..) these quantities change smoothly if the system remains in the same phase. However, if we

reach a critical value of the parameters, something dramatic could happen and some physical observables diverge. We call it phase transition point, therefore, two systems are in the same phase if, and only if, they can evolve into each other smoothly without inducing singularity in any local physical observable. In this sense, liquid water and water vapor belong to the same phase because there exists a way in the diagram phase to connect them without cross critical points as shown in figure 1.6.

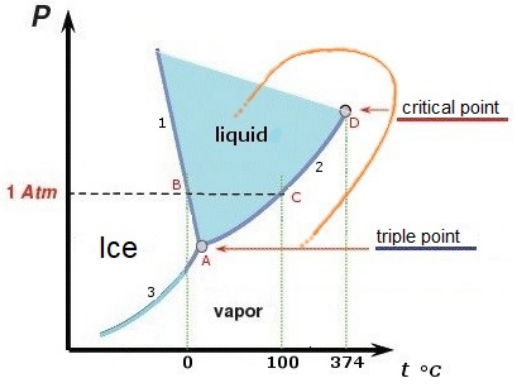

Figure 1.6: Phase diagram of water. It shows that there is a path (like the orange line) that connects two phases without crossing any critical points.

A similar definition holds for quantum systems as well. For gapped quantum systems, quantum phase transition is closely related to gap closing. In fact, let's consider a Hamiltonian $H(g)$ depending on a parameter g. At a determined value of g (i.e $g = 0$), correspond to the ground state $|\Psi(0)\rangle$ and a finite gap $\Delta(0)$ above it. If we smoothly change the value of g (i.e for 0 to 1) we obtain another ground state $|\Psi(1)\rangle$. We can also calculate the expectation value of an observable $< O >= \langle\Psi(g)| O |\Psi(g)\rangle$ that will change accordingly with the variation of the parameter g. As long as the gap $\Delta(g)$ remains finite along all the path, there will be no phase transition and the observable O will be well-define on every point of the path. Only when the gap closes there can be singularity in $\langle O\rangle$. Then it is possible to formulate this general rule: at zero temperature, two gapped systems $H(0)$ and $H(1)$ are within the same phase if, and only if, there exists a smooth path of the parameter g connecting the two and with finite gap for all g.
Now the point is how can we classify the quantum gapped systems so that systems within a set can be smoothly connected into each other and systems in different sets are not. A possible way to do a first classification is provided by symmetry-breaking mechanism: starting from Hamiltonians with the same symmetry, the ground state of them can have different symmetries, hence resulting in different phases. However, we have just realized that it is not enough, because a quantum system can be in different phases without breaking any symmetry.

Let us introduce an important notion that will allow us to make a more refined classification (based on the work of Chen et al. [6]): the Local Unitary Transformation (LU). We define a LU evolution as an unitary operation generated by time evolution of a local Hamiltonian for a finite time:

$$|\Phi(1)\rangle \sim |\Phi(0)\rangle \qquad \Longleftrightarrow \qquad |\Phi(1)\rangle = T[e^{-i\int_0^1 dg\tilde{H}(g)}]\,|\Phi(0)\rangle \tag{1.22}$$

where T is the path ordering operator and

$$\tilde{H}(g) = \sum_i O_i(g) \tag{1.23}$$

is a sum of local Hermitian operators. In general $H(g)$ and $\tilde{H}(g)$ are different quantities, the exact form of the former can be found from the latter.

In order to show the importance of local unitary transformation let us consider again the 1D transverse Ising model with the Hamiltonian given by (1.7). The gapped ground states are non-degenerate for $B > 1$ while they are two-fold degenerate for $0 < B < 1$. We said that the degeneracy is unstable against perturbation that breaks the ($\mathbb{Z}_2$ symmetry. The states of the system for $B > 0$ and $0 < B < 1$ are two distinct gapped phases (respectively trivial and non-trivial ones); this is due to a very simple reason: gapped quantum states with different ground state degeneracy (degeneracy is LU invariant) always belong to different gapped phases.

Topologically ordered phases and symmetry-breaking phases belong to the same equivalence classes induced by LU transformations. In order to distingush them, we introduce the another kind of trasformation: the stochastic local (SL) trasformation that are local invertible but not necessary unitary. Firstly, we need to define a layer of SL transformation in the following way:

$$W = \prod_i W_i \tag{1.24}$$

where W^i is a set of invertible operators that act on non-overlapping regions with size less than a finite number l (which is called range of the layer). A stochastic local transformation is then given by:

$$W^L = W^{(1)}W^{(2)}\cdots W^{(L)} \tag{1.25}$$

By using SL trasformations it possible to give a definition for short-range and long range entanglement: a state is short-range entangled (SRE) if it is convertible to a product state by a SL transformation. Otherwise it is long-range entangled (LRE).

There are states that can be transformed to product states by SL transformations but not by LU ones. The following state is an example of that:

$$|GHZ(a)\rangle = a\,|0\rangle^{\otimes L} + b\,|1\rangle^{\otimes L} \qquad with \qquad |a|^2 + |b|^2 = 1 \tag{1.26}$$

If one allows SL transformations then all $|GHZ(a)\rangle$ can be written in the form $|0\rangle^{\otimes L}$. To see this, one just applies this SL transformation:

$$W_L = \prod_{i=1}^{L} O_i \qquad where \qquad O_i = \begin{pmatrix} 1 & 0 \\ 0 & \gamma \end{pmatrix} \qquad 0 < \gamma < 1 \tag{1.27}$$

Then:

$$W_L \, |GHZ(a)\rangle = a \, |0\rangle^{\otimes L} + b\gamma^L \, |1\rangle^{\otimes L} \tag{1.28}$$

as long as L is large enough it can be arbitrarily close to the product states $|0\rangle^{\otimes L}$.
Finally we are ready to define topologically ordered states: a ground state of a gapped Hamiltonian has a nontrivial topological order if it is not convertible to a product state by any SL transformation.

1.4 Symmetry Protected Topological order

We have just seen that LU transformations induce a classification of Hamiltonians (or, equivalently, of their ground states) without requiring any symmetry constraints. Let us see what happens if we take into account the symmetries of the system. In order to implement that, one has to define a Symmetric Local Unitary (SLU) transformations. Each equivalence class of the Symmetric Local Unitary transformations is smaller and there are more kinds of classes compared to those of LU transformations. In particular, states with short-range entanglement can belong to different equivalence classes even if they do not spontaneously break any symmetry of the system. Those states have Symmetry Protected Topological Order. Haldane phase in spin-1 chains and the spin-0 chains are examples of states with the same symmetry (spin rotation) which belong to two different classes of SLU. Systems with symmetry protected topological (SPT) order cannnot have ground state degeneracy, but they are characterized by gapless edge excitations which are protected by the symmetry. The Fig. 1.7 summarizes what we have just said so far and shows a general structure of the quantum phase diagram of gapped systems at zero temperature. For systems without any symmetry all states are in the same phase (SRE) , while long-range entangled states can belong to different phases (LRE1, LRE2) due, as we said, to the different patterns in which all the particles can organize.
For a system with symmetries in which the structure is richer, there are more possibilities:

1. States with SRE belong to different phases if:

   (a) they break symmtry in different ways (SB-SRE1, SB-SRE2). They are Landau's symmetry-breaking states.

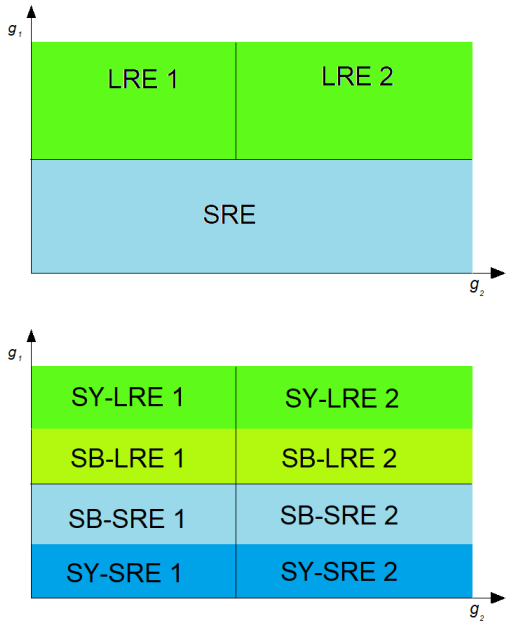

Figure 1.7: The first picture shows the possible phases of Hamiltonian $H(g_1, g_2)$ without any symmetry. The second picture shows how the phase diagram becomes richer if some symmetries are taken into account. The different shades of green (LRE) and blue (SRE) represent symmetric and symmetry-breaking phases.

(b) they belong to different symmetry protected topological phases (SY-SRE1, SY-SRE2 without breaking any symmetry)

2. State with LRE belong to different phases if:

(a) they break symmetry (SB-LRE1, SB-LRE2, so symmetry breaking and long range entangled can appear together in a state)

(b) they belong to different STP phases (SY-LRE1, SY-LRE2). In this case they are called Symmetry Enriched Topological Phases.

1.5 Adiabatic equivalence and topological invariants

In this section we are going to see, in a more formal way, how it is possible to define topologial invariants i.e. objects that have the same value as long as we remain in the same phase. They, in fact, represent a way to distinguish different topological phases. Actually there are other ways to detect topological phases such as by using Non-local Order Parameters (NLOPs) or by using the concept of entanglement. These cases will be analyzed and discussed in the netxs chapters.

As we have seen an Hamiltonian is gapped if the bulk spectrum has an energy gap between the ground state and all the other excited states. This type Hamiltonian is said to be adiabatic deformed if:

- its parameters are slowly and continuously varied
- the symmetries are respected
- the bulk gap remains open

A topological invariant of a gapped Hamiltonian is a quantity that cannot be modified by an adiabatic deformation. We realize that if two equivalent Hamiltonians share the same topological invariants then they belong to the same topological class.
Some examples of the topological invariants are the Chern number and the winding number: they are topological invariants associated to the parameter space of the model. Another important example of topological invariant is the number of edge modes, which are particular states that are manifested only in topologically non-trivial phases. Even though these examples of topological invariants are very different in character, they are related by what is called the bulk-edge correspondence. Suppose we have an interface between two topologically phases, so with different Chern numbers, then the boundary supports a certain number of edge modes. By the bulk-edge correspondence:

$$N_L - N_R = \Delta n \tag{1.29}$$

where $N_L - N_R$ is the difference between the left-moving and right-moving edge modes [43]. So we have a bridge that connects the the bulk to the excitations on the boundary that is a very important aspect for the study of topological matter.

1.5.1 The Bloch theorem and Berry phase

Let us consider a Hamiltonian in a periodic potenzial, such that $H(r) = H(\boldsymbol{r}+\boldsymbol{R})$ where $\boldsymbol{R}$ is the period of the lattice. The Bloch theorem states that the eigenfunction of such a system are in the form:

$$\Psi_{n,\boldsymbol{k}}(\boldsymbol{r}) = e^{i\boldsymbol{k}\cdot\boldsymbol{r}} u_{n,\boldsymbol{k}}(\boldsymbol{r}) \tag{1.30}$$

where $u_{n,\boldsymbol{k}}(\boldsymbol{r})$ is periodic with period $\boldsymbol{R}$. If we introduce the Bloch Hamiltonian

$$H(\boldsymbol{k}) == e^{-i\boldsymbol{k}\cdot\boldsymbol{r}} h(\boldsymbol{r}) e^{i\boldsymbol{k}\cdot\boldsymbol{r}} \tag{1.31}$$

this wave function is an eigenstate of the Bloch Hamiltonian, then it satisfies:

$$H(\boldsymbol{k}) \left|u_{n,\boldsymbol{k}}(\boldsymbol{r})\right\rangle = E_{n,\boldsymbol{k}} \left|u_{n,\boldsymbol{k}}(\boldsymbol{r})\right\rangle \tag{1.32}$$

where $E_{n,\boldsymbol{k}}$ are the eigenvalue of the Bloch Hamiltonian which depend on two quantum numbers, the band index n and the crystal momentum $\boldsymbol{k}$. The last one can only take values in the first Brillouin Zone (BZ), namely the first cell of the reciprocal lattice with periodic boundary conditions, while the first one labels the different solutions of the Bloch Hamiltonian for a fixed value of $\boldsymbol{k}$. Furthermore, n is called band index because the energies vary continuously with $\boldsymbol{k}$, providing an energy band. These energy band are usually separated by an energy gap.
Let us consider Bloch basis $|u_{n,\boldsymbol{k}}\rangle$. Since it is unique up to a phase factor, it means that we can change the phase by using a phase factor $h(\boldsymbol{k})$:

$$|u_{n,\boldsymbol{k}}\rangle \longrightarrow e^{ih(\boldsymbol{k})}\,|u_{n,\boldsymbol{k}}\rangle \tag{1.33}$$

Obviously it is easy to see that this is a manifestation of an $U(1)$ gauge symmetry that characterize the Hilbert space of the system. Let us consider a gapped Hamiltonian $H(\boldsymbol{R})$ where $\boldsymbol{R}$ belongs to the parameter space P. If this Hamiltonian is a Bloch Hamiltonian then the parameters are taken to be the BZ momenta $\boldsymbol{k}$. Let's suppose that the parameters change slowly with time that is the rate of variation of $\boldsymbol{R}(t)$ has to be slow compared to the frequencies corresponding to the energy gap [44]. This implies that the system must have enough time to reach to the new configuration. Hence, the Hamiltonian $H(\boldsymbol{R}_t)$ varies along a path C in P, that we are going to assume to be closed. We can define an orthogonal basis for the instantaneous eigenstates $H(\boldsymbol{R}_t)$ of at time t [44]:

$$H(\boldsymbol{R}_t) = |u_n(\boldsymbol{R}_t)\rangle = E_n(\boldsymbol{R}_t)\,|u_n(\boldsymbol{R}_t)\rangle \tag{1.34}$$

Furthermore we require the presence of a gap between the initial state's energy and the rest of the spectrum because it guarantees that the system will remain in an eigenstate at the end of the cycle. This is the reason why we consider gapped Hamiltonians: it is the class of systems for which the notion of adiabatic evolution is significant.
The equation (1.34) does not describe the time evolution of the state. This is achieved by the time-dependent Schrödinger equation

$$i\hbar\partial_t\,|\Phi(t)\rangle = H(\boldsymbol{R}(t))\,|\Phi(t)\rangle \tag{1.35}$$

If $|\Phi(t=0)\rangle = |u_n(\boldsymbol{R}_{t=0})\rangle$ then the state will only get a phase during its time evolution, so we can take as an Ansatz [44, 7]

$$|\Phi(t)\rangle = e^{i\gamma_n(t)}e^{-\frac{i}{\hbar}\int_0^t dt' E_n(\boldsymbol{R}_t)}\,|u_n(\boldsymbol{R}_t)\rangle \tag{1.36}$$

where

$$e^{-\frac{i}{\hbar}\int_0^t dt' E_n(\boldsymbol{R}_t)} \tag{1.37}$$

can be removed by means a gauge transformation. The first phase $e^{i\gamma_n(t)}$ cannot be removed because it depends on the geometry of the parameter space P. γ_n is called the Berry phase and can be defined as a contour integral along the path C

$$\gamma_n = i \int_C d\boldsymbol{R} \langle u_n(\boldsymbol{R}_t)| \nabla_{\boldsymbol{R}} |u_n(\boldsymbol{R}_t)\rangle = \int_C d\boldsymbol{R} \cdot \boldsymbol{A_n}(\boldsymbol{R}) \tag{1.38}$$

where

$$\boldsymbol{A_n}(\boldsymbol{R}) = i \langle u_n(\boldsymbol{R}_t)| \nabla_{\boldsymbol{R}} |u_n(\boldsymbol{R}_t)\rangle \tag{1.39}$$

is the so-called Berry connection.
The index n refer to the n-th energy band, separated from the other energy bands by a gap. Following the example of the vector potential in electrodynamics, the connection $\boldsymbol{A_n}$ is not gauge invariant. In fact, applying a gauge transformation on the basis vectors, that is changing the phases with an arbitrary function $\chi(\boldsymbol{R})$ such that $|u_n(\boldsymbol{R})\rangle \to e^{i\chi(\boldsymbol{R})} |u_n(\boldsymbol{R})\rangle$. Thus the Berry connection transforms as

$$\boldsymbol{A_n}(\boldsymbol{R}) \longrightarrow \boldsymbol{A_n}(\boldsymbol{R}) - \nabla_{\boldsymbol{R}}\chi \tag{1.40}$$

which implies that the Berry phase varies as

$$\Delta\gamma_n = \chi(\boldsymbol{R(T)}) - chi(\boldsymbol{R(0)}) \tag{1.41}$$

Hence, if C is a closed path then γ_n is gauge invariant.
Furthermore it can be expressed as a surface integral, thank to the Stokes theorem, as:

$$\gamma_n = \oint_C d\boldsymbol{R} \cdot \boldsymbol{A_n}(\boldsymbol{R}) = \int_{\tilde{F}} d\boldsymbol{S} \cdot \boldsymbol{F}_n \tag{1.42}$$

where $\tilde{F}$ is a surface whose boundary is C and $\boldsymbol{F}_n$ is the Berry curvature defined as

$$\boldsymbol{F}_n = \nabla_{\boldsymbol{R}} \times \boldsymbol{A_n}(\boldsymbol{R}). \tag{1.43}$$

Let's consider now two-dimensional manifolds. An important result in this field of topology is the Gauss-Bonnet theorem, which is a link between local properties and global properties (topology)) of compact 2D Riemannian manifolds. It states that the integral over the whole manifold M of its Gaussian curvature $F(\boldsymbol{x})$ is equal to the Euler characteristic

$$\delta = \frac{1}{2\pi} \int_M d^2x F(\boldsymbol{x}) \tag{1.44}$$

which is just $\delta = 2(1-g)$ where g is the genus i.e. the number of holes of the surface M. For example $g = 0$ for a sphere but $g = 1$ for a torus (that has one hole). The Gaussian curvature is defined by means of parallel transport of vectors living on the tangent planes, which there is one for each point of M.

As we said the main point of the Gauss-Bonnet theorem is the possibility to link local properties, like curvature, to global properties, like the genus. It is possible to show that the same argument can be done for the Berry phase. It is defined on a manifold, the BZ (a d-dimensional torus) through a local function, the Berry curvature. It is defined in a similar way to the Gaussian curvature but in this case the different fibres are Hilbert spaces attached at every point of the BZ. In the case of a two-dimensional BZ, the Berry curvature is a scalar function and, by generalizing the Gauss-Bonnet theorem, its integral over all the BZ defines the Chern number:

$$n = \frac{1}{2\pi} \int_{BZ} d^2k F(\boldsymbol{k}) \tag{1.45}$$

1.5.2 Su-Schrieffer-Heeger model

TIn this section we will introduce the SSH (Su-Schrieffer-Heeger) model in order to give an example of topological properties. It is a one-dimensional electron model which is made up of elementary cells with two atomic sites (labeled with the letters A and B). We will suppose the electrons are spinless [44, 43]. The Hamiltonian of the model is:

$$H = \sum_{i=1}^{N} (t + \delta t) c^\dagger_{A,i} c_{B,i} + (t - \delta t) c^\dagger_{A,i+1} c_{B,i} + \text{h.c.} \tag{1.46}$$

where the index i runs over all the cells, t is the hopping amplitude, δt is the dimerization factor and $c^\dagger_{A,i}, c_{A,i}$ (and $c^\dagger_{B,i}, c_{B,i}$) are Fermi operators. Assuming periodic boundary condition and passing to momentum space with Fourier transform, it possible to express the Hamiltonian as:

$$H = \begin{pmatrix} \tilde{c}^\dagger_{A,k} & \tilde{c}^\dagger_{B,k} \end{pmatrix} H(k) \begin{pmatrix} \tilde{c}_{A,k} \\ \tilde{c}_{B,k} \end{pmatrix} \tag{1.47}$$

where the Bloch Hamiltonian $H(k)$ can be written as

$$H(k) = \boldsymbol{d}(k) \cdot \boldsymbol{\sigma} \quad \text{where} \quad \boldsymbol{d}(k) = \begin{pmatrix} (t + \delta t) + (t - \delta t) \cos k \\ (t - \delta t) \sin k \\ 0 \end{pmatrix} \tag{1.48}$$

where we have set the lattice spacing $a = 1$ and $\boldsymbol{\sigma}$ is the vector whose elements are the Pauli matrices.

The Bloch Hamiltonian looks like a two-band system with eigenvalues $\pm |\boldsymbol{d}(k)|$ which implies that $\boldsymbol{d}(k) = 0$ is the only point of degeneracy. The map $k \to \hat{\boldsymbol{d}}(k) = \boldsymbol{d}(k) / |\boldsymbol{d}(k)|$ can be regarded as a map from the BZ of the chain to the two-sphere S^2. Thus, the whole image of the BZ onto S^2 is a closed curve. Furthermore, the problem can be simplified and it's possible to show [44] that the Berry phase is half of the angle swept by the vector

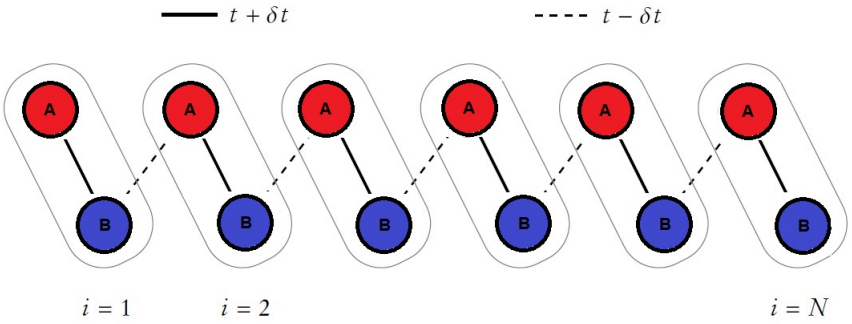

Figure 1.8: Intuitive picture of the SSH Model. We have two types of hopping: an intra-cell hopping between sites in the same cell of strength $t + \delta t$ and an inter-cell hopping between sites of neighbouring cells of strength $t - \delta t$.

$\boldsymbol{d}(k)$ in the plane, with respect to the origin $d = 0$. Therefore, we are interested in how the Berry phase changes when the parameter δt is varied.
There are two different phases of the model:

1. $\delta t > 0$, here the component d_x is always positive so $\boldsymbol{d}(k)$ sweeps no angle and the Berry phase is zero: this is the trivial phase.

2. $\delta t < 0$, in this case $d_x < 0$ and as a result by varying k across the BZ the vector $\boldsymbol{d}$ rotates by 2π and the Berry phase is π. We are going to call this case the topological phase.

Actually, what is relevant is how many times the curve encircles the origin: this defines the winding number ν, a topological invariant. In fact, the passage from $\delta t < 0$ to $\delta t > 0$ requires the curve to intersect the point of degeneracy $\boldsymbol{d} = 0$, where the gap closes. Both cases describe an insulator, because there is a gap $\pm |\boldsymbol{d}(k)|$ between the two energies, but do not describe the same phase: the trivial phase has winding number $\nu = 0$ while non-trivial phase has winding number $\nu = 1$. We can also analyze the two different phases in the fully dimerized limit $\delta t = \pm t$:

- $\delta t = t$, in this limit the Hamiltonian becomes:

$$H = 2t \sum_{i=1}^{N} c_{A,i}^{\dagger} c_{B,i} + c_{B,i}^{\dagger} c_{A,i} \tag{1.49}$$

  As we can see from the figure 1.9, there is only intra-cell hopping and the system has constant energy $\pm 2\,|t|$ and gap.

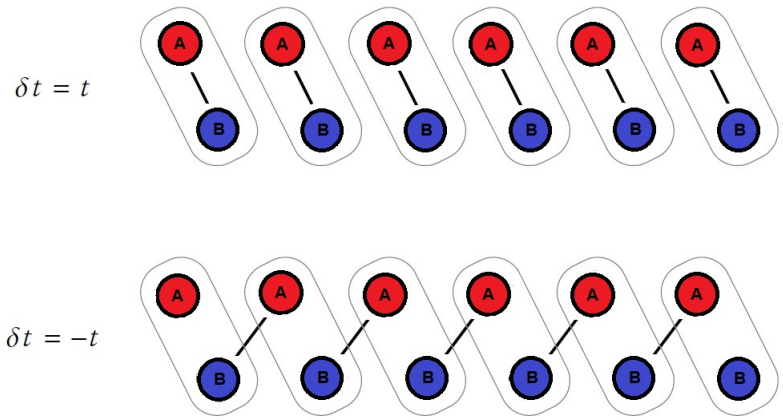

Figure 1.9: Phases of the SSH Model. The trivial phase $\delta t = t$ has no hopping between cells. The topological phase $\delta t = -t$ no hopping inside the cells then edge modes appear.

- $\delta t = -t$, this case is interesting because the Hamiltonian becomes

$$H = 2t \sum_{i=1}^{N} c^{\dagger}_{A,i+1} c_{B,i} + c^{\dagger}_{B,i} c_{A,i+1} \tag{1.50}$$

  As we can se from the figure 1.9, there is only inter-cell hopping and doesn't contains any term pairing the modes $c_{A,i}$ and $c_{b,N}$ with the rest of the chain. That means these modes can be excited with no cost in energy.

In order to explain the no-cost in energy of these edge modes, let us consider the dispersion relation. It can be got:

$$E_{\pm}(k) = \pm \left|\boldsymbol{d}(k)\right| = \pm\sqrt{2(t^2 + \delta t^2) + 2(t^2 - \delta t^2)\cos ka} \tag{1.51}$$

In both fully dimerized cases the dispersion relation becomes $E_{\pm} = \pm 2\left|t\right|$. If we are in the topological phase, this relation does not capture all the eigenstates. Indeed let us consider the excited states at the edges

$$\left|A, 1\right\rangle = c^{\dagger}_{A,1}\left|0\right\rangle, \qquad \left|B, N\right\rangle = c^{\dagger}_{B,N}\left|0\right\rangle \tag{1.52}$$

where $\left|0\right\rangle$ is the vacuum i.e. the state which is annihilated by all the annihilation operators. It is easy to show that they are annihilated by the Hamiltonian (1.50) because it does not contain any term $c_{A,1}$ or $_{B,N}$. Then, the excited states at the edges have no energy cost. Furthermore it's possible to show that these the wavefunctions are placed at the edge and have an exponential decay i.e. they don't penetrate in the bulk. [44]. The topological property of the bulk in this case is the winding number ν and the edge states are distinguished if they belong to the sublattice A or B. Thus the difference we have to look at now is $N_A - N_B$: in the trivial phase $\nu = 0$ and we don't have any edge state so $N_A - N_B$; on the other hand, in the topological phase the winding number is $\nu = 1$, so is the number of edge states on the left side $N_A - N_B = 1$ [44].

Chapter 2

Matrix Product State representation and bilinear-biquadratic model

In the previous chapter, we have established the general structure of the quantum phase diagram and the criteria for classifying gapped quantum phases. In this chapter, we are going to studying Matrix Product State representation focusing on bilinear-biquadratic model. As we'll see, this model is characterized by two massive phases i.e. the topological Haldane phase and the trivial dimer phase. The Haldane phase is a so-called symmetry protected topological phase, meaning that it remains intact even if we add small symmetry-preserving perturbations. The symmetries which need to be preserved are said to protect this topological phase, given that if those are explicitly broken then the phase disappears and becomes topological trivial. On the other hand it has been shown, using the Matrix Product State representation of quantum states, that all symmetry protected topological phases can be classified by the second cohomology group $H^2(G, \mathbb{C})$ of the corresponding symmetry group G, i.e. by the projective representations of the latter. Then, in this chapter we will better explain this aspect and, at the end, we will have all tools to define and calculate Non Local Order Parameters (NLOPs) that allows us to distinguish the different phases.

2.1 MPS representation

Let us consider a chain of spin-s variables of length L where on each site the state $|i_k\rangle$ is $d = 2s + 1$ dimensional. We can write a generic quantum state on this chain as:

$$|\Psi\rangle = \sum_{i_1 \dots i_L} C_{i_1 \dots i_L} |i_1 \dots i_L\rangle \tag{2.1}$$

where $C_{i_1 \ldots i_L}$ is a tensor with d^L components that can be expressed as a matrix product state of the form [20] :

$$A^{[1]}_{i_1} A^{[2]}_{i_2} \ldots A^{[L]}_{i_L} \quad (OBC) \qquad and \qquad Tr\left[A^{[1]}_{i_1} A^{[2]}_{i_2} \ldots A^{[L]}_{i_L}\right] \quad (PBC) \tag{2.2}$$

where $i_k = 1 \ldots d$ and $A^{[k]}_{i_k}$'s are $D_k \times D_{k+1}$ matrices on the site k. In case of OBC the first $A^{[1]}_{i_1}$ and the last matrix $A^{[L]}_{i_L}$ are respectively $1 \times D_2$ and $D_L \times 1$ matrices, i.e. a row and a column vector. D is called the inner dimension of MPS (in the following we will assume $D_k = D$) and, in general, it does not correspond to physical dimension d of Hilbert spaces. Thus, using these matrices, the generic quantum state on this chain with Open Boundary Condition and Periodic Boundary Condition, respectively, reads:

$$|\Psi\rangle = \sum_{i_1 \ldots i_L} A^{[1]}_{i_1} \ldots A^{[L]}_{i_L} |i_1 \ldots i_L\rangle \qquad and \qquad |\Psi\rangle = \sum_{i_1 \ldots i_L} Tr\left[A^{[1]}_{i_1} \ldots A^{[L]}_{i_L}\right] |i_1 \ldots i_L\rangle \tag{2.3}$$

The representation is efficient as with fixed D for a state of L spins, the number of parameters involved is at most ND^2 as compared to d^N in the generic case. If the set of matrices does not depend on site label k, then the state rapresented is translation invariant. Furthermore, it is evident that the MPS representation of a given state is not unique; in fact, if we perform the following transformation on each matrix:

$$A^{[k]}_{i_k} \longrightarrow X_k^{-1} X^{[k]}_{i_k} X_{k+1} \tag{2.4}$$

where X_k is $D \times D$ invertible matrix, then the state (2.3) remains unchanged.
The matrices A_i in an MPS representation can be put into a canonical form [18] i.e. the matrices can be chosen such that $\forall k$ (see Fig 2.1):

$$\begin{aligned} \sum_i A^{[k]}_i A^{[k]\dagger}_i &= \mathbb{I}_{\mathbb{D}\times\mathbb{D}} \\ \sum_i A^{[k]\dagger}_i \left(\Lambda^{[k-1]}\right)^2 A^{[k]}_i &= \left(\Lambda^{[k]}\right)^2 \end{aligned} \tag{2.5}$$

where $\Lambda^{[k]}$ is $D \times D$ positive diagonal matrix with $\mathrm{Tr}\left[\left(\Lambda^{[k]}\right)^2\right] = 1$.

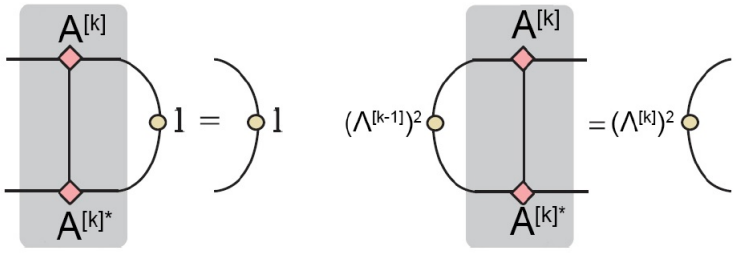

Figure 2.1: The conditions satisfied by the MPS matrices in canonical form.

It also useful to introduce the transfer matrices (see Fig.2.2):

$$T^{[k]}(X) = \sum_i A_i^{[k]} X A_i^{[k]\dagger} \tag{2.6}$$

where X is $D \times D$ matrix, then 2.5 can be restated as:

$$T^{[k]}(\mathbb{I}) = \mathbb{I} \quad T^{*[k]}((\Lambda^{[k-1]})^2) = \left(\Lambda^{[k]}\right)^2 \tag{2.7}$$

Thus, the Matrix Product State can be manipulated to give the expectation values of product of local operators $O(k)$ (see Fig.2.3):

$$\langle\Psi| \prod_{k=1}^{L} O(k) |\Psi\rangle = \prod_{k=1}^{L} T_O^{[k]}(X) \quad (OBC) \qquad and \qquad \langle\Psi| \prod_{k=1}^{L} O(k) |\Psi\rangle = Tr\left[\prod_{k=1}^{L} T_O^{[k]}(X)\right] \quad (PBC)$$

where:

$$T_O^{[k]}(X) = \sum_{ij} \langle i| O(k) |j\rangle A_j^{[k]} X A_i^{[k\dagger]} \tag{2.8}$$

so the transfer matrices T have $\mathbb{I}$ as eigenvector corresponding to the eigenvalue 1.

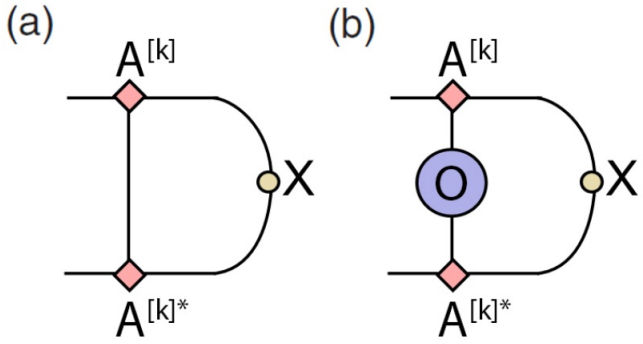

Figure 2.2: The transfer matrices (a) $T^{[k]}(X)$ and (b) $T_O^{[k]}(X)$.

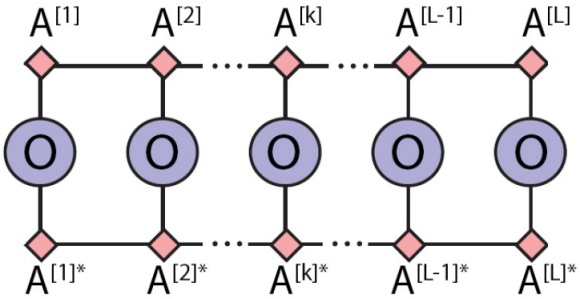

Figure 2.3: The expectation value of $\prod_{k=1}^{L} O(k)$ with OBC.

Since we are interested in the ground states of gapped Hamiltonians, which have a finite correlation length ξ, we assume that T has a non-degenerate largest eigenvalue

$\lambda_1 = 1$ in order to express this correlation length as:

$$\xi = -\frac{1}{\ln|\lambda_2|} \tag{2.9}$$

where λ_2 is the second largest eigenvalue.
Let us do some interesting example in order to become familiar with this new representation.

2.1.1 Product state

The first trivial example is the case in which the matrices $A_i^{[k]}$ are scalar. If $D = 1$, A are numbers, then $|\Psi\rangle$ is a product state. In fact, if $d = 2$ (so the spin of each particles is $s = 1/2$), we can set:

$$A_1^{[k]} = \frac{1}{\sqrt{2}} \qquad and \qquad A_2^{[k]} = \frac{1}{\sqrt{2}} \tag{2.10}$$

then $|\Psi\rangle$ describes a product state of two level spins of the form:

$$|\Psi\rangle = \left[\frac{1}{\sqrt{2}}(|0\rangle + |1\rangle)\right]\left[\frac{1}{\sqrt{2}}(|0\rangle + |1\rangle)\right]\cdots\left[\frac{1}{\sqrt{2}}(|0\rangle + |1\rangle)\right] \tag{2.11}$$

However, for $D \geq 2$ the $|\Psi\rangle$ would in general be an entangled state of many spins.

2.1.2 Greenberger–Horne–Zeilinger state

Greenberger–Horne–Zeilinger state, introduced in the previous chapter, is an entangled quantum state of $M \geq 2$ subsystems. If each system has dimension d, i.e., the local Hilbert space is isomorphic to $\mathbb{C}^d$, then the total Hilbert space of M partite system is $H_{tot} = (\mathbb{C})^{\otimes M}$. It reads:

$$|GHZ\rangle = \frac{1}{\sqrt{d}}\sum_{i=1}^{d-1}|i\rangle\otimes\cdots\otimes|i\rangle = \frac{1}{\sqrt{d}}(|0\rangle\otimes\cdots\otimes|0\rangle+|1\rangle\otimes\cdots\otimes|1\rangle+\cdots+|d-1\rangle\otimes\cdots\otimes|d-1\rangle) \tag{2.12}$$

In the case of each of the subsystems being two-dimensional, that is for qubits, it becomes:

$$|GHZ\rangle = \frac{1}{\sqrt{2}}(|0\rangle^{\otimes L} + |1\rangle^{\otimes L}) \tag{2.13}$$

It can be expressed as a Matrix Product State, up to normalization, by choosing $D = 2$ with:

$$A_0^{[k]} = \begin{pmatrix} 1 & 0 \\ 0 & 0 \end{pmatrix} \qquad A_1^{[k]} = \begin{pmatrix} 0 & 0 \\ 0 & 1 \end{pmatrix} \tag{2.14}$$

2.1.3 W state

The W state is an entangled quantum state of three qubits which has the following shape:

$$|W\rangle = \frac{1}{\sqrt{3}}(|100\rangle + |010\rangle + |001\rangle) \tag{2.15}$$

It represents a specific type of multipartite entanglement and occurs in many applications in quantum information theory. Particles prepared in this state reproduce the properties of Bell's theorem, which states that no classical theory of local hidden variables can produce the predictions of quantum mechanics. It was first reported by W. Dür, G. Vidal, and J. I. Cirac [8].
It is possible to generalize this state for n qubits:

$$|W\rangle = \frac{1}{\sqrt{n}}(|10\cdots0\rangle + |01\cdots0\rangle + \cdots + |00\cdots01\rangle) \tag{2.16}$$

where it's evident that $|W\rangle$ is nothing but a quantum superpostion with equal expansion coefficients of all possible pure states in which exactly one of the qubits is in an "excited state" $|1\rangle$, while all other ones are in the "ground state" $|0\rangle$. In order to give a matrix product state representation, let us to consider the four-particles W state (up to a normalization factor):

$$|W\rangle = \frac{1}{\sqrt{4}}(|1000\rangle + |0100\rangle + |0010\rangle + |0001\rangle) \tag{2.17}$$

As done in [9], a matrix product representation of this state is:

$$\Psi_{\alpha\beta\gamma\delta} = \sum_{ijk} A_i^\alpha B_{ij}^\beta C_{jk}^\delta D_k^\gamma \, |\alpha\beta\gamma\delta\rangle \tag{2.18}$$

where α is the index of the spin component of the first particle, β is the index of the second particle, and so on. Precisely, the matrices are:

$$A^0 = \begin{pmatrix} 1 & 0 \end{pmatrix} \qquad A^1 = \begin{pmatrix} 0 & 1 \end{pmatrix} \tag{2.19}$$

$$B^0 = C^0 = \begin{pmatrix} 1 & 0 \\ 0 & 1 \end{pmatrix} \qquad B^1 = C^1 = \begin{pmatrix} 0 & 1 \\ 0 & 0 \end{pmatrix} \tag{2.20}$$

$$D^0 = \begin{pmatrix} 1 \\ 0 \end{pmatrix} \qquad D^1 = \begin{pmatrix} 0 \\ 1 \end{pmatrix} \tag{2.21}$$

A way to represent this factorization is shown in the figures 2.4.

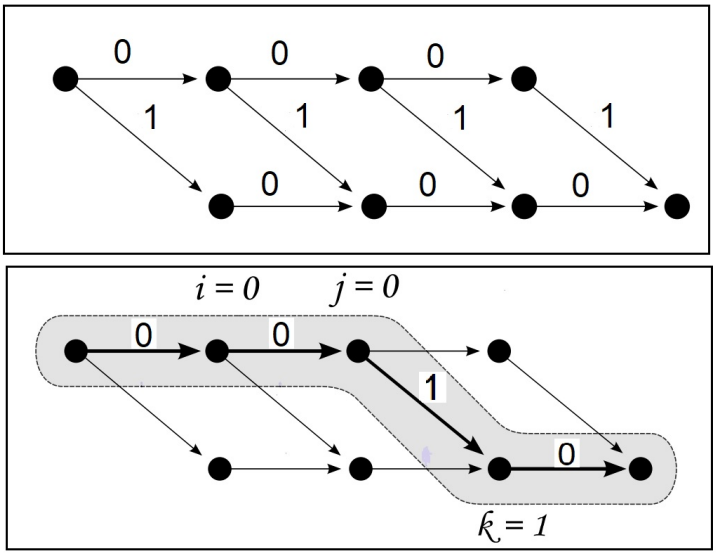

Figure 2.4: On the left: diagram representing the matrix product form of the W-state. The nodes correspond to indices, and the edges correspond to matrix elements: each possible "walk" generates a term in the state. On the right: example of a possible walk which generates the term 0010.

2.1.4 Majumdar–Ghosh model

Majumdar–Ghosh model is a periodic spin-1/2 chain where, in the ground state, only nearst-neightbor pairs of spins form valence bonds (see Fig. 2.5) [11]:

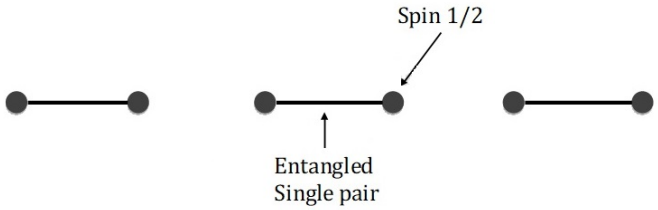

Figure 2.5: Valence bonds in dimer state on a chain of spin-1/2s, i.e. the Majumdar–Ghosh model: each point is a spin variable and each bond forms a singlet state.

$$|d\rangle_{\pm} = \bigotimes_{i=1}^{L/2} \frac{1}{\sqrt{2}} \Big(|\uparrow_{2i}\rangle \otimes |\downarrow_{2i\pm1}\rangle - |\downarrow_{2i}\rangle \otimes |\uparrow_{2i\pm1}\rangle \Big) \tag{2.22}$$

Using a projector operator we can costruct a Hamiltonian of s= 1/2 particles ad hoc for which the states (2.22) are the ground states:

$$H_{MG} = J \sum_i \left(\boldsymbol{S}_i \boldsymbol{S}_{i+1} + \frac{1}{2} \boldsymbol{S}_i \boldsymbol{S}_{i+2} \right) \tag{2.23}$$

This Hamiltonian is made up of two interaction terms: the first is between nearst-neighbor spins and the second between next-nearest-neighbor. The matrix product state representation with $D = 3$ is given by the following two matrices:

$$A_1 = \begin{pmatrix} 0 & 1 & 0 \\ 0 & 0 & -1 \\ 0 & 0 & 0 \end{pmatrix} \qquad A_2 = \begin{pmatrix} 0 & 0 & 0 \\ 1 & 0 & 0 \\ 0 & 1 & 0 \end{pmatrix} \tag{2.24}$$

Finally, two of the most important examples of matrix product states are the AKLT state and dimer state both describing an anti-ferromagnetic ground state of spin-1 chain. Before showing how we can obtain an exact MPS representation of them, let us introduce the bilinear-biquadratic model: both AKLT and dimer state are a good approximation for other systems in the same phase, i.e. the Haldane and dimer phase respectively.

2.2 Bilinear-biquadratic model

From now on we will be interested to examine a particular $s = 1$ model, the so-called bilinear-biquadratic model, whose Hamiltonian is:

$$H = J \sum_i \left[\mathbf{S}_i \cdot \mathbf{S}_{i+1} - \beta (\mathbf{S}_i \cdot \mathbf{S}_{i+1})^2 \right] \tag{2.25}$$

where J is the coupling constant and β is a real parameter.
The Hamiltonian (2.25) has a rich phase diagram obtained varying J and β. Furthermore it is the most general SU(2)-invariant s=1 Hamiltonian with nearest-neighbor interaction. Let's show the different phases of the model (see Fig 2.6). A useful way to represent the phase diagram is that shown in Fig 2.6. It can be obtained doing the following transformation:

$$J \longrightarrow J' = \cos(\theta) \qquad and \qquad \beta \longrightarrow \beta' = \tan(\theta) \tag{2.26}$$

then the Hamiltonian (2.25) can be expressed as:

$$H = J' \sum_i \left[\cos(\theta) \mathbf{S}_i \cdot \mathbf{S}_{i+1} - \sin(\theta) (\mathbf{S}_i \cdot \mathbf{S}_{i+1})^2 \right] \tag{2.27}$$

a) **Haldane phase**. This phase is the region of the phase diagram defined by:

$$1 < \beta < 1 \qquad and \qquad J > 0 \tag{2.28}$$

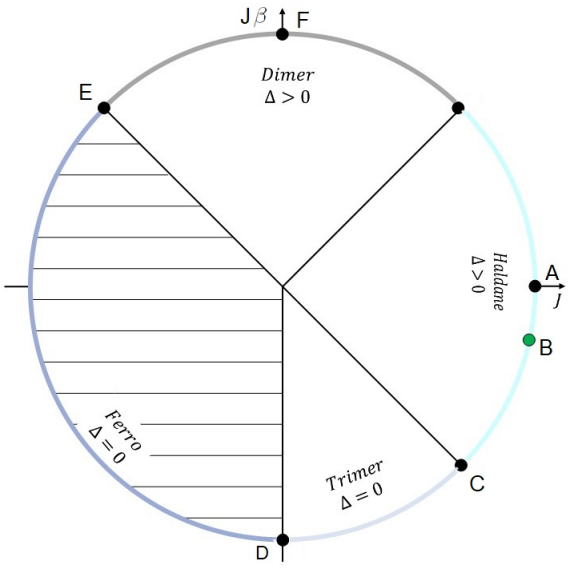

Figure 2.6: The phase diagram of bilinear-biquadratic model: on the left it is represented on the plane; on the right it is represented on the circle. In this last case we named: A the antiferromagnetic Heisenberg Model, B the AKLT point, C the Sutherland model, D the ferromagnetic biquadratic models, E the transition point ferro-Dimer, F the antiferromagnetic biquadratic models and, finally, G the Takhtajan-Babujian model

The system has a unique massive ground state with exponentially decaying correlation functions and shows an antiferromagnetic behavior. We recognize the antiferromagnetic Heisenberg model obtained for $\beta = 0$ and the AKLT model obtained for $\beta = -\frac{1}{3}$:

$$H_{Heis} = J \sum_i \left[\mathbf{S}_i \cdot \mathbf{S}_{i+1} \right] \tag{2.29}$$

$$H_{AKLT} = J \sum_i \left[\mathbf{S}_i \cdot \mathbf{S}_{i+1} - \frac{1}{3} (\mathbf{S}_i \cdot \mathbf{S}_{i+1})^2 \right] \tag{2.30}$$

The points $\beta = -1$ and $\beta = 1$ give respectively the Sutherland and Takhtajan-Babujian model [13, 22, 21].

b) **Dimer phases**. They are located in:

$$\begin{cases} \beta & > 1 \\ J & > 0 \end{cases} \qquad and \qquad \begin{cases} \beta & < -1 \\ J & < 0 \end{cases} \tag{2.31}$$

The system has a two-fold degenerate ground state and a small excitation gap [14],[17]. The degeneracy is due to the broken translation symmetry: the system tends to split its spins in pair so there is no more one-site invariance. When $\beta = \infty$

the bilinear-biquadratic model becomes purely biquadratic:

$$H_{biq} = \lim_{\beta\to\infty} \frac{H}{\beta} = -J \sum_i (\mathbf{S}_i \cdot \mathbf{S}_{i+1})^2 \tag{2.32}$$

c) **Trimerized**. This is the last antiferromagnetic region of the phase diagram for:

$$\beta < -1 \qquad and \qquad J > 0 \tag{2.33}$$

it is a gapless phase.

d) **Ferromagnetic phase**. Finally, in region delimited by:

$$\beta > -1 \qquad and \qquad J < 0 \tag{2.34}$$

we have a the only ferromagnetic phase of the model, which is gapless and contains also the Heisenberg ferromagnet for $\beta = 0$. The ground state of every model in this region is the fully aligned state:

$$|GS\rangle = |+ + + \cdots + +\rangle \tag{2.35}$$

with energy: $E = JL(1-\beta)$.

2.3 On-site unitary transformation and Projective Representation

There are a lot of systems that are invariant under on-site symmetry transformations, for example the Ising model is symmetric under the $\mathbb{Z}_2$ spin flip transformations. We shall say that a representation u of a group G is given in a certain linear space if and only if to each element $g \in G$ there is a corresponding linear operator $u(g)$ acting in the space such that to each product of the elements of the group there is a corresponding product of the linear operators, i.e.

$$u(g_1)u(g_2) = u(g_1 g_2) \tag{2.36}$$

. Furthermore, the system is symmetric under the global action of the group if the wave function transforms as:

$$u(g) \otimes \cdots \otimes u(g) \, |\Psi\rangle = \alpha^L(g) \, |\Psi\rangle \tag{2.37}$$

where L is the size of the system and $\alpha(g)$ is a one-dimensional representation of G.
Now let's define what a projective representation is. The operators $u(g)$ form a projective representation of the group G if:

$$u(g_1)u(g_2) = \omega(g_1, g_2)u(g_1 g_2) \qquad \forall g_1, g_2 \in G \tag{2.38}$$

where $\omega(g_1, g_2)$ is called factor systemand distinguishes different projective representations If $\omega(g_1, g_2) = 1$, we obtain the usual linear representation of G. However not all projective representations with $\omega \neq 1$ are non-trivial. In fact, a different choice of prefactor $u'(g) = \beta(g)u(g)$ will lead to a different ω', that is:

$$\omega'(g_1, g_2) = \frac{\beta(g_1 g_2)}{\beta(g_1)\beta(g_2)}\omega(g_1, g_2) \tag{2.39}$$

Then by redefining $\beta(g)$ we can reduce the factor system to 1 that is the usual trivial projective representation: only $\omega'(g_1, g_2)$'s which cannot be reduced to 1 belong to different classes of equivalence. The set of equivalence classes of factor system forms an abelian group called the second cohomology group of G and is denoted as $H^2(G, \mathbb{C})$ ([16]).
Now we are going to show how the matrices A_i of the MPS transform under on-site transformation. Let's consider a generic matrix product state with translational invariance and PBC:

$$|\Psi\rangle = \sum_{i_1 \dots i_L} Tr\left[A^{[1]}_{i_1} \dots A^{[L]}_{i_L}\right] |i_1 \dots i_L\rangle \tag{2.40}$$

Let be $\Omega^{[k]}(g)$ a d-dimensional unitary representation of G. This has to be linear and acting on the k-th site. Thus, if the ground state of the system is symmetric under a transformation of the group G, it transforms as:

$$\bigotimes_{k=1}^{L} \Omega^{[k]}(g) |\Psi\rangle = e^{iL\theta_\Omega(g)} |\Psi\rangle \tag{2.41}$$

where $\theta_\Omega(g)$ is a phase factor which emerges when we perform this transformation on the k-the site. It can be shown [16, 19] that A_i has to transform as (see Fig. 2.7):

$$\sum_j \Omega_{ij}(g) A_j = e^{iL\theta_\Omega(g)} R^\dagger_\Omega(g) A_i R_\Omega(g) \tag{2.42}$$

where $R_\Omega(g)$ is D-dimensional unitary projective representation of G, belonging to a class ω of $H^2(G, \mathbb{C})$, while $e^{iL\theta_\Omega(g)}$ is a one-dimensional representation of G.
The key point for the classification of the various SPT phases for a given symmetry G is that two ground states belong to the same phase if the corresponding projective representations belong to the same class w. Indeed as shown in [16] it is possible to construct explicitly a local unitary transformation that connects the two ground states without breaking the symmetry or facing a phase transition when the corresponding MPS are related to equivalent projective representations, while it is not possible when they are inequivalent. So the STP phases of spin systems can be labeled by $\{\omega, \theta_\Omega(g)\}$.

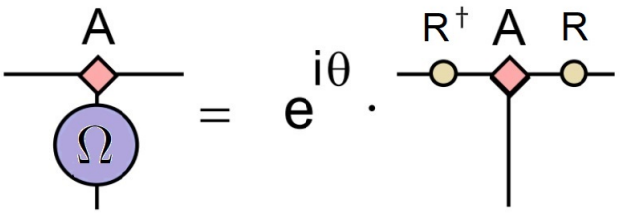

Figure 2.7: Symmetry transformation of the matrix A_i

Furthermore, in order to show an important result about $R_\Omega(g)$, let us introduce a useful alternative form of the matrices in the MPS. Indeed, from the Singular Value Decomposition, the matrices $A_i^{[k]}$ can be written as (see [23]):

$$A_i^{[k]} = \Gamma_i^{[k]}\Lambda^{[k]} \tag{2.43}$$

where $\Gamma_i^{[k]}$ is a D dimensional matrix. Dropping the index k (we are considering traslation invariance), the state $|\Psi\rangle$ can be written as:

$$|\Psi\rangle = \sum_{i_1\dots i_L} Tr\left[\Gamma_{i_1}\Lambda\cdots\Gamma_{i_L}\Lambda\right]|i_1\dots i_L\rangle \tag{2.44}$$

and the canonical condition (2.5) becomes:

$$\sum_i \Gamma_i\Lambda^2\Gamma_i^\dagger = \mathbb{I} \tag{2.45}$$

Now we have all the tools to show that $R_\Omega^\dagger(g)$ is an eigenvector of the transfer matrix. Indeed:

$$\begin{aligned} T_\Omega(R_\Omega^\dagger) &= \sum_{ij}\Omega_{ij}\Gamma_i\Lambda R_\Omega^\dagger\Lambda\Gamma_j^\dagger \\ &= \sum_j\left(\sum_i\Omega_{ij}\Gamma_i\right)\Lambda R_\Omega^\dagger\Lambda\Gamma_j^\dagger \\ &= e^{i\theta_\Omega}\sum_j R_\Omega^\dagger\Gamma_j R_\Omega\Lambda R_\Omega^\dagger\Lambda\Gamma_j^\dagger \\ &= e^{i\theta_\Omega}\sum_j R_\Omega^\dagger\Gamma_j\Lambda^2\Gamma_j^\dagger \\ &= e^{i\theta_\Omega}R_\Omega^\dagger \end{aligned} \tag{2.46}$$

where we used the property [23]: $[\Lambda, R_\Omega] = 0$. Then if we are able to find R_Ω, we can read off the factor system ω and determine the corresponding phase.
Useful tools that permit us to distinguish SPT phases are the so-called Non Local Order Parameters. Indeed, if Ω is a symmetry transformation then we can define it as:

$$\mathbf{O}_\Omega(O^A, O^B) = \lim_{n\to\infty}\langle\Psi|\,O^A(1)\left(\prod_{k=2}^{n-1}\Omega(k)\right)O^B(n)\,|\Psi\rangle \tag{2.47}$$

where O^A and O^B are two generic local operators, placed, respectively, on the first site and on the n-th site of the chain. Let's see how we can choose O^A and O^B in order to distinguish topological states. It's easy to check that (2.47) can be expressed as (see Fig **??**):

$$\begin{aligned}\mathbf{O}_\Omega(O^A,O^B) &= \lim_{n\to\infty} Tr\left[\Lambda^2 T_{O^A} T_\Omega^n T_{O^B}\right] \\ &= Tr\left[\Lambda^2 T_{O^A}(R_\Omega^\dagger)\right]\cdot Tr\left[\Lambda R_\Omega \Lambda T_{\Omega^B}(\mathbb{I})\right] \\ &= Tr\left[\Lambda^2 R_\Omega^\dagger \tilde{O}^A\right]\cdot Tr\left[\Lambda^2 R_\Omega \tilde{O}^B\right]\end{aligned} \tag{2.48}$$

where

$$\tilde{O}^A = \sum_{ij} O^A_{ij}\Gamma_i^\dagger \Lambda^2 \Gamma_j \qquad and \qquad \tilde{O}^B = \sum_{ij} O^B_{ij}\Gamma_i \Lambda^2 \Gamma_j^\dagger \tag{2.49}$$

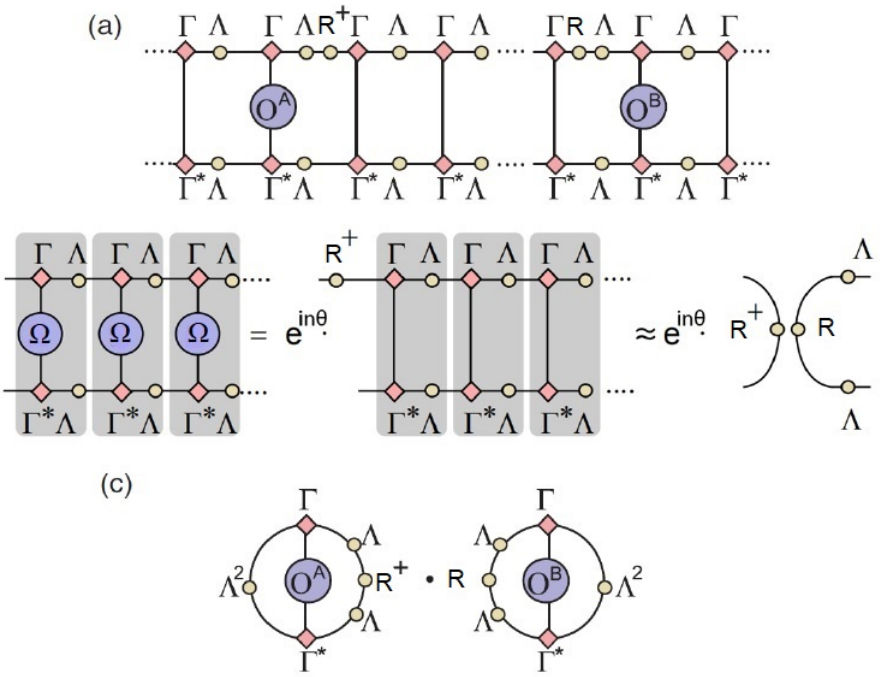

Figure 2.8: Evaluation of the NLOP $\mathbf{O}_\Omega(O^A,O^B)$. The matrices R_Ω and $R_\Omega^\dagger$ involved in the transformation of the Γ's all vanish except the ones at the edges. (b,c) Approximation of the NLOP in the thermodynamic limit where we are ignore the overall phase.

Now we suppose to have another symmetry Ω' that commutes with the previous one

$$[\Omega',\Omega] = 0 \tag{2.50}$$

but its projective representation not:

$$R_{\Omega'}R_\Omega = e^{i\Phi}R_\Omega R_{\Omega'} \tag{2.51}$$

If we choose a local operator O^A so that, under this new symmetry, it transforms as:

$$\Omega' O^A \Omega'^\dagger = e^{i\sigma}O^A \tag{2.52}$$

where σ is a phase factor. $\tilde{O}^A$ transforms in the same way:

$$R_{\Omega'}\tilde{O}^A R^\dagger_{\Omega'} = e^{i\sigma}\tilde{O}^A. \tag{2.53}$$

Then it follows that:

$$\begin{aligned} Tr\left[\Lambda^2 R^\dagger_\Omega \tilde{O}^A\right] &= e^{i\sigma} Tr\left[\Lambda^2 R^\dagger_\Omega R^\dagger_{\Omega'} \tilde{O}^A R_{\Omega'}\right] \\ &= e^{i(\sigma-\Phi)} Tr\left[\Lambda^2 R^\dagger_\Omega \tilde{O}^A\right] \end{aligned} \tag{2.54}$$

The importance of this result (2.54) will be clear in the last section of this Chapter where we will discuss how to define properly Non-Local Order Parameters.

2.4 MPS representation of AKTL and dimer states

As we said, we are interested to two particular states of bilinear-biquadratic model that is AKLT (Affleck-Kennedy-Lieb-Tasaki) states, representing the whole Haldane phase, and the dimer state. They belong to two different STP phases which can be detected by NLOP just defined.

2.4.1 AKTL state

The AKLT Hamiltonian is given by:

$$H_{AKLT} = J\sum_i \left[\mathbf{S}_i \cdot \mathbf{S}_{i+1} - \frac{1}{3}(\mathbf{S}_i \cdot \mathbf{S}_{i+1})^2\right] \tag{2.55}$$

where $\boldsymbol{S}_i$ are spin 1 operator. It easy to check that H_{AKLT} can be written as:

$$H_{AKLT} = 2J\sum_i P_2(i, i+1) - \frac{2}{3}NJ \tag{2.56}$$

where $\mathbf{S}_i$ is the spin operator of the i-th site and $P_2(i, i+1)$ is the projection onto the total spin $J = 2$ subspace of each neighboring pair particles. The ground state of this Hamiltonian can be obtained using the picture of the valence-bond solid, which is illustrated in Fig 2.9, where each bond denotes the singlet state:

$$|singlet\rangle = \frac{1}{\sqrt{2}}(|\uparrow\downarrow\rangle - |\downarrow\uparrow\rangle) \tag{2.57}$$

and each oval represent the projection onto the triplet subspace:

$$\Pi_{Triplet} = |+1\rangle\langle 00| + |0\rangle\left[\frac{1}{\sqrt{2}}(\langle\uparrow\downarrow| + \langle\downarrow\uparrow|)\right] + |-1\rangle\langle 11| \tag{2.58}$$

where $|1\rangle, |0\rangle$ and $|1\rangle$ are the eigenstates of the spin S_z operator, corresponding to the eigenvalues $1, 0$ and -1 respectively. This gives us a state of a spin-1 chain denoted by

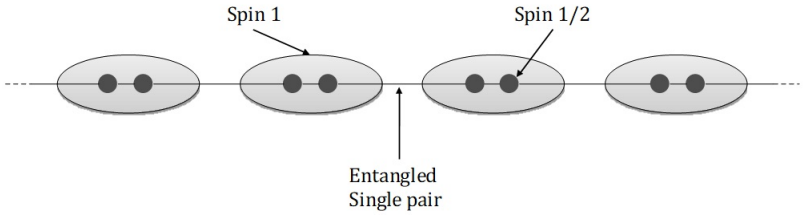

Figure 2.9: Entangled pair structure of the AKLT wave function

$|\Psi_{AKLT}\rangle$.

It is the ground state of the system because it is the ground state of each projection $P_2(i, i+1)$. This is because, among the four spin-1/2s making up a pair of neighboring spin-1s, the two in the middle form a spin singlet. Therefore, the total spin of the four spin-1/2s can only be 0 and 1 but not 2. On a ring with periodic boundary condition, the ground state preserves spin rotation symmetry and it is unique and gapped. On the other hand, on a chain with boundary there are isolated spin-1/2s at each end of the chain that are not coupled with anything and give rise to a two-fold degenerate edge state. The full ground state on an open chain is four-fold degenerate. This degeneracy is stable as long as spin rotation symmetry is preserved.

Let's show now how we can calculate the MPS representation of that. We think at AKLT state as a symmetrical combination of two spin-1/2's in the same site and as antisymmetrical combination of two spin-1/2's on the nearest neighbor's sites. As done in [20] a generic quantum state on a chain made of $2L$ spin-1/2's can be expressed as:

$$|\Psi_{AKLT}\rangle = \sum_{a_1 \ldots a_L} \sum_{b_1 \ldots b_L} C_{a_1 \ldots a_L b_1 \ldots b_L} |a_1 \ldots a_L\rangle |b_1 \ldots b_L\rangle \tag{2.59}$$

where we have denoted $|a_k\rangle = |0\rangle$ and $|b_k\rangle = |1\rangle$. In order to create a singlet bonds between spins b_k and a_{k+1} we can apply a matrix of the form:

$$N^{b_k a_{k+1}} = \begin{pmatrix} 0 & \frac{1}{\sqrt{2}} \\ -\frac{1}{\sqrt{2}} & 0 \end{pmatrix} \tag{2.60}$$

thus we get:

$$|\Psi_{AKLT}\rangle = \sum_{a_1 \ldots a_L} \sum_{b_1 \ldots b_L} N^{b_1 a_2} \cdots N^{b_L a_1} |a_1 \ldots a_L\rangle |b_1 \ldots b_L\rangle \qquad PBC \tag{2.61}$$

$$|\Psi_{AKLT}\rangle = \sum_{a_1 \ldots a_L} \sum_{b_1 \ldots b_L} N^{b_1 a_2} \cdots N^{b_{L-1} a_L} |a_1 \ldots a_L\rangle |b_1 \ldots b_L\rangle \qquad OBC \tag{2.62}$$

However, we want to obtain that each pair of spins on the same site is a spin-1 variable. In order to implement this, we need to introduce a set of three matrices $M_{i_K}^{a_k b_k}$ which

give rise to the correct symmetrization:

$$M_+ = \begin{pmatrix} 1 & 0 \\ 0 & 0 \end{pmatrix} \qquad M_0 = \begin{pmatrix} 0 & \frac{1}{\sqrt{2}} \\ \frac{1}{\sqrt{2}} & 0 \end{pmatrix} \qquad M_- = \begin{pmatrix} 0 & 0 \\ 0 & 1 \end{pmatrix} \tag{2.63}$$

indeed the matrix $M_{i_K}^{a_k b_k}$ project the local state $|a_k b_k\rangle$ onto $|i_k\rangle = |+\rangle, |0\rangle, |-\rangle$. Replacing, the AKLT state reads:

$$|\Psi_{AKLT}\rangle = \sum_{a_1 \dots a_L} \sum_{b_1 \dots b_L} M_{i_1}^{a_1 b_1} N^{b_1 a_2} \cdots M_{i_L}^{a_L b_L} N^{b_L a_1} |a_1 \dots a_L\rangle |b_1 \dots b_L\rangle \qquad PBC \tag{2.64}$$

$$|\Psi_{AKLT}\rangle = \sum_{i_1 \cdots i_L} \sum_{a_1 \dots a_L} \sum_{b_1 \dots b_L} M_{i_1}^{a_1 b_1} N^{b_1 a_2} \cdots N^{b_{L-1} a_L} M_{i_L}^{a_L b_L} |a_1 \dots a_L\rangle |b_1 \dots b_L\rangle \qquad OBC \tag{2.65}$$

or equivalently:

$$|\Psi_{AKLT}\rangle = \sum_{i_1 \cdots i_L} Tr\big[M_{i_1} N \cdots M_{i_L} N |a_1 \dots a_L\rangle\big] |b_1 \dots b_L\rangle \qquad PBC \tag{2.66}$$

$$|\Psi_{AKLT}\rangle = \sum_{i_1 \cdots i_L} M_{i_1}^{a_1} N \cdots M_{i_{L-1}} N M_{i_L}^{b_L} |a_1 \dots a_L\rangle |b_1 \dots b_L\rangle \qquad OBC. \tag{2.67}$$

It easy to check that MPS representation is given by $A_{i_k} = M_{i_k} N$:

$$A_+ = \begin{pmatrix} 0 & \frac{1}{\sqrt{2}} \\ 0 & 0 \end{pmatrix} \qquad A_0 = \begin{pmatrix} -\frac{1}{2} & 0 \\ 0 & \frac{1}{2} \end{pmatrix} \qquad A_- = \begin{pmatrix} 0 & 0 \\ -\frac{1}{\sqrt{2}} & 0 \end{pmatrix} \tag{2.68}$$

Futhermore, we get:

$$\sum A_i A_i^\dagger = \frac{3}{4} \mathbb{I} \tag{2.69}$$

but we want the canonical form, so all we have to do is rescaling by a factor $\frac{2}{\sqrt{3}}$:

$$A_+ = \begin{pmatrix} 0 & \sqrt{\frac{2}{3}} \\ 0 & 0 \end{pmatrix} \qquad A_0 = \begin{pmatrix} -\frac{1}{\sqrt{3}} & 0 \\ 0 & \frac{1}{\sqrt{3}} \end{pmatrix} \qquad A_- = \begin{pmatrix} 0 & 0 \\ -\sqrt{\frac{2}{3}} & 0 \end{pmatrix} \tag{2.70}$$

If we want the useful form in (2.43), we need to define:

$$\Lambda = \begin{pmatrix} \frac{1}{\sqrt{2}} & 0 \\ 0 & \frac{1}{\sqrt{2}} \end{pmatrix} = \frac{1}{\sqrt{2}} \mathbb{I} \tag{2.71}$$

and the corresponding Γ_i matrices are:

$$\Gamma_+ = \begin{pmatrix} 0 & \frac{2}{\sqrt{3}} \\ 0 & 0 \end{pmatrix} \qquad \Gamma_0 = \begin{pmatrix} -\sqrt{\frac{2}{3}} & 0 \\ 0 & \sqrt{\frac{2}{3}} \end{pmatrix} \qquad \Gamma_- = \begin{pmatrix} 0 & 0 \\ -\frac{2}{\sqrt{3}} & 0 \end{pmatrix} \tag{2.72}$$

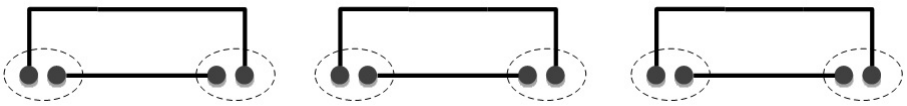

Figure 2.10: The spin-1 dimer state: each valence bond represents a singlet state, every site is represents by an oval containing two spin-1/2.

For our purposes, it's more convenient to use a different basis for the local Hilbert space on each site, that is:

$$|x\rangle = -\frac{1}{\sqrt{2}}(|+\rangle - |-\rangle) \qquad |y\rangle = \frac{i}{\sqrt{2}}(|+\rangle + |-\rangle) \qquad |z\rangle = |0\rangle \tag{2.73}$$

In this basis the spin matrices become:

$$S^x = \begin{pmatrix} 0 & 0 & 0 \\ 0 & 0 & -i \\ 0 & i & 0 \end{pmatrix} \qquad S^y = \begin{pmatrix} 0 & 0 & i \\ 0 & 0 & 0 \\ -i & 0 & 0 \end{pmatrix} \qquad S^z = \begin{pmatrix} 0 & -i & 0 \\ i & 0 & 0 \\ 0 & 0 & 0 \end{pmatrix} \tag{2.74}$$

whereas the matrices Γ_i become:

$$\Gamma_x = -\sqrt{\frac{2}{3}}X \qquad \Gamma_y = -\sqrt{\frac{2}{3}}Y \qquad \Gamma_z = -\sqrt{\frac{2}{3}}Z \tag{2.75}$$

where X, Y and Z are the Pauli's matrices (1.8).

2.4.2 Dimer state

Using valence bond states, we can costruct the dimer states as:

$$|d\rangle_{\pm} = \bigotimes_i^{L/2} \frac{1}{\sqrt{3}} \Big(|+\rangle_{2i} \otimes |-\rangle_{2i\pm1} + |-\rangle_{2i} \otimes |+\rangle_{2i\pm1} - |0\rangle_{2i} \otimes |0\rangle_{2i\pm1} \Big) \tag{2.76}$$

As we can see from the figure 2.10, each valence bond emanating from the site $2i$ has to terminate on the neighboring site $2i \pm 1$. We said that VBS for the AKLT model is the exact ground state and it can represent a good approximation for other systems in the same phase (Haldane phase). Also for dimer state, there is no value of β for which (2.76) is the exact ground state; nevertheless, it good approximates the ground state for the dimer phase as defined in (2.31). Now we use the basis (2.73) to express (2.76) as:

$$|d\rangle = \bigotimes_i \frac{1}{\sqrt{3}} \Big(|x\rangle_{2i-1} \otimes |x\rangle_{2i} \quad + \quad |y\rangle_{2i-1} \otimes |y\rangle_{2i} \quad + \quad |z\rangle_{2i-1} \otimes |z\rangle_{2i} \Big) \tag{2.77}$$

This state is no invariant under one-site translation but it is still invariant under translation of two sites. Correspondingly we expect to find two different MPS representations

defined in odd and even sites. Like we have shown in the subsection 2.1.1, we can obtain the MPS representation of product state using 1×1 matrices, i.e. scalars. Then, given that the dimer state is a product state of singlets, a possible choice of A_i (odd site) and $\tilde{A}_i$ (even site) is:

$$A_x = \frac{1}{\sqrt{3}} \begin{pmatrix} 1 & 0 & 0 \end{pmatrix} \qquad \tilde{A}_x = \begin{pmatrix} 1 \\ 0 \\ 0 \end{pmatrix} \tag{2.78}$$

where A_i and $\tilde{A}_i$ are respectively D-dimensional row and column vectors. Indeed, in this way, their contraction gives rise a scalar.

$$A_y = \frac{1}{\sqrt{3}} \begin{pmatrix} 0 & 1 & 0 \end{pmatrix} \qquad \tilde{A}_y = \begin{pmatrix} 0 \\ 1 \\ 0 \end{pmatrix} \tag{2.79}$$

$$A_z = \frac{1}{\sqrt{3}} \begin{pmatrix} 0 & 0 & 1 \end{pmatrix} \qquad \tilde{A}_z = \begin{pmatrix} 0 \\ 0 \\ 1 \end{pmatrix} \tag{2.80}$$

Again, if we want to put them in the form (2.43) such that the condition (2.45) are satisfied, we have:

$$\Lambda = \frac{1}{\sqrt{3}} \begin{pmatrix} 1 & 0 & 0 \\ 0 & 1 & 0 \\ 0 & 0 & 1 \end{pmatrix} \qquad \tilde{\Lambda} = 1 \tag{2.81}$$

Finally, the Γ_i and $\tilde{\Gamma}_i$ are:

$$\Gamma_x = \begin{pmatrix} 1 & 0 & 0 \end{pmatrix} \qquad \tilde{\Gamma}_x = \begin{pmatrix} 1 \\ 0 \\ 0 \end{pmatrix} \tag{2.82}$$

$$\Gamma_y = \begin{pmatrix} 0 & 1 & 0 \end{pmatrix} \qquad \tilde{\Gamma}_y = \begin{pmatrix} 0 \\ 1 \\ 0 \end{pmatrix} \tag{2.83}$$

$$\Gamma_z = \begin{pmatrix} 0 & 0 & 1 \end{pmatrix} \qquad \tilde{\Gamma}_z = \begin{pmatrix} 0 \\ 0 \\ 1 \end{pmatrix} \tag{2.84}$$

2.5 Characterization of the phases by their projective representation

Let's see how nontrivial SPT order is manifested in the AKLT model:

$$H_{AKLT} = J \sum_i \left[\mathbf{S}_i \cdot \mathbf{S}_{i+1} - \frac{1}{3} (\mathbf{S}_i \cdot \mathbf{S}_{i+1})^2 \right] \tag{2.85}$$

which is invariant under the SU(2) spin rotation symmetry generated by S_x, S_y and S_z. In the previous section we've show how get MPS representation in a basis given by (2.73). In this section we're going to use another equivalent MPS representation of AKLT state that is:

$$A_x = X, \qquad A_y = Y \qquad A_z = Z \tag{2.86}$$

where now the basis states are:

$$|x\rangle = \frac{1}{\sqrt{2}}(|+\rangle - |-\rangle) \qquad |y\rangle = -\frac{i}{\sqrt{2}}(|+\rangle + |-\rangle) \qquad |z\rangle = -|0\rangle \tag{2.87}$$

that are egual to 2.73 up to a minus sign. Obviously, this representation is not in the canonical form but, for our purpose, it does not matter. We can compute the symmetry tranformation matrices $M(g)$ acting on A_i. For example, under the rotation on z axis for an angle α, the matrices change into:

$$\begin{aligned} A_x &\longrightarrow \tilde{A}_x = \cos(\alpha/2) X - Y \sin(\alpha/2) \\ A_y &\longrightarrow \tilde{A}_x = \cos(\alpha/2) Y + Y \sin(\alpha/2) \\ A_z &\longrightarrow \tilde{A}_z = Z \end{aligned} \tag{2.88}$$

from which we can see that $M_z(\alpha) = e^{i\frac{\alpha}{2}Z}$. So, for a generic rotation we can write:

$$M(\alpha) = e^{\frac{i}{2}(\alpha_x X + \alpha_y Y + \alpha_z Z)} \tag{2.89}$$

let us to re-define Pauli's matrices as $\sigma_1 = X$, $\sigma_2 = Y$, $\sigma_3 = Z$ and introduce $\tau_i = \frac{i\sigma_i}{2}$ and the vector $(\alpha_x, \alpha_y, \alpha_z) = \boldsymbol{\alpha} = \alpha\ \hat{\mathbf{n}}$, [1] then:

$$\begin{aligned} M(\alpha) = e^{\frac{i\alpha}{2}(n_x X + n_y Y + n_z Z)} = e^{\sigma_i \alpha^i} = \sum_{k=0}^{\infty} \frac{1}{k!} (\sigma_i \alpha^i)^k = \\ = \cos\left(\frac{1}{2}|\boldsymbol{\alpha}|\right) + i \frac{\sigma_i \alpha^i}{|\boldsymbol{\alpha}|} \sin\left(\frac{1}{2}|\boldsymbol{\alpha}|\right) \end{aligned} \tag{2.90}$$

[1] $\hat{\mathbf{n}}$ is an oriented unit vector with origin in the center of rotation and directed along the axis of rotation.

The most important property of M(g) is that it forms a non-trivial projective representation of the SO(3) group which can be seen from 2π rotations using the expression (2.90) just deduced:

$$M(2\pi) = -\mathbb{I}_2 \tag{2.91}$$

A rotation of 2π in the $SO(3)$ group representation gives rise to the identity operation while the matrix representation $M(g)$ (that is nothing but $SU(2)$ group [2]) Therefore a sign factor $\omega(g_1, g_2)$ occur in composing $M(g_1)$ and $M(g_2)$. For example:

$$M(\boldsymbol{\pi})M(\boldsymbol{\pi}) = -M(\mathbf{0}). \tag{2.92}$$

Then $M(\boldsymbol{\alpha})$, generated by spin operators form a projective representation of the $SO(3)$ rotation symmetry. In particular, let us consider the symmetry operation given by π-rotation about α-axis ($\alpha = x, y, z$). A way to find the projective representation is given by (2.46). It is easy to check that the matrix we are looking for is σ_α. For example, let us to fix $\alpha = z$, then:

$$\begin{aligned} T_z(\sigma_z) &= \sum_{ij} \left(e_{ij}^{i\pi S^z} \Gamma_i \Lambda \sigma_z \Lambda . \Gamma_j^\dagger \right) \\ &= -\frac{1}{2}\left[\Gamma_x \sigma_z \Gamma_x^\dagger + \Gamma_y \sigma_z \Gamma_y^\dagger - \Gamma_z \sigma_z \Gamma_z^\dagger \right] = \\ &= -\frac{1}{3}\left[\sigma_x \sigma_z \sigma_x + \sigma_y \sigma_z \sigma_y + \sigma_z \sigma_z \sigma_z \right] \\ &= \frac{1}{3}\left[\sigma_z + \sigma_z + \sigma_z \right] = \sigma_z \end{aligned} \tag{2.93}$$

Comparing this result with (2.46) it is clear that:

$$e^{i\theta} = 1 \qquad \longrightarrow \qquad \theta = 0 \tag{2.94}$$

Furthermore, we know that Pauli's matrices have the following commutation and anti-commutation relationship:

$$\left[\sigma_i, \sigma_j \right] = 2i\epsilon^{ijk}\sigma_k \qquad and \qquad \left\{ \sigma_i, \sigma_j \right\} = 2\delta_{ij} \tag{2.95}$$

in particular, when $i \neq j$ and remember how we defined Φ from (2.51), we have:

$$\sigma_i \sigma_j = -\sigma_j \sigma_i = e^{i\pi} \sigma_j \sigma_i = e^{i\Phi} \sigma_j \sigma_i \qquad \longrightarrow \qquad \Phi = \pi \tag{2.96}$$

[2]The $SU(2)$ group of matrices constitutes the lowest dimensional non-trivial faithful irreducible unitary representation of the rotation group, which is thereby named its fundamental representation or spinor representation of the rotation group. It is simply connected, though the vector representation $SO(3)$ is not. Owing to this SU(2) is said to be the universal covering of SO(3).

Then the AKLT state is characterized by $\theta = 0$ and $\Phi = \pi$. They cannot change without facing a phase transition so they remain the same in the whole Haldane phase.
Let us now show the MPS representation of the dimer state. It is not site independent state, so we will find two different representation. From the equation (2.42) we know that:

$$\sum_j \Omega_{ij}(g) A_j = e^{i\theta_\Omega(g)} R_\Omega^\dagger(g) A_i R_\Omega(g) \tag{2.97}$$

So, in the canonical form, they read:

$$\sum_j \Omega_{ij}(g) \Gamma_j = e^{i\theta_\Omega(g)} \tilde{R}_\Omega^\dagger(g) \Gamma_i R_\Omega(g) \tag{2.98}$$

$$\sum_j \Omega_{ij}(g) \tilde{\Gamma}_j = e^{i\theta_\Omega(g)} R_\Omega^\dagger(g) \tilde{\Gamma}_i \tilde{R}_\Omega(g) \tag{2.99}$$

where the projective representations R_Ω and $\tilde{R}_\Omega$ are:

$$\begin{aligned} R_x &= \begin{pmatrix} 1 & 0 & 0 \\ 0 & -1 & 0 \\ 0 & 0 & -1 \end{pmatrix} \qquad \tilde{R}_x = 1 \\ R_y &= \begin{pmatrix} -1 & 0 & 0 \\ 0 & 1 & 0 \\ 0 & 0 & -1 \end{pmatrix} \qquad \tilde{R}_y = 1 \\ R_z &= \begin{pmatrix} -1 & 0 & 0 \\ 0 & -1 & 0 \\ 0 & 0 & 1 \end{pmatrix} \qquad \tilde{R}_z = 1 \end{aligned} \tag{2.100}$$

The first matrices correspond to the rotation of a π-angle around x,y, and z axes of SO(3) group. It is easy to see that a generic element of this group can be written

$$R(\alpha) = e^{i\alpha^i J_i} \tag{2.101}$$

where the generators J_i coincide with spin matrices (2.74):

$$J_x = \begin{pmatrix} 0 & 0 & 0 \\ 0 & 0 & -i \\ 0 & i & 0 \end{pmatrix} \qquad J_y = \begin{pmatrix} 0 & 0 & i \\ 0 & 0 & 0 \\ -i & 0 & 0 \end{pmatrix} \qquad J_z = \begin{pmatrix} 0 & -i & 0 \\ i & 0 & 0 \\ 0 & 0 & 0 \end{pmatrix} \tag{2.102}$$

Furthermore, the commutation relations are:

$$\big[R_i, R_j\big] = 0 \tag{2.103}$$

thus this is the trivial projective representation with $\theta = 0$ and $\Phi = 0$ which characterized the dimer state and remain the same for the whole dimer phase.

2.6 New non-local order parameters

As it is shown in [24], it is possible using Non-Local Order Parameters to detect different symmetric phases. We have previously seen that NLOP has the form (2.47):

$$\mathbf{O}_{\Omega}(O^A, O^B) = \lim_{n\to\infty} \langle\Psi|\, O^A(1)\Big(\prod_{k=2}^{n-1}\Omega(k)\Big)O^B(n)\,|\Psi\rangle \tag{2.104}$$

where O^A and O^B are local operators while $\Omega(k)$ is the on-site symmetry transformation. We also said that we need another non-trivial symmetry $\Omega'(k)$ which commutes with $\Omega(k)$:

$$\big[\Omega, \Omega'\big] = 0 \tag{2.105}$$

A possible choice could be $\Omega = e^{i\pi J^z}$ and $\Omega' = e^{i\pi J^\alpha}$ with $\alpha = x, y$. The local operators O^A and O^B are matrices 3×3 and each of them can be expressed as linear combination of elements, shown in figure 2.11, belonging to basis of a 9-dimensional vector space.

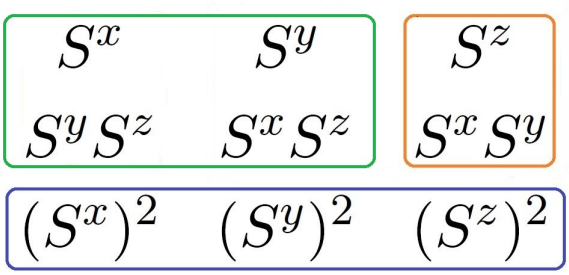

Figure 2.11: Basis of 9-dimensional vector space. Operators in the orange rectangle are odd under Ω' both for $\alpha = x, y$. Instead, operators in the blue rectangle are even under Ω' both for $\alpha = x, y$. The parity of operators inside the green rectangle depends on the choice of $\alpha = x, y$

As it is stressed in figure above, we can separate those operators into three classes based on how they change under Ω' transformation:

1. Class of operators that are odd under Ω' transformation for both $\alpha = x, y$ (in orange rectangle in figure 2.11). If we choose operators of this class ($\sigma = \pi$) to evaluate NLOP, they will certainly, vanish in the dimmer phase ($\Phi = 0$).

2. Class of operators that are even under Ω' transformation for both $\alpha = x, y$ (in blue rectangle in figure 2.11). If we choose operators of this class ($\sigma = 0$) to evaluate NLOP, they will certainly vanish in the Haldane phase ($\Phi = \pi$).

3. Class of operators that can be even or odd under Ω' depending on the axis of rotation chosen $\alpha = x, y$ (in the green rectangle in figure 2.11). If we choose operators of this class to evaluate NLOP, they certainly vanish in both Haldane and dimer phases.

In the other cases the operators have to be calculated: for example, an operator, which belongs to the first class, has to be calculate in the Haldane phase because it will be generally non-zero, but it could accidentally vanish. The same holds for an operator of the second class in the dimer state.
Let's evaluate NLOPs in the AKLT point. Hence we have to evaluate the following traces:

$$\mathbf{O}_\Omega(O^A, O^B) = Tr\big[\Lambda^2 R_\Omega^\dagger \tilde{O}^A\big] \cdot Tr\big[\Lambda^2 R_\Omega \tilde{O}^B\big] \tag{2.106}$$

where

$$\tilde{O}^A = \sum_{ij} O^A_{ij} \Gamma_i^\dagger \Lambda^2 \Gamma_j \qquad and \qquad \tilde{O}^B = \sum_{ij} O^B_{ij} \Gamma_i \Lambda^2 \Gamma_j^\dagger \tag{2.107}$$

and $R_\Omega = R_z = \sigma_z$. Let us to verify that choosing O^A and O^B within the second class, the NLOPs vanish. For simplicity we set $O^A = O^B = (S^z)^2$, thus:

$$\begin{aligned} \mathbf{O}_z((S^z)^2, (S^z)^2) &= \frac{1}{4} Tr\left[\sigma_z \left(\sum_{ij} (S^z)^2_{ij} \Gamma_i^\dagger \Lambda^2 \Gamma_j \right)\right] \cdot Tr\left[\sigma_z \left(\sum_{ij} (S^z)^2_{ij} \Gamma_i \Lambda^2 \Gamma_j^\dagger \right)\right] \\ &= \frac{1}{4} Tr\left[\frac{2\sigma_z}{3}\mathbb{I}\right] \cdot Tr\left[\frac{2\sigma_z}{3}\mathbb{I}\right] = 0 \end{aligned} \tag{2.108}$$

It is easy to show that, in the same way, the other NLOPs (obtained choosing other operators of the second class) are zero:

$$\mathbf{O}_z((S^x)^2, (S^x)^2) = \mathbf{O}_z((S^y)^2, (S^y)^2) = 0 \tag{2.109}$$

We said that if we choose operators from the third class, the corresponding NLOP has to vanish too. Indeed, let $O^A = O^B = S^y S^z$, we find:

$$\begin{aligned} \mathbf{O}_z((S^y S^z), (S^y S^z)) &= \frac{1}{4} Tr\left[\sigma_z \left(\sum_{ij} (S^y S^z)_{ij} \Gamma_i^\dagger \Lambda^2 \Gamma_j \right)\right] \cdot Tr\left[\sigma_z \left(\sum_{ij} (S^y S^z)_{ij} \Gamma_i \Lambda^2 \Gamma_j^\dagger \right)\right] \\ &= \frac{1}{4} Tr\left[i\frac{\sigma_z \sigma_x}{3}\right] \cdot Tr\left[-i\frac{\sigma_z \sigma_x}{3}\right] = 0 \end{aligned} \tag{2.110}$$

In the same way, it can be shown that:

$$\mathbf{O}_z((S^x S^z), (S^x S^z)) = \mathbf{O}_z((S^x), (S^x) = \mathbf{O}_z((S^y), (S^y) = 0 \tag{2.111}$$

Conversely, with operators of the first class we can get NLOPs that don't vanish. Indeed:

$$\begin{aligned}\mathbf{O}_z((S^xS^y),(S^xS^y)) &= \frac{1}{4}Tr\left[\sigma_z\left(\sum_{ij}(S^xS^y)_{ij}\Gamma_i^\dagger\Lambda^2\Gamma_j\right)\right]\cdot Tr\left[\sigma_z\left(\sum_{ij}(S^xS^y)_{ij}\Gamma_i\Lambda^2\Gamma_j^\dagger\right)\right] \\ &= \frac{1}{4}Tr\left[i\frac{\sigma_z\sigma_z}{3}\right]\cdot Tr\left[-i\frac{\sigma_z\sigma_z}{3}\right] = \frac{1}{9}\end{aligned} \tag{2.112}$$

Similarly if we use $O^A = O^B = S^z$, we get:

$$\mathbf{O}_z((S^z),(S^z)) = -\frac{4}{9} \tag{2.113}$$

For the dimer state, we have to remember that it is not translational invariant and it has not a site-independent MPS representation as showed before. Therefore, we can get different values of NLOPs depending where we place the local operator O^A and O^B. In particular, we can place them both on even sites or both on odd sites, but also O^A on an even site and O^B on an odd site (and vice versa). Consequently, we have four different expression for non-local order parameters.

Again, there are classes of local operators that, if they were used to build NLOPs, give rise to zero value of NLOPs. In this case (dimer state), they are the first and the third class. Indeed, for the first class, we get:

$$\mathbf{O}_z((S^xS^y),(S^xS^y)) = \mathbf{O}_z((S^z),(S^z)) = 0 \tag{2.114}$$

whereas for the third class:

$$\mathbf{O}_z((S^yS^z),(S^yS^z)) = \mathbf{O}_z((S^xS^z),(S^xS^z)) = \mathbf{O}_z((S^y),(S^y)) = \mathbf{O}_z((S^x),(S^x)) = 0 \tag{2.115}$$

Clearly, these results are independent of where we place the local operator. If we calculate NLOPs built with local operator of the second class, they can be non-zero; this time the exact value obtained depends on where we place O^A and O^B. We don't show the calculations for each case but we just summarize the results in the table below 2.6

	$\mathbf{O}_z((S^x)^2,(S^x)^2)$	$\mathbf{O}_z((S^x)^2,(S^x)^2)$	$\mathbf{O}_z((S^x)^2,(S^x)^2)$
Even-Odd	$\frac{4}{9}$	$\frac{4}{9}$	$\frac{4}{9}$
Odd-Even	$\frac{4}{9}$	0	0
Even-Even	$-\frac{4}{9}$	0	0
Odd-Odd	$-\frac{4}{9}$	0	0

Chapter 3

Entanglement and the Quantum Fisher Information

In this chapter we discuss correlation and entanglement in many-body systems. We start from introducing the concepts of independence and correlation in probability theory, which leads to understanding of the concepts of entropy and mutual information, which are of vital importance in modern information theory.

The concept of correlation is used in almost every branch of sciences. Intuitively, correlations describe the dependence of certain properties for different parts of a composite object. If these properties of different parts are independent of each other, then we say that there do not exist correlations between (or among) them. For instance, in many-body physics, people usually characterize correlations in terms of correlation functions $\langle O_i O_j \rangle - \langle O_i \rangle \langle O_j \rangle$, where O_i is some observable on the site i, and $\langle \cdot \rangle$ denotes the expectation value with respect to the quantum state of the system. The behavior of these correlation functions gives a lot of useful information such as the correlation length. In this chapter we would like to treat correlation in a more formal way. It will later become clearer that doing so helps with a better understanding of manybody physics. In other words, there is something beyond just correlation function to look at, which turns out to provide new information and characterization of some rather interesting new physical phenomena, such as the topological phase of matter.

We start looking at correlation in terms of elementary probability theory. First of all it is the formal mathematical language of characterizing the concept of independence and correlation. This formal language will then be further linked to the concept of entropy and mutual information, which are key concepts in information theory. Physicists are indeed familiar with the concept of entropy, which is in some sense a measure of how chaotic a system is. By looking at it slight differently, it is then a measure of how much

information the system carries. One important success in quantum information is the development of the theory of entanglement. 'Entanglement' is widely heard nowadays but what we would like to emphasize here is that there is nothing mysterious, in a sense that almost all quantum many-body systems are entangled. We would also like to introduce the theory of entanglement in a more formal manner, which naturally follows the information theoretic point of view. We will start our discussion from the simplest case, where we only consider two objects and their independence/correlation. We look at the classical correlation case first, and then move to the case of quantum systems, where the concept of entanglement can be naturally introduced.
Following up all that, we move into looking at the theory of Ficher Information, from both the classical and the quantum point of view. In particular, in order to understand the role that the Quantum Fisher Information plays in quantum scenario, we will provide a criterion that allows us to detect k-partite entanglement.

3.1 Information and correlation in classical probability theory

We start from looking at the simplest case: two independent objects A and B. Conventionally in literature, we usually deal with two people, Alice and Bob, performing some joint experiments. In this case, assume that Alice has d_A possible outcomes and let us denote the set of these possible outcomes by:

$$A = \{a_0, a_1, a_2, \cdots, \quad a_{d_A-1}\} \tag{3.1}$$

Analogously, let's assume that Bob has total d_B possible outcomes, with:

$$B = \{b_0, b_1, b_2, \cdots, \qquad b_{d_B-1}\} \tag{3.2}$$

denotes the set of these possible outcomes. A joint possible outcome for Alice and Bob is (a_i, b_m). All such joint possible outcomes form a set that we denote by $A \times B$, which is nothing but the Cartesian product of these two sets A and B :

$$\begin{aligned} A \times B = \Big\{ & (a_0, b_0), (a_0, b_1), \cdots, (a_0, b_m), \cdots, (a_0, b_{d_B-1}), \\ & (a_1, b_0), (a_1, b_1), \cdots, (a_1, b_m), \cdots, (a_1, b_{d_B-1}), \\ & \cdots \qquad \cdots \qquad \cdots \\ & (a_i, b_0), (a_i, b_1), \cdots, (a_i, b_m), \cdots, (a_i, b_{d_B-1}), \\ & \cdots \qquad \cdots \qquad \cdots \\ & (a_{d_A-1}, b_0), (a_{d_A-1}, b_1), \cdots, (a_{d_A-1}, b_m), \cdots, (a_{d_A-1}, b_{d_B-1}) \Big\} \end{aligned} \tag{3.3}$$

The joint probability distribution $P_{AB}(a_i, b_m)$ for the joint experiment Alice and Bob perform needs to satisfy the following conditions

$$P_{AB}(a_i, b_m) \geq 0, \tag{3.4}$$

$$\sum_{i=0}^{d_A-1} \sum_{m=0}^{d_B-1} P_{AB}(a_i, b_m) = 1. \tag{3.5}$$

The probability for Alice to get the outcome $a_i \in A$ is then:

$$P_A(a_i) = \sum_{m=0}^{d_B-1} P_{AB}(a_i, b_m). \tag{3.6}$$

In the same, the probability for Bob to get the outcome $b_m \in B$ is then:

$$P_B(b_m) = \sum_{i=0}^{d_A-1} P_{AB}(a_i, b_m). \tag{3.7}$$

For example, a simple case could be that Alice and Bob have only two different possible outcomes:

$$A = \{a_0, a_1\} \qquad and \qquad B = \{b_0, b_1\} \tag{3.8}$$

so the Cartesian products is:

$$A \times B = \big\{(a_0, b_0), (a_0, b_1), (a_1, b_0), (a_1, b_1)\big\} \tag{3.9}$$

We want to undestand under which circumstance a joint probability distribution $P_{AB}(a_i, b_m)$ has some correlation between the outcomes of Alice and Bob. When Bob obtains the outcome b_m, the probability for Alice to get the outcome a_i is:

$$P_{A|B}(a_i, b_m) = \frac{P_{AB}(a_i, b_m)}{P_B(b_m)} \tag{3.10}$$

which is called the conditional probability distribution for A. Similarly one can write down the conditional probability distribution $P_{B|A}(a_i, b_m)$ for B. That is, when Alice gets the outcome a_i, the conditional probability for Bob to get the outcome b_m is

$$P_{B|A}(a_i, b_m) = \frac{P_{AB}(a_i, b_m)}{P_B(b_m)} \tag{3.11}$$

Now suppose that the joint distribution $P_{A|B}(a_i, b_m)$ has no correlation at all, then from Alice's point of view, her outcome is independent of Bob's outcome. In other words, whatever Bob's outcome is, the probability distribution of Alice's outcome should be just the same. This means that the conditional probability should not depend on b_m, i.e.

$$P_{A|B}(a_i, b_m) = P_{A|B}(a_i, b_n) \qquad \forall i, m, n. \tag{3.12}$$

Similary, from for Bob we should have:

$$P_{B|A}(a_i, b_m) = P_{B|A}(a_j, b_m) \qquad \forall i, j, m. \tag{3.13}$$

We can prove that these equations imply that the joint probability distribution equals the product of the probability distributions of each party and vice versa:

$$P_{AB}(a_i, b_m) = P_A(a_i)P_B(b_m) \qquad \forall i, m. \tag{3.14}$$

In fact, from (3.13) we have:

$$P_{B|A}(a_i, b_m) = P_{B|A}(a_j, b_m) = \frac{P_{AB}(a_j, b_m)}{P_A(a_j)} \tag{3.15}$$

and this has to hold for every j. Thus we can write:

$$P_{B|A}(a_i, b_m) = \frac{\sum_{j=0}^{d_A-1} P_{AB}(a_j, b_m)}{\sum_{j=0}^{d_A-1} P_A(a_j)} = P_B(b_m) \tag{3.16}$$

Inserting (3.16) inyo (3.11) we will get (3.14).
We can summarize these results saying that the following statements are equivalent:

- There is no correlation in the joint probability distribution $P_{AB}(a_i, b_m)$.
- The probability for Bob's outcome is independent of Alice's outcome.
- The probability for Alice's outcome is independent of Bob's outcome.
- The joint probability equals the product of probabilities for the two parties:

$$P_{AB}(a_i, b_m) = P_A(a_i)P_B(b_m) \qquad \forall i, m. \tag{3.17}$$

3.1.1 Correlation fuctions

When the above equivalent conditions do not hold, then there must be correlation between the outcomes of Alice and Bob. We first introduce a random variable $X(A)$, which is a real function whose domain is the set of all possible outcomes of Alice. The average value of this random variable can then be given by:

$$E(X) = \sum_{i=0}^{d_A-1} P_A(a_i)X(a_i) \tag{3.18}$$

Sometimes for simplicity one will write:

$$E(X) = \sum_{x \in X} P(x)x \tag{3.19}$$

where the sum runs over all possible values in X, and indeed $P(x) = P(X(a_i) = x) = P_A(a_i)$. We assume that there is a one-to-one correspondence between a_i and x. Similarly, a random variable $Y(B)$, a real function whose domain is the set of all possible outcomes of Bob, has the average value:

$$E(Y) = \sum_{m=0}^{d_B-1} P_B(b_i)Y(b_i) = \sum_{y\in Y} P(y)y \tag{3.20}$$

Let us write the joint probability distribution

$$P_{AB}(a_i, b_m) = P(X(a_i) = x, Y(b_m) = y) = P(x, y) \tag{3.21}$$

then the average value of the random variable $X \times Y$ is:

$$E(X, Y) = \sum_{x\in X}\sum_{y\in Y} P(x)xP(y)y. \tag{3.22}$$

As an example, again consider that $A = \{a_0, a_1\}$ and $B = \{b_0, b_1\}$. Choose the random variables $X(a_0) = Y(b_0) = 0$ and $X(a_1) = Y(b_1) = 1$. A variable like these is called a bit that is a random variable with only two possible values 0 or 1. Then the possible values of $X \times Y$ will be $\{(0, 0), (0, 1), (1, 0), (1, 1)\}$.
The correlation fuction is defined as:

$$C(X, Y) = E(X, Y) - E(X)E(Y) \tag{3.23}$$

One can immediately see that if the joint distribution $P_{AB}(a_i, b_m)$ has no correlation (that is $P(x, y) = P(x)P(y)$), then $E(X, Y) = E(X)E(Y)$ and $C(X, Y) = 0$. Futhermore, the converse is also true, hence $C(X, Y) = 0$ implies that $P_{AB}(a_i, b_m) = P_A(a_i)P_B(b_m)$.
We can summarize these observations saying that: a joint probability distribution P_{AB} does not have correlation if and only if $C(X, Y) = 0, \quad \forall X, Y$.

3.1.2 Mutual Information

We have just seen how correlation function is useful to give some information about the correlation in a system formed by two subsystems. In the context of information theory, there is a concept, introduced by Shannon, that nicely quantifies the degree of correlation between the two subsystems. This concept is called the mutual information, which, for two random variables, is defined as:

$$I(X, Y) = \sum_{x\in X}\sum_{y\in Y} P(x, y)\log\left(\frac{P(x, y)}{P(x)P(y)}\right). \tag{3.24}$$

Intuitively, mutual information measures the information that X and Y share. Or in other words, how correlated they are in a sense that how much knowing one of these two variables reduces the uncertainty about knowing the other. For instance, if X and Y are independent, then knowing X does not give any information about Y and vice versa, so their mutual information should be zero. This can be easy verify just requiring that equation (3.14) holds, then:

$$P(x,y) = P(x)P(y) \qquad \Longrightarrow \qquad I(X,Y) = 0. \tag{3.25}$$

On the other hand, if X and Y are the same (i.e. the case of "perfect correlation"), so all information carries by X is shared with Y. In this case, the mutual information should be the same as the uncertainty contained in X (or Y) alone.
In order to clarify what "uncertainty contained in X" means, we know that in physics uncertanty is quantify by entropy. Let us introduce Shannon's entropy defined as:

$$S(X) = -\sum_{x\in X} P(x)\log P(x) \tag{3.26}$$

where, just for definition, the base of log is 2. The case of perfect correlation, mathematically means:

$$P(x,y) = \begin{cases} 0 & if \quad x \neq y \\ P(x) = P(y) & otherwise \end{cases} \tag{3.27}$$

then

$$I(X,Y) = \sum_{x\in X}\left(\sum_{y\in Y} P(x,y)\right)\log\left(\frac{P(x)}{P(x)P(y)}\right) = \sum_{x\in X} P(x)\log\left(\frac{1}{P(x)}\right) = S(X). \tag{3.28}$$

where we used (3.6) written as:

$$P(x) = \sum_{y\in Y} P(x,y) \tag{3.29}$$

So we essentially got what we expected: the mutual information is the same as the uncertainty contained in X alone. Let's consider the case in which the random variable X is a bit and the probability distribution is given by:

$$P(0) = p, \qquad and \qquad P(1) = 1-p \tag{3.30}$$

So the Shannon's entropy is:

$$S(p) = -p\log p - (1-p)\log(1-p) \tag{3.31}$$

The plot of this function is shown in Fig 3.1 where we can see that it vanishes for $p = 0$ or $p = 1$ and it has a maximum at $p = 1/2$. Here, indeed, one has the most uncertainty: the probability of getting values 0 and 1 is just half and half.

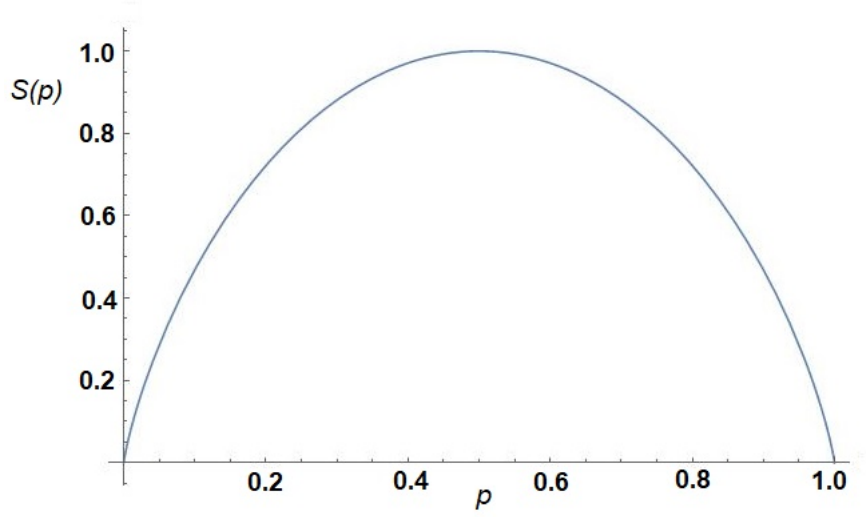

Figure 3.1: Shape of binary entropy function $S(p)$.

The Shannon's entropy for the joint probability distribution of two random variables is:

$$S(X,Y) = -\sum_{x\in X}\sum_{y\in Y} P(x,y)\log P(x,y) \tag{3.32}$$

We can write quantity $S(X|Y=\tilde{y})$, i.e. the entropy of X conditional on the variable of Y taking the value $\tilde{y}$, as:

$$S(X|Y=\tilde{y}) = -\sum_{x\in X} P(x|\tilde{y})\log P(x|\tilde{y}) \tag{3.33}$$

Hence, the total conditional entropy $S(X|Y)$ will be:

$$\begin{aligned} S(X|Y) &= \sum_{y\in Y} P(y)H(X|Y=y) = -\sum_{y\in Y}\sum_{x\in X} P(y)P(x|y)\log P(x|y) \\ &= -\sum_{y\in Y}\sum_{x\in X} P(x,y)\log\left(\frac{P(x,y)}{P(y)}\right) \end{aligned} \tag{3.34}$$

where we used (3.10) written as:

$$P(x|y) = \frac{P(x,y)}{P(y)} \tag{3.35}$$

In term of all these quantities the mutual information (3.24) can be written in a very

significant form:

$$\begin{aligned} I(X,Y) &= \sum_{x\in X}\sum_{y\in Y} P(x,y)\log P(x,y) - \sum_{x\in X}\left(\sum_{y\in Y} P(x,y)\right)\log P(x) - \sum_{y\in Y}\left(\sum_{x\in X} P(x,y)\right)\log P(y) \\ &= \sum_{x\in X}\sum_{y\in Y} P(x,y)\log P(x,y) - \sum_{x\in X} P(x)\log P(x) - \sum_{y\in Y} P(y)\log P(y) \\ &= S(X) + S(Y) - S(X,Y) \end{aligned} \tag{3.36}$$

In the same way, one can prove other relations such as:

$$\begin{aligned} I(X,Y) &= S(X) - S(X|Y) = S(Y) - S(Y|X) \\ &= S(X,Y) - S(X|Y) - S(Y|X) \end{aligned} \tag{3.37}$$

which are all intuitively summarized in the figure 3.2.

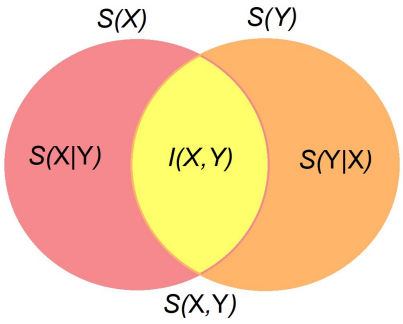

Figure 3.2: $S(X)$ and $S(Y)$ are plotted as the regions inside two circles, and the mutual information $I(X,Y)$ is just their overlap (in yellow). The quantities $S(X|Y)$ and $S(Y|X)$ are also illustrated.

3.2 Quantum Entanglement

In quantum mechanics, the state of a quantm system is represented by a normalized vector in the Hilbert space. Hence if $|\psi_1\rangle$ and $|\psi_2\rangle$ are two orthogonal quantum states, then any superposition of them is also a quantum state:

$$|\psi\rangle = c_1|\psi_1\rangle + c_2|\psi_2\rangle \tag{3.38}$$

with c_1 and c_2 are complex numbers satisfying $|c_1|^2 + |c_2|^2 = 1$. This famous propery is called superposition principle of quantum states which is a foundamental feature of quantum mechanics. Furthermore, at every state $|\psi\rangle$ is always possible to associate a projection operator $\mathbb{P}_\psi = |\psi\rangle\langle\psi|$ satisfying the following properties:

1. $\mathbb{P}_\psi$ is bounded.
2. $\mathbb{P}_\psi$ is Hermitian.
3. $\mathbb{P}_\psi$ is positive (that is $\langle\alpha|\,\mathbb{P}_\psi\,|\alpha\rangle \geq 0$, $\forall\,|\alpha\rangle \in H$).
4. $\mathrm{Tr}\big[\mathbb{P}_\psi\big] = 1$.
5. $\mathbb{P}_\psi^2 = \mathbb{P}_\psi$.

It is also called density matrix and denoted by ρ_ψ. When a quantum measurement of an observable (i.e. a Hermitian operator) M is made on the system, we will get one of the eigenvalues of the operator M. We know that M can be written as:

$$M = \sum_i c_i\,|\phi_i\rangle\,\langle\phi_i| \tag{3.39}$$

where each c_i and $|\phi_i\rangle$ are the eigenvalues and eigenvectors of M respectively.
So the probability of getting the value c_i is:

$$p_i = \langle\psi|\phi_i\rangle\,\langle\phi_i|\psi\rangle \tag{3.40}$$

Sometime we cannot establish a priori that a system is in a well defined state, but we can only say that it can be found in a state chosen from a set of compatible states $\big\{\,|\psi_k\rangle\,\big\}$. Let us suppose that p_k is the probability to find the system in the state $|\psi_k\rangle$, obviously the following conditions holds:

$$0 \leq p_k \leq 1, \quad \textit{and} \quad \sum_k p_k = 1 \tag{3.41}$$

In this case one says that the system is in a mixed state. The set $\big\{\,|\psi_k\rangle\,\big\}$ is called statistical ensemble and define a density operator given by:

$$\rho = \sum_k p_k\,|\phi_k\rangle\,\langle\phi_k| \tag{3.42}$$

It esay to check that also ρ satisfy the properties of $\mathbb{P}_\psi$ except for the last one.
In general $\rho \neq \rho^2$ while the following theorem holds:

$$\rho = \rho^2 \quad \Longleftrightarrow \quad \rho = |\psi\rangle\,\langle\psi| \quad \text{(i.e. } \rho \text{ is a pure state)} \tag{3.43}$$

Now we introduce a measure of uncertainty for a state ρ, i.e. the von Neumman entropy

$$S(\rho) = -\mathrm{Tr}\big[\rho\log\rho\big] \tag{3.44}$$

which is a generalization of the Shannon entropy. Indeed, from the spectral decomposition $\rho = \sum_k p_k\,|\phi_k\rangle\,\langle\phi_k|$, we have $S(\rho) = -\sum_k p_k \log p_k$.

3.2.1 Bipartite quantum system and Shmidt decomposition

Now we consider the case of composite quantum system, formed by two subsystems, one for Alice and the other for Bob. We denote Alice's Hilbert by H_A (whose dimension is d_A with an orthonormal basis $\{|i_A\rangle\}$) and Bob's Hilber space by H_B (whose dimension is d_B with an orthonormal basis $\{|m_B\rangle\}$). The corresponding total Hilbert space, denoted by H_{AB}=$H_A \otimes H_B$ (where $\otimes$ is the tensor product of two spaces), will have a basis which is the Cartesian product of $\{|i_A\rangle\}$) and $\{|m_B\rangle\}$ which is of dimension $d_A d_B$. Hence, a pure state $|\psi_{AB}\rangle \in H_{AB}$ can be written as

$$|\psi_{AB}\rangle = \sum_{i=0}^{d_A-1} \sum_{m=0}^{d_B-1} c_{im} |i_A m_B\rangle \tag{3.45}$$

where $|i_A m_B\rangle = |i_A\rangle \otimes |m_B\rangle$. The way to find the quantum state ρ_B for the system B from the state $|\psi_{AB}\rangle$ is to trace over the subsystem A:

$$\rho_B = \mathrm{Tr}_A\big[\, |\psi_{AB}\rangle \langle\psi_{AB}| \,\big] = \sum_{i=0}^{d_A-1} \langle i_A|\psi_{AB}\rangle \langle\psi_{AB}|i_A\rangle = \sum_{i=0}^{d_A-1} \sum_{m,n=0}^{d_B-1} c_{im} c_{in}^* |m_B\rangle \langle n_B| \tag{3.46}$$

The density matrix ρ_B is called the reduced matrix for the system B.
By choosing carefully the basis of subsystems A and B, one can write the state $|\psi_{AB}\rangle$ in an important standard form, namely, the Schmidt decomposition:

$$|\psi_{AB}\rangle = \sum_{k=1}^{r} \sqrt{\lambda_k} |\psi_k\rangle_A |\phi_k\rangle_B \tag{3.47}$$

where

$$\lambda_k > 0, \quad \sum_{k=1}^{r} \lambda_k = 1, \quad r \leq min\{d_A, d_B\}, \quad \text{and} \quad \langle\psi_i|\psi_j\rangle = \langle\phi_j|\phi_i\rangle = \delta_{ij} \tag{3.48}$$

In order to prove this result, we suppose that $d = d_A = d_B$. From the singular value decomposition we know that a matrix can be deconposed like $C = UDV$ where U and V are unitary matrices and D is diagonal. Then, we can write $c_{im} = \sum_k u_{ik} d_{kk} v_{km}$ and we get:

$$\begin{aligned} |\psi_{AB}\rangle &= \sum_i \sum_m c_{im} |i_A\rangle \otimes |m_B\rangle = \sum_k d_{kk} \Big(\sum_i u_{ik} |i_A\rangle \Big) \otimes \Big(\sum_m v_{km} |m_A\rangle \Big) \\ &= \sum_k d_{kk} |\psi_k\rangle_A |\phi_k\rangle_B \end{aligned} \tag{3.49}$$

so we can just set $d_{kk} = \sqrt{\lambda_k}$ to complete the proof.
The Schmidt decomposition plays a key role in characterization of correlations in a pure bipartite quantum state. The coefficients λ_k are called Schmidt coefficients, and the

bases $|\psi_k\rangle_A$ and $|\phi_k\rangle_B$ are called Schmidt bases. When a joint projective measurement is performed, then we get a joint probability distribution:

$$P_{AB}(i,m) = \langle\psi_{AB}| \left(|\psi_i\rangle \langle\psi_i| \otimes |\phi_m\rangle \langle\phi_m| \right) |\psi_{AB}\rangle \tag{3.50}$$

There is no correlation in the state $|\psi_{AB}\rangle$ if none of the joint probability distributions has any correlation. Furthermore, recall that each Hermitian operator corresponds to a random variable in classical probability theory. Then for two observables O_A acting locally on the subsystem A, and O_B acting locally on subsystem B, the correlation function is given by

$$C(O_A, O_B) = \langle O_A \otimes O_B\rangle - \langle O_A \otimes \mathbb{I}_B\rangle\langle \mathbb{I}_A \otimes O_B\rangle \tag{3.51}$$

where $\langle\cdot\rangle = \langle\psi_{AB}| \cdot |\psi_{AB}\rangle$.
We now ready to state the conditions under which a bipartite pure state is without correlation:
a pure bipartite state has no correlation if and only if

1. $|\psi_{AB}\rangle = |\psi_A\rangle \otimes |\psi_B\rangle$ or, equivalently
2. $C(O_A, O_B) = 0, \quad \forall\ O_A$,$O_B$.

Note that a pure state of the form $|\psi_A\rangle \otimes |\psi_B\rangle$ is called a product state and it has $r = 1$ (unitary rank). Indeed the Schmidt's rank is a "measure" of the non-separability of a state. Furthermore, if $|\psi_{AB}\rangle$ cannot be written as a product state, it called entangled.
We now show the necessary and sufficient condition 1. If $|\psi_{AB}\rangle = |\psi_A\rangle \otimes |\psi_B\rangle$ then:

$$P_{AB}(i,m) = |\langle\psi_A|i_A\rangle|^2 \, |\langle\psi_B|m_B\rangle|^2 = P_A(i)P_B(m) \tag{3.52}$$

Vice versa, if we use the Schmidt's basis for $|\psi_{AB}\rangle$ then $P_{AB} = \lambda_i\delta_{ij}$. Hence the condition for $|\psi_{AB}\rangle$ to have no correlation is $r = 1$, i.e., it is a product state.
Furthermore, similar as the case of classical joint probability, we have the concept of quantum mutual information which measures the total amount of correlation between A and B:

$$I(A,B) = S_A + S_B - S_{AB} \tag{3.53}$$

Here for simplicity we write S_A for $S(\rho_A)$, S_B for $S(\rho_B)$ and S_{AB} for $S(\rho_{AB})$.
It easy to verify that the von Neumman entropy has the following propertis:

- $S(\rho)$ is zero if and only if ρ represents a pure state.
- $S(\rho)$ is maximal and equal to $\ln d$ for a maximally mixed state, d being the dimension of the Hilbert space.

- $S(\rho)$ is invariant under changes in the basis of ρ, that is, $S(\rho) = S(U\rho U^\dagger)$, with U a unitary transformation.

- $S(\rho)$ is concave, that is, given a collection of positive numbers λ_i which sum to unity ($\sum_i \lambda_i = 1$) and density operators ρ_i, we have:

$$S\Big(\sum_{i=1}^{k} \lambda_i \rho_i\Big) \geq \sum_{i=1}^{k} \lambda_i S(\rho_i) \tag{3.54}$$

- $S(\rho)$ satisfies the bound:

$$S\Big(\sum_{i=1}^{k} \lambda_i \rho_i\Big) \leq \sum_{i=1}^{k} \lambda_i S(\rho_i) - \sum_{i=1}^{k} \lambda_i \log \lambda_i \tag{3.55}$$

- $S(\rho_i)$ is additive for independent systems. Given two density matrices ρ_A, ρ_B describing independent systems A and B, we have:

$$S(\rho_A \otimes \rho_B) = S(\rho_A) + S(\rho_B) \tag{3.56}$$

3.2.2 Tripartite quantum system

Similar to the bipartite case, we can discuss the correlation for a tripartite pure state ρ_{ABC}: a state ρ_{ABC} has no correlation if and only if it can be written as:

$$\rho_{ABC} = \rho_A \otimes \rho_B \otimes \rho_C \tag{3.57}$$

Then we will say that a tripartite state is ρ_{ABC} genuine entangled if it cannot be written as a product state with respect to any bipartition of the system. This induces a classification of the 'degree' of entanglement as it shown in Fig 3.3. Later we will generalize the classification for a system with N particles.

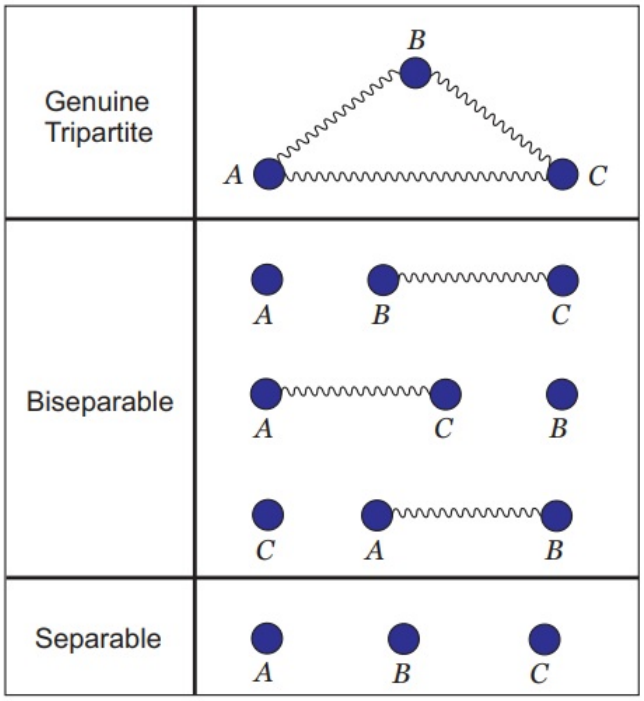

Figure 3.3: All the possibilities of entanglement with three particles. From the top: first, genuine tripartite entanglement, where all particles are in a entangled state. Biseparable states, where two particles are entangled, and another one it is separated. Three particles in a fully separable state.

Naturally, the degree of the total correlation in a state ρ_{ABC} equals the generalized mutual information of the state, i.e.,

$$I(\rho_{ABC}) = S_A + S_B + S_C - S_{ABC} \tag{3.58}$$

In general, this total correlation $I(\rho_{ABC})$ contains both bipartite correlations and tripartite correlations. Since the bipartite correlations are given by the quantum mutual information $I(A,B)$, $I(B,C)$, $I(A,C)$ respectively, we can say that the true tripartite correlation $I_{tri}(\rho_{ABC})$ should be given by:

$$\begin{aligned} I_{tri}(\rho_{ABC}) &= I(\rho_{ABC}) - \big[I(A,B) + I(A,C) + I(B,C)\big] \\ &= S_{AB} + S_{AC} + S_{BC} - S_A - S_B - S_C - S_{ABC} \end{aligned} \tag{3.59}$$

which can be viewed in the graphical manner as illustrated in Fig 3.4.

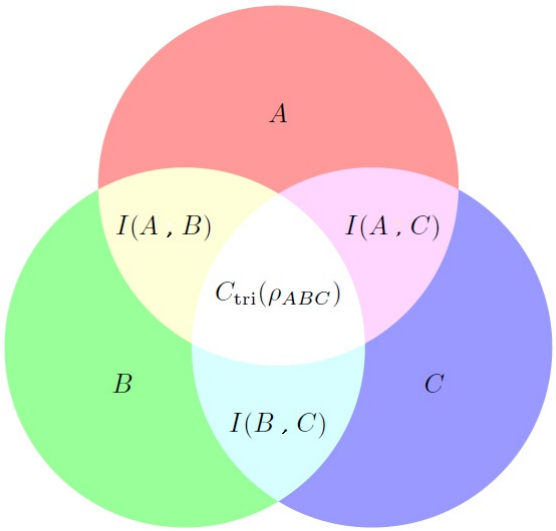

Figure 3.4: An inituitive distribution of correlations in a tripartite quantum state ρ_{ABC}. The true threebody correlation is the overlap of A, B, C, and the two-body correlations between A and B, between A and C, between B and C are represented by the mutual information $I(A, B)$, $I(A, C)$, $I(B, C)$ respectively.

3.3 Fisher Information

So far we have seen how it is possible to use mutual information or von Neumman entropy to detect correlation in a k-partite systems. In mathematical statistics and information theory, another important fuction used for the same task is the so-called Fisher Information (FI). After a brief section describing how FI is defined in classical theory of probability, then, we will explain how it is introduced in quantum mechanics and the role it plays in order to detect quantum k-partite entenglement.

3.3.1 Classical Fisher Information

In statistics, the Fisher information (sometimes simply called information) is a way of measuring the amount of information that an observable random variable X carries about an unknown parameter θ of a distribution that models X. It is defined as the variance of the score (logarithmic derivate) of the likelihood function. Denoting the Fisher Information with F, the variance of the score will be:

$$F(\theta) = \left\langle \left(\frac{\partial \ln f(x,\theta)}{\partial \theta} - \left\langle \frac{\partial \ln f(x,\theta)}{\partial \theta} \right\rangle \right)^2 \right\rangle \tag{3.60}$$

where $f(x,\theta)$ is the likelihood function. It is possible to show that the mean value of the score is zero:

$$\left\langle \frac{\partial \ln f(x,\theta)}{\partial \theta} \right\rangle = \int \frac{1}{f(x,\theta)} \frac{\partial f(x,\theta)}{\partial \theta} f(x,\theta) dx = \frac{\partial}{\partial \theta} \int f(x,\theta) dx = \frac{\partial}{\partial \theta} 1 = 0 \tag{3.61}$$

then the Fisher Information reduces to:

$$F(\theta) = \left\langle \left(\frac{\partial}{\partial \theta} \ln f(x,\theta) \right)^2 \right\rangle \tag{3.62}$$

The likelihood function is usually defined differently for discrete and continuous probability distributions. A general definition is also possible, as discussed below.
Let X be a discrete random variable with probability function $P(\theta, X)$ depending on a parameter. Then the function:

$$f(x,\theta) = P(\theta, X = x) \tag{3.63}$$

considered as a function of θ is the likelihood function, given a certain outcome x of the random variable X. For the sake of completeness, we report an important result the so-called the Cramér–Rao bound. It states that the inverse of the Fisher information is a lower bound on the variance of any unbiased estimator of θ:

$$\mathrm{Var}\big(\tilde{\theta}\big) \geq \frac{1}{F(\theta)} \tag{3.64}$$

where unbiased estimetor means: $\langle \tilde{\theta} \rangle = \theta$.

3.3.2 Quantum Fisher Information

The Quantum Fisher Information (QFI) is the information of a parameter that we can get from a quantum state. Consider a quantum state $\rho(\theta)$, depending by a parameter θ. The QFI of θ is defined as:

$$F_Q(\theta) = \mathrm{Tr}\big[\rho(\theta) L^2\big] \tag{3.65}$$

where L is the so-called symmetry logarithmic derivative, determined by the following equation [19]:

$$\frac{\partial \rho(\theta)}{\partial \theta} = \frac{1}{2}\big[L\rho(\theta) + \rho(\theta)L\big] \tag{3.66}$$

It is possible to show [46] that QFI can be written as:

$$F_Q(\theta) = \sum_i \frac{(\partial_\theta \lambda_i)^2}{\lambda_i} + 4 \sum_{ij} \frac{\lambda_i (\lambda_i - \lambda_j)^2}{(\lambda_i + \lambda_j)^2} \left| \langle \psi_i | \partial_\theta \psi_j \rangle \right|^2 \tag{3.67}$$

where $\partial_\theta \equiv \frac{\partial \rho(\theta)}{\partial \theta}$, λ_i and $|\psi_i\rangle$ are eigenvalues and eigenvectors of ρ, respectively. Let us to prove it.

Proof. Assume that the spectral decomposition of the density operator is given by:

$$\rho(\theta) = \sum_i \lambda_i |\psi_i\rangle \langle\psi_i| \tag{3.68}$$

In the eigenbasis of $\rho(\theta)$, the equation (3.66) reads:

$$\langle\psi_i| \partial_\theta \rho |\psi_j\rangle = \frac{1}{2}(\lambda_i + \lambda_j) L_{ij} \tag{3.69}$$

By substing (3.68) and the normalization relation $\mathbb{I} = \sum_j |\psi_j\rangle \langle\psi_j|$ into (3.66), one can obtain the quantum Fisher Information as:

$$F_Q(\theta) = \sum_{ij} \lambda_i L_{ij} L_{ji} \tag{3.70}$$

As $\lambda_i > 0$, Eq. (3.69) can be written into:

$$L_{ij} = \frac{2(\partial_\theta \rho)_{ij}}{\lambda_i + \lambda_j} \tag{3.71}$$

where $(\partial_\theta \rho)_{ij} \equiv \langle\psi_i| \partial_\theta \rho |\psi_j\rangle$. Utilizing this expression, Eq (3.70) can be written in the form:

$$F_Q(\theta) = \sum_{ij} \frac{4\lambda_i}{(\lambda_i + \lambda_j)^2} |(\partial_\theta \rho)_{ij}|^2 \tag{3.72}$$

Next, from the spectral decomposition of $\rho(\theta)$ one can find that:

$$(\partial_\theta \rho)_{ij} = \partial_\theta \lambda_i \delta_{ij} + (\lambda_j - \lambda_i) \langle\psi_i|\partial_\theta \psi_j\rangle \tag{3.73}$$

Finally, substituting this last equation in (3.72) we have:

$$F_Q(\theta) = \sum_i \frac{(\partial_\theta \lambda_i)^2}{\lambda_i} + 4 \sum_{ij} \frac{\lambda_i (\lambda_i - \lambda_j)^2}{(\lambda_i + \lambda_j)^2} |\langle\psi_i|\partial_\theta \psi_j\rangle|^2 \tag{3.74}$$

that completes the proof.

3.3.3 An Upper Bound for Quantum Fisher Information

Let H be an observable (Hermitian operator) on some Hilbert space of quantum states. Let $\rho(\theta)$, be a parameterized family of density operators which satisfy the von Neumann equation:

$$i\frac{\partial \rho(\theta)}{\partial \theta} = H\rho(\theta) - \rho(\theta)H \tag{3.75}$$

Let M be a measurement of the parameter θ, that is, M is a positive operator-valued measure, and the probability $P_\theta(x) = \mathrm{Tr}\rho(\theta)M(x)$ describes the probability distribution

of the results being in x when the state is $\rho(\theta)$. The mean value and the variance of the measurement M are:

$$\langle M\rangle_\theta = \int xP_\theta(x)dx \tag{3.76}$$

and

$$(\Delta_{\rho(\theta)}M)^2 = \int \big(x - \langle M\rangle_\theta\big)^2 P_\theta(x)dx \tag{3.77}$$

respectively. The measurement is called unbiased if $\langle M\rangle_\theta = \theta$. In this situation, the quantum Cramer Rao inequality for QFI states that [8]:

$$F_Q\big[\rho(\theta), H\big] \geq \frac{1}{(\Delta_{\rho(\theta)}M)^2} \tag{3.78}$$

This inequality gives a lower bound for quantum Fisher information, in terms of the variance of any measurement (estimator) of the parameter.

Now we are going to present two important theorems that will be used later. The first one establishes an upper bound for quantum Fisher information, in terms of the variance $(\Delta_{\rho(\theta)}H)^2 = \mathrm{Tr}(H - \langle H\rangle_\theta)^2$ of the generator H of the quantum motion. The second one gives us a way to calculate the QFI for a pure state. The proofs of these theorems can be found in Appendix A.

Theorem 1 Let $\rho(\theta)$ satisfy the von Neumann equation (3.75), then $F_Q\big[\rho(\theta), H\big] \leq 4(\Delta_{\rho(\theta)}H)^2$

Theorem 2 If $\rho(\theta)$ is a pure state, then $F_Q\big[\rho(\theta), H\big] = 4(\Delta_{\rho(\theta)}H)^2$

3.3.4 Uncertainty Relations from Quantum Fisher Information

Combining the quantum Cramer-Rao inequality and Theorem 1, we have the following inequality chain:

$$4(\Delta_{\rho(\theta)}H)^2 \geq F_Q\big[\rho(\theta), H\big] \geq \frac{1}{(\Delta_{\rho(\theta)}M)^2} \tag{3.79}$$

and, in particular, we have:

$$(\Delta_{\rho(\theta)}H)^2 \cdot (\Delta_{\rho(\theta)}M)^2 \geq \frac{1}{4} \tag{3.80}$$

which is a generalization of the Heisenberg uncertainty relations. To see how the above inequality implies the conventional Heisenberg uncertainty relation, we consider the canonical position and momentum pair $Q = x$ and $P = -i\partial_x$. Let be $|\psi\rangle$ a wavefunction, and put:

$$\begin{aligned} (\Delta_\psi Q)^2 &= \langle\psi|\, Q - \langle Q\rangle_\psi \,|\psi\rangle\,, \qquad \langle Q\rangle_\psi = \langle\psi|\, Q\,|\psi\rangle \\ (\Delta_\psi P)^2 &= \langle\psi|\, P - \langle P\rangle_\psi \,|\psi\rangle\,, \qquad \text{with} \qquad \langle P\rangle_\psi = \langle\psi|\, P\,|\psi\rangle \end{aligned} \tag{3.81}$$

Now in inequality (3.79), we take $\rho(\theta) = |\psi_\theta\rangle \langle\psi_\theta|$ with:

$$|\psi_\theta\rangle = \exp -i\theta P |\psi\rangle , \qquad \text{with} \qquad H = P \quad \text{and} \quad Q = Q - \langle Q\rangle \tag{3.82}$$

Noting that by the translation invariance of the Lebesgue measure, M is an unbiased estimator for θ, and:

$$(\Delta_{\rho(\theta)} H)^2 = (\Delta_\psi P)^2 \qquad (\Delta_{\rho(\theta)} M)^2 = (\Delta_\psi Q)^2 \tag{3.83}$$

we immediately obtain:

$$(\Delta_\psi P)^2 \cdot (\Delta_\psi Q)^2 \geqslant \frac{1}{4} \tag{3.84}$$

which is precisely the familiar Heisenberg uncertainty relation for the canonical pair of position and momentum.

3.4 Entanglement criterion derived from F_Q

So far we provided a description of the Quantum Fisher Information for a generic state ρ and H. Now let us consider a state of N particles and a linear operator defined as:

$$\hat{H} = \frac{1}{2} \sum_{i=1}^{N} \hat{J}^i_{\vec{n}} \tag{3.85}$$

where the local operator $\hat{J}^i_{\vec{n}}$ has the form:

$$\hat{J}^i_{\vec{n}} = \vec{n} \cdot \vec{\hat{J}^i} = \alpha_i \hat{J}^i_x + \beta_i \hat{J}^i_y + \gamma_i \hat{J}^i_z \tag{3.86}$$

with $\alpha_i^2 + \beta_i^2 + \gamma_i^2 = 1$. The operators $\hat{J}^i_x$,$\hat{J}^i_y$ and $\hat{J}^i_z$ fulfill the commutation relations of angular momentum operators. It has been recently shown that QFI, for N-particle states and linear generator $\hat{H}$ the QFI has to satysfy [49]:

$$F_Q\big[\rho, \hat{H}\big] \leq N^2 \tag{3.87}$$

where the equality can be reached only for certain maximally entangled states.
In particular, if ρ is not entangled, it can be written as separable state of the form:

$$\rho_{sep} = \sum_\alpha p_\alpha \bigotimes_{l=1}^{N} \left|\psi^{(l)}_\alpha\right\rangle \left\langle\psi^{(l)}_\alpha\right| \tag{3.88}$$

where $\{p_\alpha\}$ form a probability distribution. In this case the inequality (3.87) becomes:

$$F_Q\big[\rho, \hat{H}\big] \leq N \tag{3.89}$$

Let us now consider the fallowing classification of multipartite entanglement [48]. A pure state of N particles is k-entangled if can be written as:

$$|\psi_{k-ent}\rangle = \bigotimes_{l=1}^{M} |\psi_l\rangle \tag{3.90}$$

where $|\psi_l\rangle$ is a state with N_l entangled particles and M is the number of parties in which it is possible to split up the state. Then:

$$N = \sum_{l=1}^{M} N_l \tag{3.91}$$

In the product (3.90), we consider the state $|\psi_l\rangle$ for which N_l is maximum and so we set $k \equiv \max\{N_l\}$. Therefore, a k-particle entangled state can be wrtitten as a product $|\psi_k\rangle$ which containts at least one state $|\psi_l\rangle$ of $N_l = k$ particles which does not factorize. Let us illustate classification with the following example. Let be $N = 8$ and:

$$|\psi_{3-ent}\rangle = |\psi_1\rangle \otimes |\psi_{23}\rangle \otimes |\psi_4\rangle \otimes |\psi_{567}\rangle \otimes |\psi_8\rangle \tag{3.92}$$

This state has $M = 5$ and $k = 3$. Indeed, as we can see, the maximum entangled state is $|\psi_{567}\rangle$ which contains $N_{567} = 3$ particles. Since $|\psi_{567}\rangle$ cannot be further factorized we say that $|\psi_{3-ent}\rangle$ is three-particles entangled. So in this notation a state $|\psi_{1-ent}\rangle$ is fully separable while a state $|\psi_{N-ent}\rangle$ is extremelly entangled.

3.4.1 Theorem 3: F_Q^{k+1} criterion.

For k-entangled state and an arbitrary linear operator $\hat{H}$ of the form (3.85), the QFI is bounded by:

$$F_Q\big[\rho, \hat{H}\big] \leq kN \tag{3.93}$$

Proof Let us define $\bar{M} \equiv \frac{N}{k}$ and, for simplicity, we suppose that is an integer. The basic ingedients of the derivations are:

1. The QFI is convex in the states; that is:

$$F_Q\big[[p\rho_1 + (1-p)\rho_2]\big] \leq pF_Q[\rho_1] + (1-p)F_Q[\rho_2] \tag{3.94}$$

   for $p \in [0, 1]$.

2. For a product state $|\psi_{AB}\rangle = |\psi_A\rangle \otimes |\psi_B\rangle$ we have:

$$(\Delta_{\rho_{AB}} \hat{H}^{AB})^2 = (\Delta_{\rho_A} \hat{H}^A)^2 + (\Delta_{\rho_B} \hat{H}^B)^2 \tag{3.95}$$

   Here H^{AB} acts on all particles while H^A acts on the particles of ψ_A only and in analogy for ψ_B.

It follows from 1) that maximum for F_Q is reached on pure k-entangled state [47]. Therefore, from Theorem 2 we get that $F_Q[\rho_{k-ent}, \hat{H}] = 4(\Delta_\rho \hat{H})^2$. Our task is to massimize $4(\Delta_\rho \hat{H})^2$ with respect to the probe state $|\psi_{k-ent}\rangle$.
Due to 2) we obtain:

$$F_Q[\rho_{k-ent}, \hat{H}] = 4(\Delta_\rho H)^2 = 4\sum_{l=1}^{M}(\Delta_{\rho_l}\hat{H})^2 \tag{3.96}$$

Then, by using (3.87) for l-th system, we get:

$$4\sum_{l=1}^{M}(\Delta_{\rho_l}\hat{H})^2 = \sum_{l=1}^{M}(\Delta_{\rho_l}\hat{J}^l_{\vec{n}})^2 \leq \sum_{l=1}^{M} N_l^2 \tag{3.97}$$

The QFI is increased by making N_l as large as possible. Hence, the maximum is reached by the product of $M = \bar{M}$ state of $N_l = k$ particles that is:

$$\max\Big[\sum_{l=1}^{M} N_l^2\Big] = MN_l^2 \tag{3.98}$$

then:

$$F_Q[\rho_{k-ent}, \hat{H}] \leq \bar{M}k^2 \tag{3.99}$$

with $\bar{M} = \frac{N}{k}$ that completes the proof.
Similarly, with some algebric calculation, it can possible to show that if $\bar{M}$ is not integer, equation (3.93) becomes:

$$F_Q\big[\rho, \hat{H}\big] \leq sk^2 + (N - sk)^2 \tag{3.100}$$

where $s = \lfloor \bar{M} \rfloor$ is the largest integer smaller than or equal to M.
Furthermore, if the equality is reached than we have k-partite entanglement whereas if the bound is surpassed, then the state contains $k+1$ entangled particles (see Fig 3.5).
In simple cases, it is esay to verify, by algebraic calculation, that this criterion works. For example if we considerate a q-bit state of the form:

$$|GHZ\rangle = \frac{1}{\sqrt{2}}\big(\,|0\rangle^{\otimes N} + |1\rangle^{\otimes N}\,\big) \tag{3.101}$$

and choosing $\hat{H}$ as:

$$\hat{H} = \frac{1}{2}\sum_{i=1}^{N}\hat{\sigma}_z^i, \qquad \text{where} \qquad \hat{\sigma}_z = \begin{pmatrix} 1 & 0 \\ 0 & -1 \end{pmatrix} \tag{3.102}$$

it can be possible to show that GHZ-states satured the inequality, that is:

$$F_Q\big[\,|GHZ\rangle\,, \hat{H}\big] = 4\big[\,\langle GHZ|\,\hat{H}^2\,|GHZ\rangle - \big(\,\langle GHZ|\,\hat{H}\,|GHZ\rangle\,\big)^2\big] = N^2 \tag{3.103}$$

Thus we have $k = N$ which means that $|GHZ\rangle$ is N-entangled state. On the other hand, if we take a product state $|0\rangle^{\otimes N}$, we find $F_Q = N$ that implies $k = 1$ as expected.

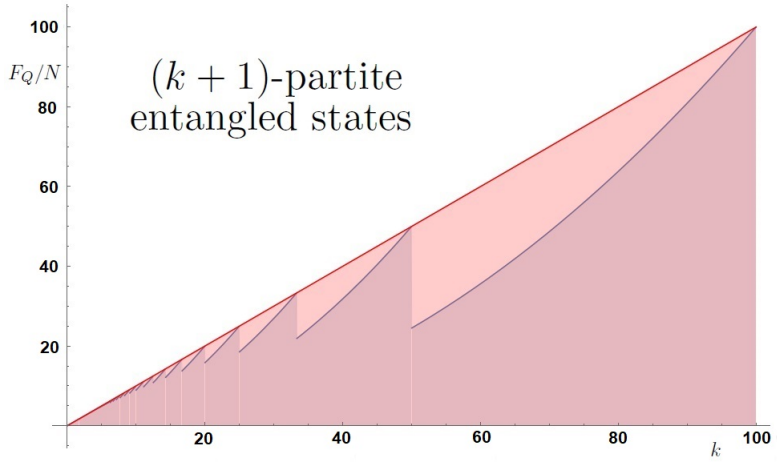

Figure 3.5: F_Q^{k+1} criterion. The blu line is the bound $F_Q\left[\rho, \hat{H}\right] = sk^2 + (N - sk)^2$ which separates product states (below the line) from $(k + 1)$-particle entangled states (above the line). For comparison, the function $F_Q[\rho_{k-ent}, \hat{H}] = Nk$ is plotted (red line). Here N=100.

Chapter 4

Evaluation of the QFI by NLOP

In the previous Chapter we introduced the Quantum Fisher Information and we derived a criterion which allows us to establish the 'degree' of entanglement of a system. In this section, our task is to evaluate the QFI in the Haldane and dimer phases of bilinear-biquadratic model by using numerical techniques. In particular we'll be interested to the scaling behavior of the Fisher density f_Q as function of N. The idea of carrying out this type of study on our model, started from a paper of Pezzè et al [25] which is part of a series of several studies, done in the last years, aimed at finding a method to detect mulpipartite entanglement structure of certain models.

4.1 Multipartite entanglement in topological quantum phases

The characterization of quantum phases and quantum phase transitions (QPTs) via entanglement measures [26, 27] is an intriguing problem at the verge of quantum information and many-body physics [28]. The study of entanglement pushes our understanding of QPTs [29, 30] beyond standard approaches in statistical mechanics and sheds new light on the creation, and manipulation of useful resources for quantum technologies.
The literature [28] has mostly focused on bipartite entanglement. A benchmark is the so-called area law that relates the amount of bipartite entanglement entropy among two partition of a many-body system to the surface area between the two blocks. For models with shortrange interactions in one dimension, the Von Neumann entropy is constant in the gapped phases while it increases logarithmically with the system size at criticality. Yet, violations of the area law are not always related to a closing gap: a logarithmic increase of the Von Neumann entropy occurs also in some gapped phases of one-dimensional models with long-range interaction, as well as for peculiar short-range models [34].The

complex structure of a many-body quantum state is of course much richer than that caught by bipartite/pairwise entanglement. Yet, multipartite entanglement (ME) has been much less studied. Recently [35, 36] ME in models exhibiting Ginzburg-Landau-type QPTs has been witnessed using the quantum Fisher information calculated for the local order parameter, exploiting well-known relations between the QFI and ME [39] as we have shown in the Chapter 3.

However, it has been emphasized that this approach, based on local operators, fails to detect ME at topological QPTs [37]. For this task, methods based on the QFI generally require the extension of entanglement criteria for nonlocal operators.

Indeed, recently, Pezzè et al [25] really used nonlocal operators to calculate the QFI for a paradigmatic model showing topological phases: the Kitaev chain of spinless fermions in a lattice [41, 42] with variable-range pairing [31, 33] whose Hamiltonian is:

$$H = -\frac{J}{2}\sum_{j=1}^{L}\left(\hat{a}_j^\dagger \hat{a}_{j+1} + \text{h.c}\right) - \mu\sum_{j=1}^{L}\left(\hat{n}_j - \frac{1}{2}\right) + \frac{\Delta}{2}\sum_{j=1}^{L}\sum_{l=1}^{L-j} d_l^{-\alpha}\left(\hat{a}_j\hat{a}_{j+l} + \hat{a}_{j+l}^\dagger\hat{a}_j^\dagger\right) \quad (4.1)$$

where $J > 0$, $\hat{a}_j$ is a fermionic annihilation operator on the site j, $\hat{n}_j = \hat{a}_j^\dagger\hat{a}_j$ and L is the total number of sites. By using the non-local operator

$$\hat{O}_\rho = \sum_{j=1}^{L}\hat{o}_\rho^j \qquad \text{with} \quad \rho = x, y \quad (4.2)$$

where

$$\hat{o}_\rho^j = (-1)^{\delta_{\rho,y}}\left(\hat{a}_j^\dagger e^{i\pi\sum_{l=1}^{j-1}\hat{n}_l} + (-1)^{\delta_{\rho,y}} e^{-i\pi\sum_{l=1}^{j-1}\hat{n}_l}\hat{a}_j\right) \quad (4.3)$$

they showed how the scaling behaviour of Fisher density changes in different points of the phase diagram chacacterized by different values of winding number. We summarize their results in Fig. 4.1.

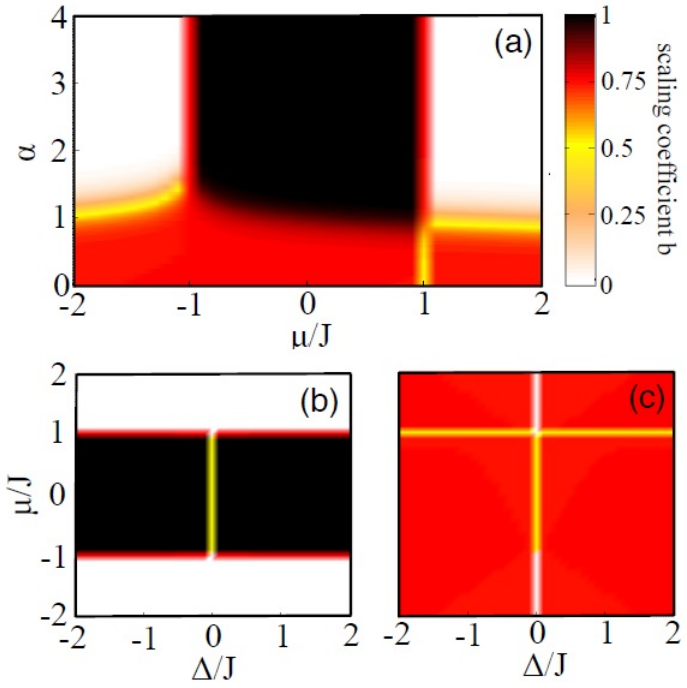

Figure 4.1: Phase diagram of the Kitaev chain obtained numerically from the scaling of the Fisher density as a function of the system size L, $f_Q = 1 + cL^b$. The color scale show the scaling coefficent b in the μ/J-α plane for $\Delta = J$ (a) and in the Δ/J-μ/J plane (b) and infinite-range (c) pairing (figure taken from [25]).

Then, they concluded that QFI can detect multipartite entanglement in the topological and long-range phases (with nonvanishing winding numbers) of the Kitaev chain. In particular, Pezzè et al emphasize how a key aspect of the calculation was the use of nonlocal operators: the quantum Fisher information relative to local operators in unable to detect entanglement for Kitaev model, as noted in [37].

4.2 String order parameters

Both the Haldane and the dimer phases are antiferromagnetic gapped phases separated by a phase transition at $\beta = 1$. As we have seen in the previous sections, in order to distinguish the two phases, we need to define Non-Local Order Parameters (NLOPs) as:

$$\mathbf{O}_\Omega(O^A, O^B) = \lim_{n\to\infty} \langle\Psi|\, O^A(1)\Big(\prod_{k=2}^{n-1}\Omega(k)\Big)O^B(n)\,|\Psi\rangle \tag{4.4}$$

where, by an appropriate choise of O_A and O_B, its value can be zero or different from zero in the two phases. The reason why this works is due to the non-local nature of these parameters. Indeed the AKLT model has exponatially decaying correlations and

this applies to the whole Haldane phase. Therefore we may conclude that there is no order in this antiferromagnetic phase but, as we will see, a different kind of hidden order is actually there. We are going to show this on the valence bond state. As we can see from the Fig.2.9, we know that, in a finite chain, the ground state of AKLT model is four-fold degenerate due to the effective spin-1/2's at the boundaries. Let us to write the ground state of AKLT as Φ_σ, where σ is a string of $+$'s, $-$'s and 0's so that Φ_σ can be expressed as a tensor product of a single site states $|+\rangle$, $|-\rangle$ and $|0\rangle$.
For instance, if the first spin-1/2 of the chain is in the $|\uparrow\rangle$ state, then for the first site we cannot have a $|-\rangle$ state but only $|+\rangle$ or $|0\rangle$. In the latter case we still must have the first non-zero character to be a $+$ in σ in order to satisfy the construction of the valence bond state. It can be verified that there has to be the same number of $+$'s and $-$'s alternating all along the σ string, with no further restrictions on the number of 0's between them. So a typical permitted state Φ_σ, could look like this:

$$\Phi_\sigma = |000+-0+-+0-+0-+-0\rangle \tag{4.5}$$

If we take a look at (4.5) it is apparent that there is a sort of Néel order (antiferromagnetic order) if we ignore the 0's. Still we cannot predict what the spins will be in two distant sites as we have no control on the number of the 0's. Indeed there is no local order parameter that can be found to be non-zero in the Haldane phase and that can be used to distinguish this phase from the others. As it turned out, there actually is a non-local order parameter, the string order parameter, that reveals the hidden order of the Haldane phase. In order to see how we can arrive to define it, let us to introduce a nonlocal unitary transformation U:

$$U = \prod_{j<k} \exp\left(i\pi S_j^z S_k^x\right) \tag{4.6}$$

such that:

$$U\Phi_\sigma = (-1)^{z(\sigma)}\Phi_{\bar{\sigma}} \tag{4.7}$$

where $z(\sigma)$ is the number of 0 characters in odd sites. Here the configuration of $\bar{\sigma}$ is defined as follow:

- if $\sigma_i = +(-)$ and the number of non.sero characters to the left of the site i is odd then $\bar{\sigma}_i = -(+)$
- otherwise $\sigma_i = \bar{\sigma}_i$

where σ_i is the i-th character of the string. We give an example of the action of U on a random state:

$$|0+-++++0+-+0++0\rangle \quad \longrightarrow \quad -|0+++-+0---0+-+\rangle \tag{4.8}$$

In particular, if we apply this transformation on the permitted state (4.5), it becomes:

$$U\Phi_\sigma = |000++0+-+0++0+++0\rangle \tag{4.9}$$

Then this unitary transformation aligns all the non-zero spins i.e. if the first non-zero character is $+(-)$ all the other non-zero characters become $+(-)$. It is also evident that $U^{-1} = U$.

Let us show now how the spin operators transform under the action of U [12]:

$$\begin{aligned}
\widetilde{S}_j^x &= US_j^xU^{-1} = S_j^x \exp\left(i\pi \sum_{l>j} S_l^x\right) \\
\widetilde{S}_j^y &= US_j^yU^{-1} = \exp\left(i\pi \sum_{l<j} S_l^z\right) S_j^y \exp\left(i\pi \sum_{l>j} S_l^x\right) \\
\widetilde{S}_j^z &= US_j^zU^{-1} = \exp\left(i\pi \sum_{l<j} S_l^z\right) S_j^z
\end{aligned} \tag{4.10}$$

Notice that local operators have been mapped onto non-local operators as they contain a sum of spin operators acting on different sites. This is not surprising given that U itself is a non-local unitary transformation. For the same reason we should expect that, in general, also the transformed Hamiltonian $\widetilde{H} = UHU^{-1}$ will be non-local and thus have long-range interactions but, using the transformed spin operators (4.10), it actually turns out to be a local operator:

$$\widetilde{H} = J \sum_j \left[h_j + \beta(h_j)^2\right] \tag{4.11}$$

where

$$h_j = -S_j^x S_{j+1}^x + S_j^y \exp\left(i\pi\left(S_j^z + S_{j+1}^x\right)\right) S_{j+1}^y - S_j^z S_{j+1}^z \tag{4.12}$$

The transformed Hamiltonian $\widetilde{H}$ still has the same symmetries of the original Hamiltonian H, but they may not be local symmetries anymore. Actually the only local symmetry H has is related to its invariance under rotations of π about each coordinate axis. This symmetry group is equivalent to $Z_2 \times Z_2$: indeed the product of two π-rotations about two different axes produce a π- rotation about the third axis.

4.3 Quantum Fisher Information for string operators

As we have seen in the chapter 3, the QFI for a pure state is:

$$F_Q\left[\,|\psi\rangle\,, H\right] = 4(\Delta_{|\psi\rangle} H)^2 = 4\left[\,\langle\psi|\, H^2\,|\psi\rangle - \langle\psi|\, H\,|\psi\rangle^2\,\right] \tag{4.13}$$

Then, since our aim is to evaluate this quantity on the ground state of bilinear-biquadratic model by using non-local operators (i.e. string operators (4.10)), we can choose $H \equiv \widetilde{S}^z$. Consequently, we get:

$$\begin{aligned}\langle\psi_{GS}|\left(\widetilde{S}^z\right)^2|\psi_{GS}\rangle &= \sum_{j=1}^{N-1}\sum_{l>j}^{N}\left\langle S_j^z \exp\left(i\pi\sum_{k=j+1}^{l-1}S_k^z\right)S_l^z\right\rangle \\ &= \sum_{j=1}^{N-1}\sum_{l>j}^{N}\left\langle S_j^z\left(\prod_{k=1+j}^{l-1}\Omega(k)\right)S_l^z\right\rangle\end{aligned} \tag{4.14}$$

and

$$\begin{aligned}\langle\psi_{GS}|\,\widetilde{S}^z\,|\psi_{GS}\rangle &= \sum_{l=1}^{N}\left\langle \exp\left(i\pi\sum_{k=0}^{l-1}S_k^z\right)S_l^z\right\rangle \\ &= \sum_{l=1}^{N}\left\langle\left(\prod_{k=0}^{l-1}\Omega(k)\right)S_l^z\right\rangle\end{aligned} \tag{4.15}$$

where, as usual:

$$\Omega(k) = \exp\left(i\pi S_k^z\right) \tag{4.16}$$

For the first term (4.14), is useful to define a matrix M (with matrix elements M_{jl}) as:

$$M = \begin{pmatrix} / & \langle S_1^z S_2^z\rangle & \langle S_1^z\Omega(2)S_3^z\rangle & \langle S_1^z\Omega(2)\Omega(3)S_4^z\rangle & \cdots & \langle S_1^z\Omega(2)\cdots\Omega(N-1)S_N^z\rangle \\ / & / & \langle S_2^z S_3^z\rangle & \langle S_2^z\Omega(3)S_4^z\rangle & \cdots & \langle S_2^z\Omega(3)\cdots\Omega(N-1)S_N^z\rangle \\ / & / & / & \langle S_3^z S_4^z\rangle & \cdots & \cdots \\ \cdots & \cdots & \cdots & \cdots & \cdots & \cdots \\ / & / & / & / & \cdots & \langle S_{N-1}^z S_N^z\rangle \end{pmatrix} \tag{4.17}$$

Thus, $\langle\psi_{GS}|\left(\widetilde{S}^z\right)^2|\psi_{GS}\rangle$ turns out to be the sum of all matrix elements of M.
Similarly, for the term (4.15), we can define a verctor N:

$$N = \left(\langle S_1^z\rangle, \langle\Omega(1)S_2^z\rangle, \langle\Omega(1)\Omega(2)S_3^z\rangle, \cdots, \langle\Omega(1)\Omega(2)\cdots\Omega(N-1))S_N^z\rangle\right) \tag{4.18}$$

such that $\langle\psi_{GS}|\,\widetilde{S}^z\,|\psi_{GS}\rangle$ turns out to be the sum of all its elements. In this way the QFI can be written as:

$$F_Q\left[\,|\psi_{GS}\rangle\,,\widetilde{S}^z\right] = 4\left[\left(\sum_{j=1}^{N-1}\sum_{l>j}^{N}M_{jl}\right) - \left(\sum_{l=1}^{N}N_l\right)^2\right] \tag{4.19}$$

The QFI written in this form is very useful for numerical approach. Indeed we can easy implement a code to calculate every element of M (or N) and add them together.

4.4 Numerical evaluation of QFI by using string order operator

Now we are ready to perform numerical evaluation of the QFI for our model in different points of the phase diagram. For this purpose, we use ITensor (that is a C++ library for implementing tensor network calculations and performing DMRG procedures [45]) whose feauters are described in (Appendix B). First of all we have implemented a C++ code which was able to

- simulate the ground state of the model for every value of β and J;
- calculate the ground state energy;
- calculate the expected value of some local operator on the ground state;

Then, verified it worked, we calculated the expected value of some string operator. Since we knew the exact result of some non-local order parameters in the thermodynamic limit (see Chapter 2), then we first tried to evaluate them in order to verify the correct implementation of our code. For instance, we fixed $N = 120$ (in order to be as near as possible to thermodynamic limit) and tried to evaluate:

$$\mathbf{O}_z((S^z),(S^z)) = -\frac{4}{9} \tag{4.20}$$

In the notation just introduced, it corresponds to the matrix element $M_{1,120}$ and, performing numerical calculation we obatined $-0,4444$ as expected. Other checks have been made with other NLOPs and, once again our analytical calculations are in agreement with the numerical results.
Finally, we performed numerical evalutation of QFI. It's important to stress that every numerical estimate of QFI we did, satisfies:

$$F_Q \leq N^2 \tag{4.21}$$

as it was recently established in [32]. Furthermore, as we have seen in Chapter 3, in order to make the multipartite entanglement structure clearer, it is useful to work with the density of QFI, defined as:

$$f_Q = \frac{\left| F_Q\left[\, |\psi_{GS}]\right\rangle, \widetilde{S}^z\right]\right|}{N} \tag{4.22}$$

where the absolute value was introduced to avoid problems with the sign of F_Q.
What we find is that analyzing f_Q one can:

- distinguish the Haldane phase from dimer phase: in the former the shape of f_Q is linear, in the latter the data trend tends to be flat for sufficiently high values of N (we find that the best function that fit these data is $\tan^{-1}$).
- detect the phase transition at $\beta = 1$. Here f_Q shows a power law scaling.
- identify, for every value of N and β, the multipartite structure of entanglement (which is maximum at AKLT point as expected).
- verify how much the valence-bound state (VBS) representations are good approximations for whole Haldane and dimer phases.

4.4.1 Haldane phase

In this section we show the shape of f_Q as function of N in the Haldane phase. In figures 4.2, 4.4, 4.3, 4.5 we have set $J = 1$ and $\beta = -1/3$, 0, 1/3, 2/3 progressively. As we can see, the whole Haldane phase is chacacterized by a linear trend of f_Q. For this reason we try to fit a function of the form:

$$f_Q = a + bN \tag{4.23}$$

with a and b free parameters. In particular, at AKLT point we have that every value of $f_Q(N) \simeq k = N - 1$ which implies a N-partite entangled state. This is exactly what we expected becouse, as we can see from the intuite picture of VBS (Fig. 2.9), at AKLT point we have the maximum entangled ground state. Progressively, for the other volues of β, the slope of f_Q decreases and which witnesses a less entangled multipartite structure.

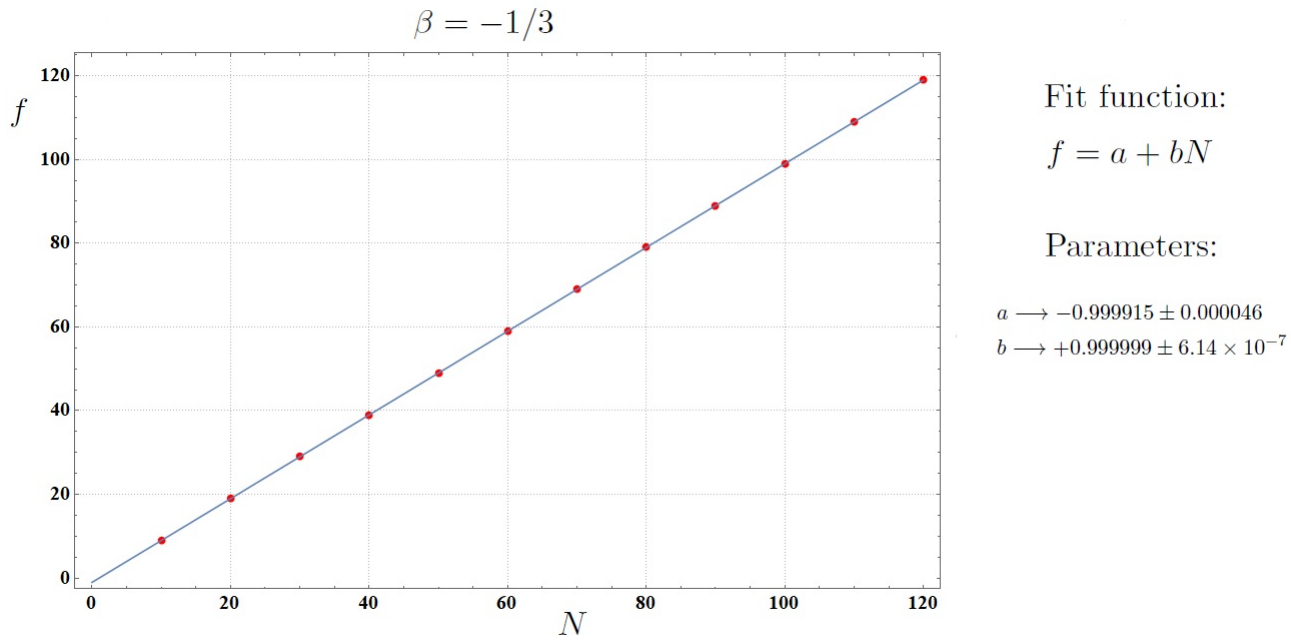

Figure 4.2: Linear behavior emerging from numerical evaluation of f_Q at AKLT point.

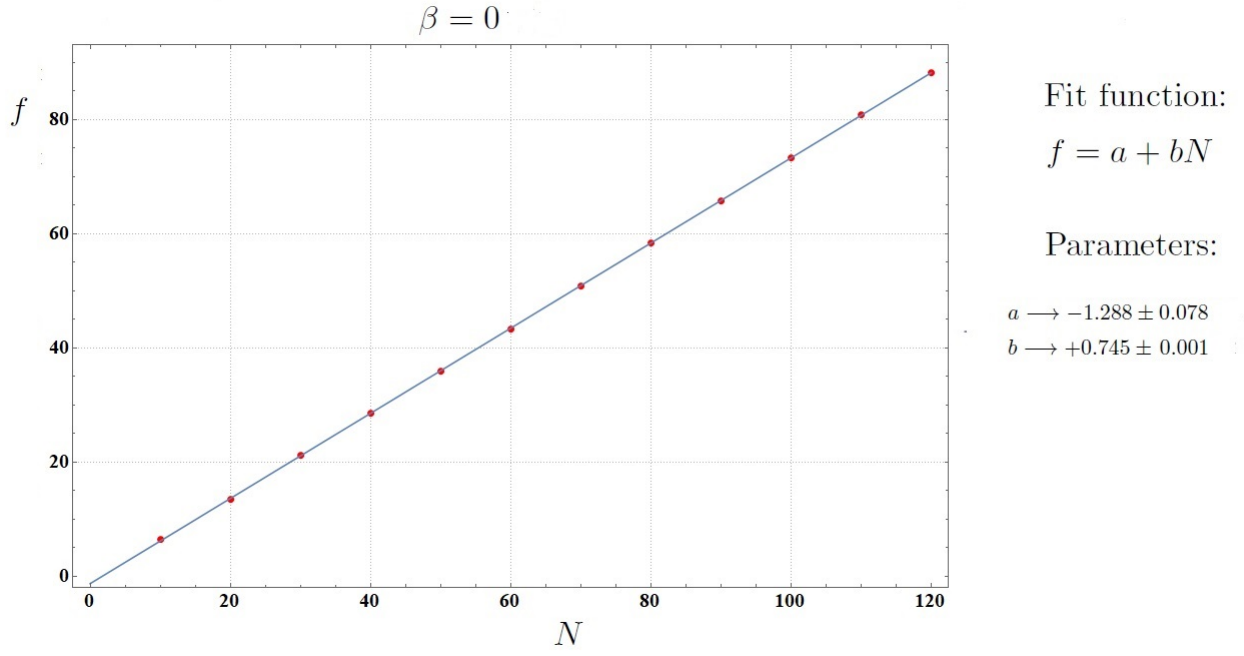

Figure 4.3: Linear behavior emerging from numerical evaluation of f_Q at Heisemberg point.

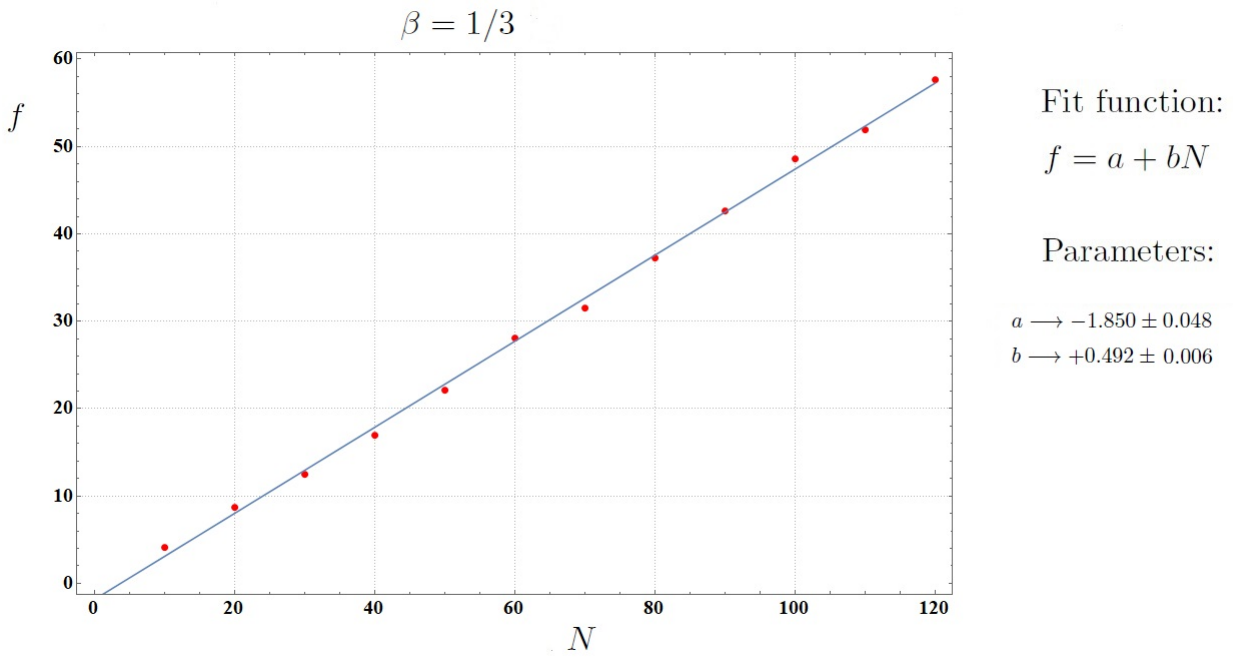

Figure 4.4: Linear behavior emerging from numerical evaluation of f_Q at $\beta = 1/3$.

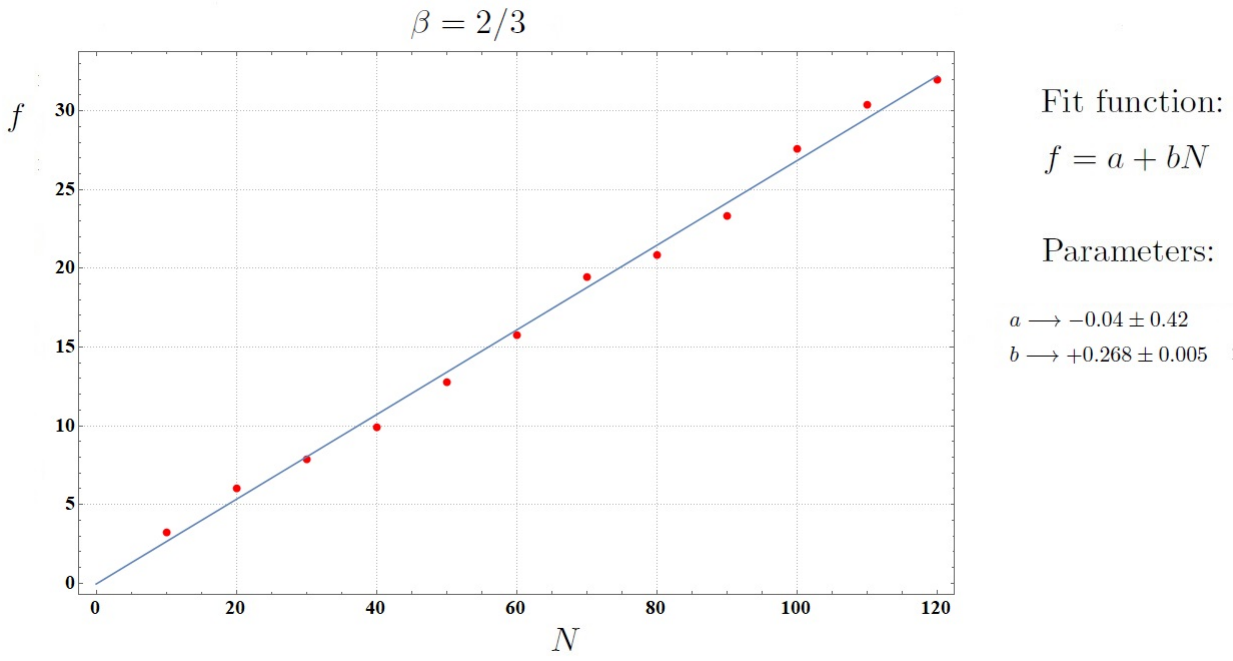

Figure 4.5: Linear behavior emerging from numerical evaluation of f_Q at $\beta = 2/3$.

4.4.2 Phase transition $\beta = 1$

Here we show the power law scaling of f_Q as function of N at the phase transtion point $\beta = 1$. Indeed, observing the trend of the data and after trying different functions, we realized that the best fit is obtained using a function of the form:

$$f_Q = c + dN^e \tag{4.24}$$

which gives us back free parameters c, d and e with the lowest standard error.

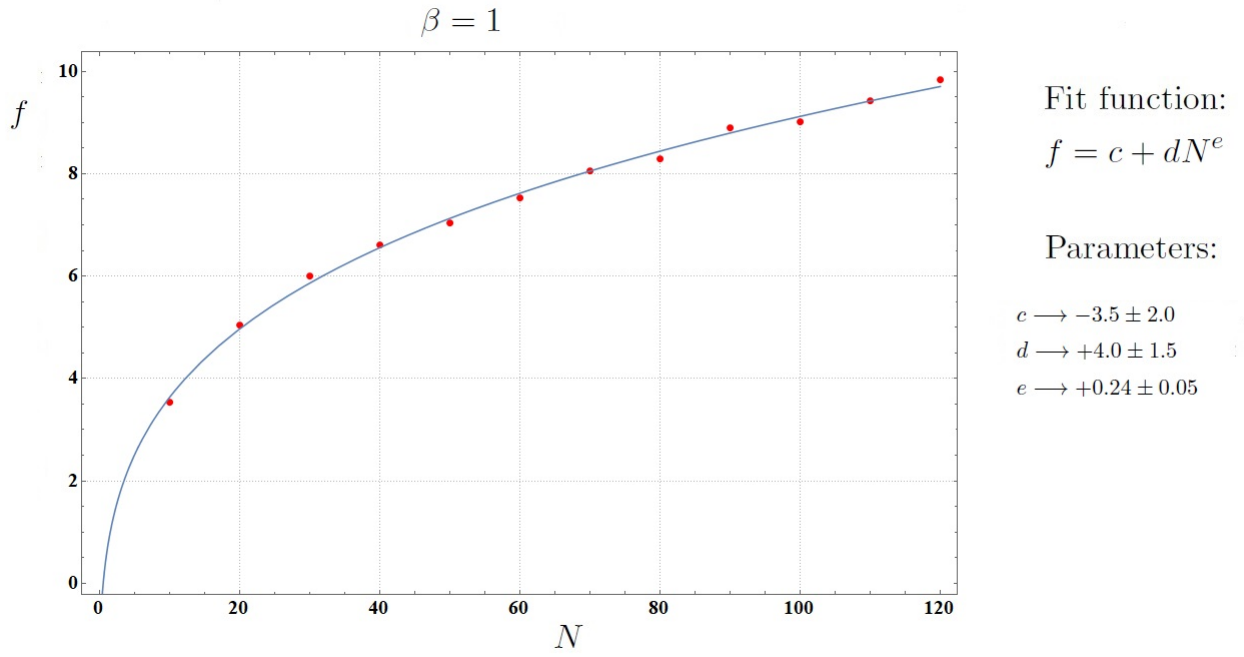

Figure 4.6: Power scaling law emerging from numerical evaluation of f_Q at the phase transition.

4.4.3 Dimer phase

Finally, in this section we show the shape of f_Q as function of N in the dimer phase In figures 4.7, 4.8, 4.9 we have set $J = 1$ and $\beta = 2$, 4, 10 progressively. As we can see, the whole dimer phase is chacacterized by a particular distribution of data: it seems that, for large values of N, f_Q follows a flat trend. This becomes even clearer for high values of β. For this reason we try to fit a function of the form:

$$f_Q = g \tan^{-1}(hN + m) \tag{4.25}$$

Furthermore, we have to remember that a good approximation for the ground states in the dimer phase is given by VBS shown in Fig 2.10. From our fits, we should conclude that such approximation is more accurate for higher values of β. Indeed for $\beta = 10$, all

values of f_Q are between 1 and 2, which means that for every value of N the correspondig ground state is 2-partite entanged.

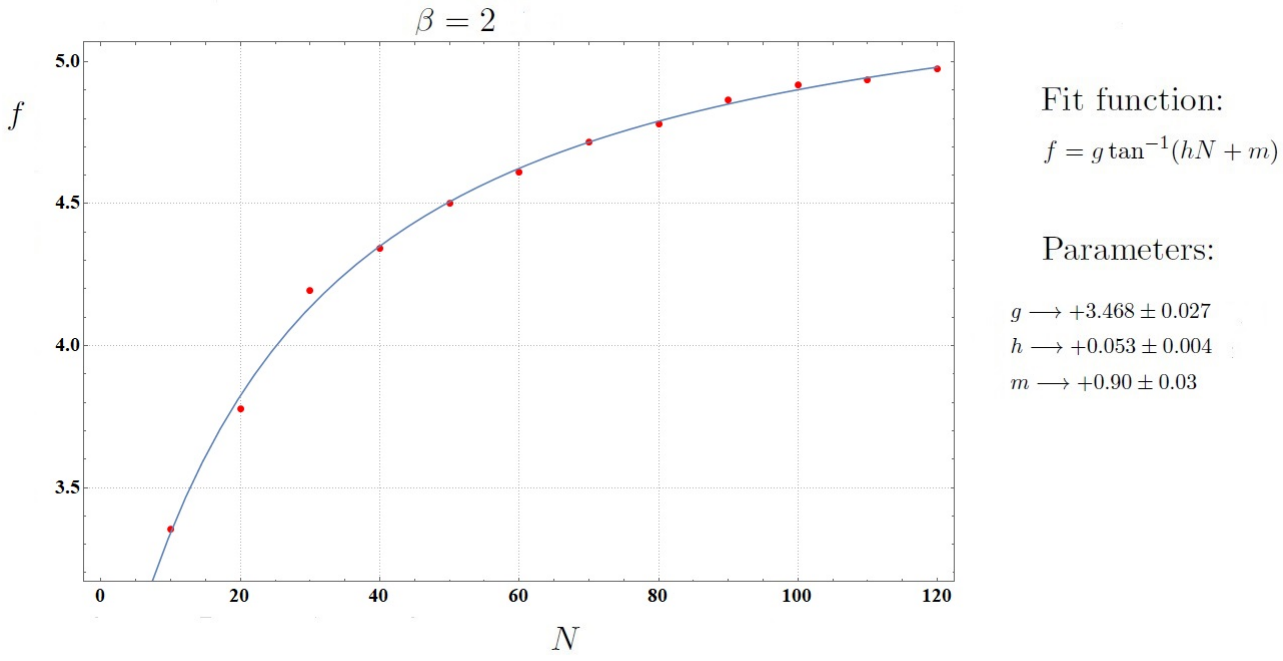

Figure 4.7: Shape of f_Q emerging from numerical evaluation for $\beta = 2$

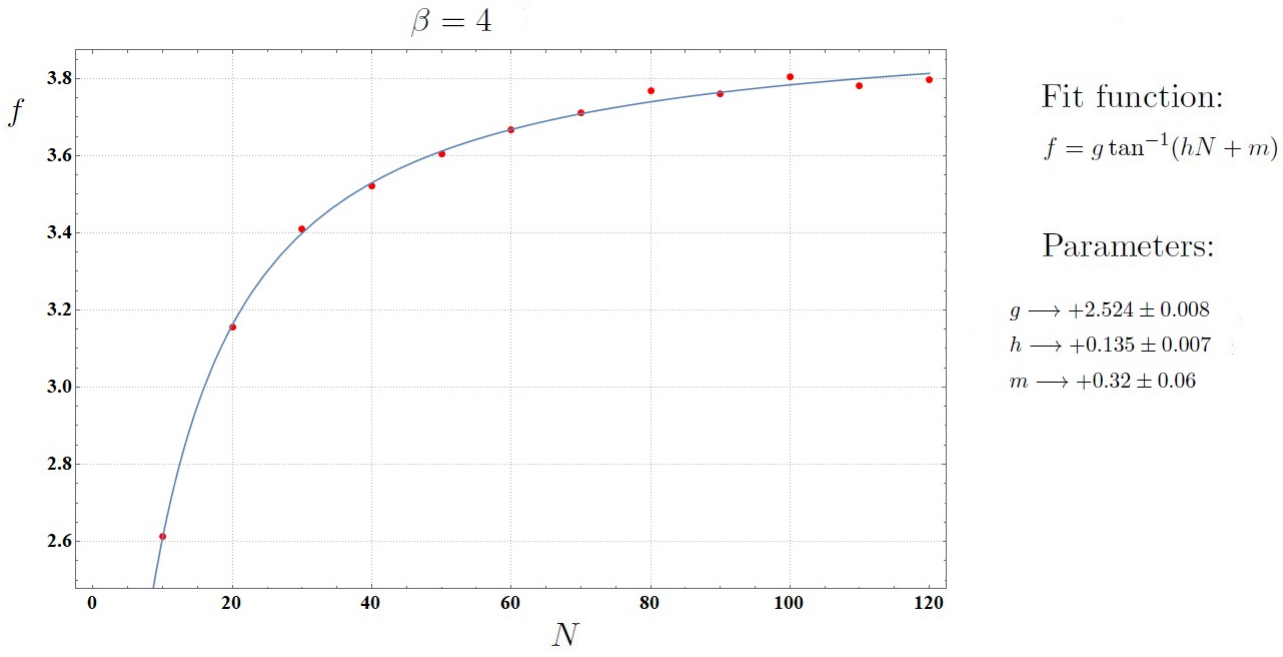

Figure 4.8: Shape of f_Q emerging from numerical evaluation for $\beta = 4$

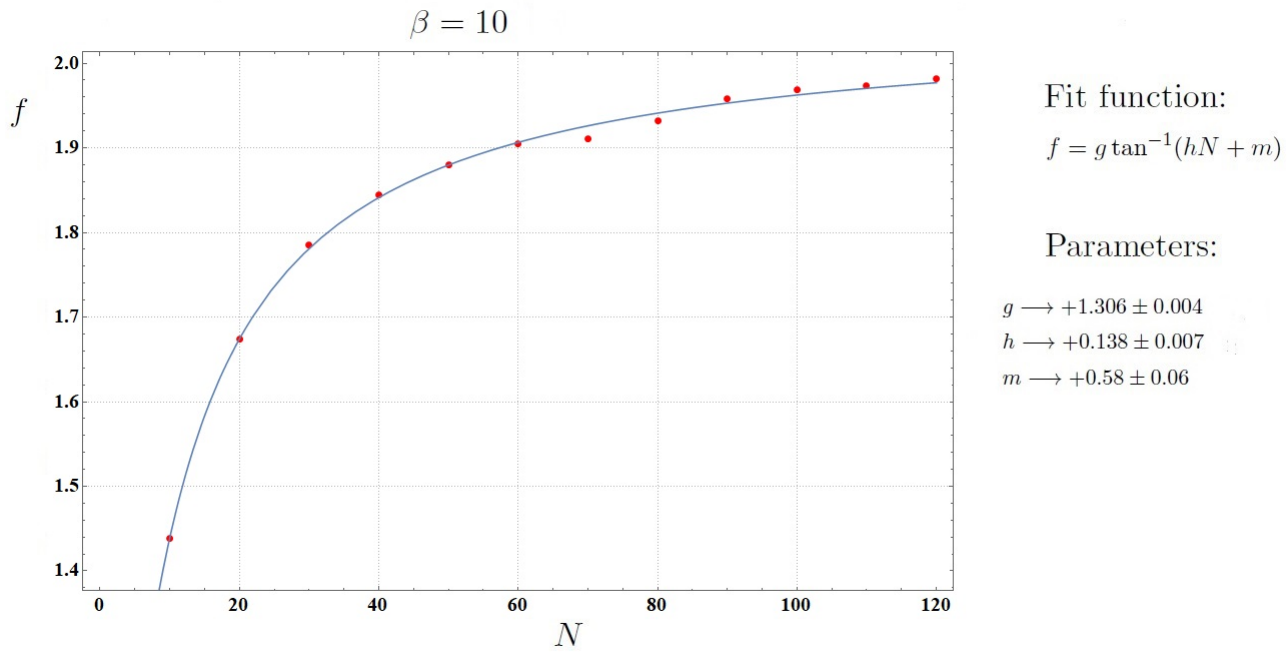

Figure 4.9: Shape of f_Q emerging from numerical evaluation for $\beta = 10$. We note the flat trend for large values of N.

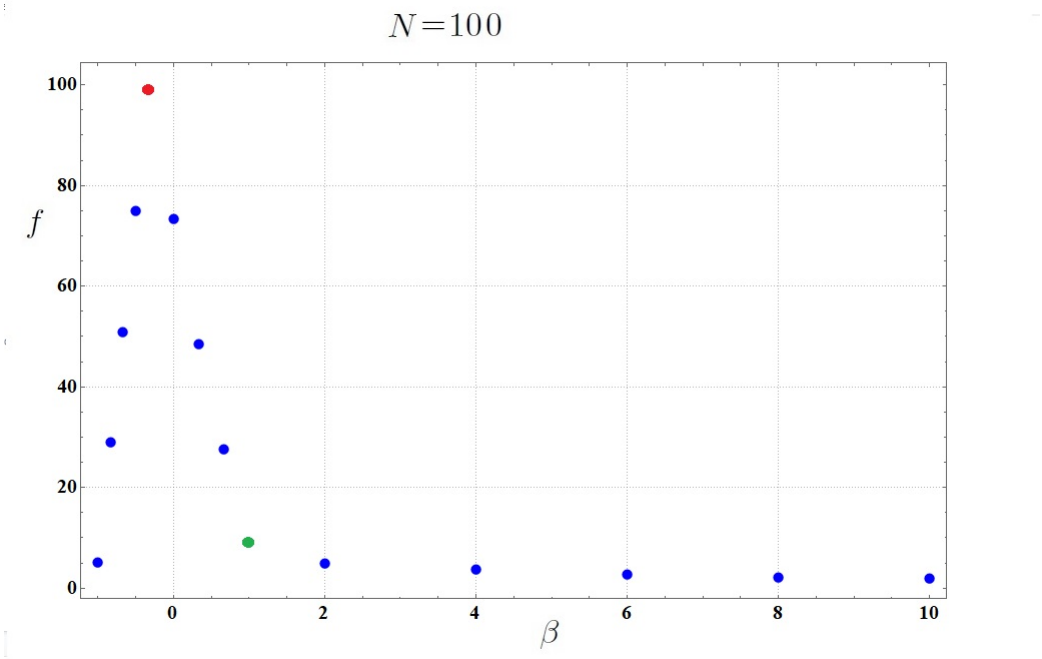

Figure 4.10: Shape of f_Q as function of β. The red and green points are the AKLT and Heisenberg state respectively.

Finally we show the data distribution we get fixing $N = 100$ and varying β, Fig. 4.10. This type of picture well summarize our results: the peak is reached at AKLT point (red

point in figure) while, at the Heisenberg point (green point in figure), the trend starts to be flat.

Conclusions

In this work we have shown that is possible to define and use correctly the Quantum Fisher Information in order to detect the multipartite structure of entanglement in the topological phases for the bilinear-biquadratic model. It is evident how matrix product state representation has helped us in the general understanding of how the expectation values of certain non-local order parameters (NLOPs) are sensitive to topological order. As we have seen in Chapter 2, from MPS representation of a ground state we can easily extract a lot of information about the phase in which the state is. Furthermore we have used these analytical results also to test our numerical methods. Indeed we have checked that the values of the different non-local order parameters were coherent with our exact calculations. We found indeed no discrepancies.

After that, we provided the analytical form of QFI by using string operators. In particular we were interested to the shape of the density of QFI (f_Q) because, as we have seen in Chapter 3, it provides directly a measure of entanglement for the ground state of a system. The first obviuos result we obtained was finding that, all QFI we evaluated satisfied the upper buond represented by N^2 as probed in [32]. Then, we performed numerical calculation in different points of phase diagram. Fixing $J = 1$, we started with Haldane phase setting progressively $\beta = -1/3,\ 0,\ 1/3,\ 2/3$. The first of these points is the AKLT state which has an exact matrix product state representation and, as we can see from the valence bond rapresentation, its ground state is maximally entangled. The linear behaviour of f_Q and its slope confirmed this picture. In fact, the estimated value of b is essentially 1 with a paltry standard error, then we can conclude that the ground state of AKLT point is N-entangled. For the other points of the Haldane phase, we can simply see that the slope of f_Q decreases and this witnesses a less entangled multipartite structure. At the phase transtion point ($\beta = 1$) we have obtained that the best fit we could perfom with our data was a power law scaling of f_Q. Finally, in the dimer phase we have chosen $J = 1$ and $\beta = 2,\ 4,\ 10$ progressively. As we can see, the whole dimer phase seems to be chacacterized by a flat trend of data for large values of N. This becomes even clearer for high values of β. For this reason we tried to fit a function which has a horizontal asymptote. Furthermore, for $\beta = 10$, all data are between 1 and

2, so this testifies 2-partite entangled states. Then we could say that the valence bond representation for dimer phase is more accurate for higher values of β.
We want to conclude pointing out that the properties of the QFI hold in general, then, it can be used to detect the multipartite structure of entanglement for whatever model we want to study. It would be therefore interesting to investigate whether it is feasible to use it for systems with more complicated degrees of freedom, such as models with a higher symmetry -such as $SU(3)$- or with constraints, as for example models with gauge symmetries.

Appendix A

Proofs of Theorems 1 and 2.

In this section we are going to give an algebraic proofs of Theorems 1 and 2 exposed in the Chapter 3.

A.0.1 Theorem 1

Let $\rho(\theta)$ satisfy the von Neumann equation (3.75), then $F_Q\big[\rho(\theta), H\big] \leq 4(\Delta_{\rho(\theta)}H)^2$

Proof. We only treat the case when ρ is nondegenerate. When ρ is degenerate, simple modification of the following procedure yields the same conclusion. Thus suppose that $\rho(\theta)$ has the orthogonal spectral representation like:

$$\rho(\theta) = \sum_m \lambda_m \left|\psi_m\right\rangle \left\langle\psi_m\right| \tag{A.1}$$

Here $\{\lambda_m\}$ are the different (positive) eigenvalues of $\rho(\theta)$, and $\{|\psi_m\rangle\}$ constitutes an orthonormal base (we have suppressed the parameter θ to simplify notations). Using the orthonormal, we also have:

$$\mathbb{I} = \sum_m \left|\psi_m\right\rangle \left\langle\psi_m\right| \tag{A.2}$$

So, for all m and n,

$$\begin{aligned}\left\langle\psi_m\right| \partial_\theta\rho \left|\psi_n\right\rangle &= \left\langle\psi_m\right| - iH\rho + i\rho H \left|\psi_n\right\rangle = -i\lambda_n \left\langle\psi_m\right| H \left|\psi_n\right\rangle + i\lambda_m \left\langle\psi_m\right| H \left|\psi_n\right\rangle \\ &= i(\lambda_m - \lambda_n) \left\langle\psi_m\right| H \left|\psi_n\right\rangle\end{aligned} \tag{A.3}$$

In particular, for any m,

$$\left\langle\psi_m\right| \partial_\theta\rho \left|\psi_m\right\rangle = 0 \tag{A.4}$$

From (A.3), for all $m \neq n$, we have:

$$\left\langle\psi_m\right| H \left|\psi_m\right\rangle = \frac{1}{i(\lambda_m - \lambda_n)} \left\langle\psi_m\right| \partial_\theta\rho \left|\psi_m\right\rangle . \tag{A.5}$$

Since

$$\mathrm{Tr}(\rho H) = \sum_m \langle\psi_m|\, \rho H\, |\psi_m\rangle = \sum_m \lambda_m \langle\psi_m|\, H\, |\psi_m\rangle \tag{A.6}$$

and

$$\begin{aligned}\mathrm{Tr}(\rho H^2) &= \sum_m \langle\psi_m|\, \rho H^2\, |\psi_m\rangle = \sum_m \lambda_m \langle\psi_m|\, H^2\, |\psi_m\rangle \\ &= \sum_m \lambda_m \langle\psi_m|\, H \Big[\sum_n |\psi_n\rangle \langle\psi_n| \Big] H\, |\psi_m\rangle \\ &= \sum_m \sum_n \lambda_m \langle\psi_m|\, H\, |\psi_n\rangle \langle\psi_n|\, H\, |\psi_m\rangle \\ &= \sum_m \sum_n \lambda_m |\langle\psi_m|\, H\, |\psi_n\rangle|^2\end{aligned} \tag{A.7}$$

Symmetrically, we also have

$$\mathrm{Tr}(\rho H^2) = \sum_m \sum_n \lambda_n |\langle\psi_m|\, H\, |\psi_n\rangle|^2 \tag{A.8}$$

then, combining equations (A.7) and (A.8) , we can write

$$\mathrm{Tr}(\rho H^2) = \sum_m \sum_n \frac{\lambda_m + \lambda_n}{2} |\langle\psi_m|\, H\, |\psi_n\rangle|^2 \tag{A.9}$$

Thus, the variance of H in the state ρ satis¢es:

$$\begin{aligned}(\Delta_{\rho(\theta)} H)^2 &= Tr(\rho H^2) - (Tr(\rho H))^2 \\ &= \sum_{mn} \frac{\lambda_m + \lambda_n}{2} |\langle\psi_m|\, H\, |\psi_n\rangle|^2 - \Big(\sum_m \lambda_m \langle\psi_m|\, H\, |\psi_m\rangle \Big)^2 \\ &= \sum_{m\neq n} \frac{\lambda_m + \lambda_n}{2} |\langle\psi_m|\, H\, |\psi_n\rangle|^2 + \sum_m \lambda_m |\langle\psi_m|\, H\, |\psi_n\rangle|^2 - \Big(\sum_m \lambda_m \langle\psi_m|\, H\, |\psi_m\rangle \Big)^2 \\ &\geq \sum_{m\neq n} \frac{\lambda_m + \lambda_n}{2} |\langle\psi_m|\, H\, |\psi_n\rangle|^2 \qquad \text{(by using Schwarz inequality)} \\ &= \sum_{m\neq n} \frac{\lambda_m + \lambda_n}{2(\lambda_m - \lambda_n)^2} |\langle\psi_m|\, H\, |\psi_n\rangle|^2 \qquad \text{(by using equation (A.5))}\end{aligned} \tag{A.10}$$

On the other hand,

$$\begin{aligned}\langle\psi_m|\, \partial_\theta \rho\, |\psi_n\rangle &= \frac{1}{2} \langle\psi_m|\, L\rho + \rho L\, |\psi_n\rangle = \frac{1}{2} \Big(\lambda_n \langle\psi_m|\, L\, |\psi_n\rangle + \lambda_m \langle\psi_m|\, L\, |\psi_n\rangle \Big) \\ &= \frac{(\lambda_m + \lambda_n)}{2} \langle\psi_m|\, L\, |\psi_n\rangle\end{aligned} \tag{A.11}$$

Thus quantum Fisher information of ρ is

$$\begin{aligned}F_Q(\rho) &= \mathrm{Tr}(\partial_\theta \rho L) = \sum_m \langle\psi_m|\, \partial_\theta \rho L\, |\psi_m\rangle \\ &= \sum_m \langle\psi_m|\, \partial_\theta \rho \Big[\sum_n |\psi_n\rangle \langle\psi_n| \Big] L\, |\psi_m\rangle = \sum_{m\neq n} \frac{2}{\lambda_m + \lambda_n} |\langle\psi_m|\, \partial_\theta \rho\, |\psi_n\rangle|^2\end{aligned} \tag{A.12}$$

The conclusion of the theorem follows since:

$$\frac{(\lambda_m + \lambda_n)}{(\lambda_m - \lambda_n)^2} \geq \frac{1}{(\lambda_m + \lambda_n)} \tag{A.13}$$

.

A.0.2 Theorem 2

If $\rho(\theta)$ is a pure state, then $F_Q\big[\rho(\theta), H\big] = 4(\Delta_{\rho(\theta)}H)^2$

Proof. Since $\rho(\theta)$ is a pure state, we have $\rho(\theta) = \rho^2(\theta)$. Differentiating both sides with respect to θ gives:

$$\frac{\partial\rho(\theta)}{\partial\theta} = \frac{\partial\rho(\theta)}{\partial\theta}\rho(\theta) + \rho(\theta)\frac{\partial\rho(\theta)}{\partial\theta} \tag{A.14}$$

The symmetrized logarithmic derivative of $\rho(\theta)$ is $L = 2\partial_\theta\rho(\theta)$. Consequently, noting that $\rho(\theta) = \rho^2(\theta)$ and the cyclic invariance of the trace, we have:

$$\begin{aligned} F_Q\big[\rho(\theta), H\big] &= \mathrm{Tr}\bigg[\frac{\partial\rho(\theta)}{\partial\theta}L\bigg] \\ &= 2\mathrm{Tr}\bigg[\bigg(\frac{\partial\rho(\theta)}{\partial\theta}\bigg)^2\bigg] \\ &= 2\mathrm{Tr}\big[-H\rho(\theta)H\rho(\theta) + H\rho^2(\theta)H + \rho(\theta)H^2 - \rho(\theta)H\rho(\theta)H\rho(\theta)\big] \\ &= 4\bigg[\mathrm{Tr}\big[\rho(\theta)H^2\big] - \mathrm{Tr}\big[\rho(\theta)H\rho(\theta)H\big]\bigg] \end{aligned} \tag{A.15}$$

But when $\rho(\theta)$ is a pure state, we have:

$$\mathrm{Tr}\big[\rho(\theta)H\rho(\theta)H\big] = \bigg[\mathrm{Tr}\big[\rho(\theta)H^2\big]\bigg]^2 \tag{A.16}$$

Consequently, $F_Q\big[\rho(\theta), H\big] = 4(\Delta_{\rho(\theta)}H)^2$.

Appendix B

ITensor library and numerical code

ITensor (Intelligent Tensor) is a C++ library for implementing tensor network calculations. Features include:

- Ordering of tensor indices is handled automatically.
- Full-featured matrix product state / tensor train and DMRG layer.
- Quantum number conserving (block-sparse) tensors; same interface as dense tensors.
- Complex numbers handled automatically and efficiently.

ITensors have an interface resembling tensor diagram notation, making them nearly as easy to multiply as scalars: tensors indices have unique identities and matching indices automatically contract when two ITensors are multiplied. This type of interface makes it simple to transcribe tensor network diagrams into correct, efficient code. Tensor methods are a powerful approach for problems in physics and applied math, but keeping track of tensor indices by hand can be tedious and make your code fragile and prone to bugs. Inspired by diagrammatic notation for tensor networks, ITensor lets you focus on the connectivity of tensor networks without thinking about low-level details like index ordering and data permutation. Indices in ITensor carry extra information so that "multiplying" two ITensors contracts all matching indices, similar to Einstein summation.
The density matrix renormalization group (DMRG) is an adaptive algorithm for optimizing a matrix product state (MPS) (or tensor train) tensor network, such that after optimization, the MPS is approximately the dominant eigenvector of a large matrix . The matrix is usually assumed to be a Hermitian matrix, but the algorithm can also be formulated for more general matrices.

The DMRG algorithm works by optimizing two neighboring MPS tensors at a time, combining them into a single tensor to be optimized. The optimization is performed using

an iterative eigensolver approach. Before the next step, the single tensor is factorized using an SVD or density matrix decomposition in order to restore the MPS form. During this factorization, the bond dimension (or tensor train rank) of the MPS can be adapted. This adaptation is optimal in the sense of preserving the distance between the network just after the optimization step and the network with restored MPS form.

In physics and chemistry applications, DMRG is mainly used to find ground states of Hamiltonians of many-body quantum systems. It has also been extended to compute excited states, and to simulate dynamical, finite-temperature, and non-equilibrium systems. Algorithms similar to or inspired by DMRG have been developed for more general MPS computations, such as summing two MPS; multiplying MPS by MPO networks; or finding MPS solutions to linear systems.

B.0.1 Numerical code

In this section we will show the code we use to perform numerical analysis. It is essentially composed by two blocks:

1. **Simulation of Hamiltonian and calculation of the ground state by DMRG**
   In the following, we display the section of the code where we produce the ground state of the our model by DMRG algorithm.

```
using namespace itensor;
using std::vector;
int main()
{
        // Parameters
    int N_tot =120, l, m, pos_Oa;
    Real J=1;
    Real Beta=2;
    std::ofstream dati("dati.dat");
    std::ofstream do2s("do2s.dat");
    printf(do2s,"Beta=␣%.12f␣\n\n",Beta);
    for (int N = 10; N < N_tot+1; N += 10)
    {
     // Creation of the M matrix
        auto s1 = Index(N);
        auto M=ITensor(s1,prime(s1));

    // Creation of 120 sites with Spin=1
        auto sites = SpinOne(N,{"ConserveQNs=",false});

    //  Hamiltonian
```

```
auto ampo = AutoMPO(sites);
       for( auto j : range1(N-1) )
       {
              ampo += J,"Sx",j,"Sx",j+1;
              ampo += J,"Sy",j,"Sy",j+1;
              ampo += J,"Sz",j,"Sz",j+1;
              ampo += -J*Beta,"Sx",j,"Sx",j+1,"Sx",j,"Sx",j+1;
              ampo += -J*Beta,"Sy",j,"Sy",j+1,"Sy",j,"Sy",j+1;
              ampo += -J*Beta,"Sz",j,"Sz",j+1,"Sz",j,"Sz",j+1;
              ampo += -J*Beta,"Sx",j,"Sx",j+1,"Sy",j,"Sy",j+1;
              ampo += -J*Beta,"Sx",j,"Sx",j+1,"Sz",j,"Sz",j+1;
              ampo += -J*Beta,"Sy",j,"Sy",j+1,"Sx",j,"Sx",j+1;
              ampo += -J*Beta,"Sy",j,"Sy",j+1,"Sz",j,"Sz",j+1;
              ampo += -J*Beta,"Sz",j,"Sz",j+1,"Sx",j,"Sx",j+1;
              ampo += -J*Beta,"Sz",j,"Sz",j+1,"Sy",j,"Sy",j+1;
       }
              auto H = toMPO(ampo);
              auto psi0 = randomMPS(sites);

// Run DMRG to get the ground state
       auto sweeps = Sweeps(5);
       sweeps.maxdim() = 5,10,20;
       sweeps.cutoff() = 1E-10;
       auto [E,psi] = dmrg(H,psi0,sweeps,{"Quiet",true});
       println("Ground␣state␣energy␣E=␣",E);
       printf(dati,"Energy=␣%.f␣\n", E);
```

2. **Evaluation of expected value of string operators**. Here we show the part of the code in which we calculate the first term of QFI that is the sum over all elements of M matrix (see Chapter 4). We have implemented a similar code for N matrix.

```
// Evaluation of the first term of QFI by string operator
       for (int pos_Oa=1; pos_Oa< N; pos_Oa += 1)
       {
              for (int l = pos_Oa+1; l < N+1; l += 1)
              {
                     auto Oa= op(sites,"Sz",pos_Oa);
                     auto Ob= op(sites,"Sz",l);
                     psi.position(pos_Oa);
                     ITensor C=psi(pos_Oa)
                     C*=Oa;
                     auto ir = commonIndex(psi(pos_Oa),psi(pos_Oa + 1),"Link");
                     C *= dag(prime(prime(psi(pos_Oa),"Site"),ir));
```

```
                                        for (int k = pos_Oa+1; k < l; k += 1)
                                        {
                                                auto a=op(sites,"expSz",k);
                                                C *= psi(k);
                                                C *= a;
                                                C *= dag(prime(prime(psi(k), "Site"),"Link"));
                                        }
                                C *= psi(l);
                                C *= Ob;
                                auto il = commonIndex(psi(l-1),psi(l),"Link");
                                C *= dag(prime(prime(psi(l),"Site"),il));
                                ITensor F=realPart(C);
                                auto T=elt(F);
                                M.set(s1(pos_Oa),prime(s1)(l), T);
                                println("M(",pos_Oa,",",l,")=",T);
                                printf(dati,"%.12f\n", T);
                        }
                }
        Real R=sumels(M);

                        // Printing on file
                        printf(dati,"N=%.␣\t␣\t␣O2=␣%.12f␣\n\n",N,R);
                                printf(do2s,"N=%.␣\t␣\t␣O2=␣%.12f␣\n",N,R);
        }
                dati.close();
                do2s.close();
return 0;
}
```

Bibliography

[1] V. Klitzing, G. Dorda, M. Pepper, *"New Method for High-Accuracy Determination of the Fine-Structure Constant Based on Quantized Hall Resistance"*, In: Phys. Rev. Lett. 45 494.

[2] R.B. Laughlin, *"Anomalus quantum Hall Effect: An incompressible quantum fluid with fractionally charged excitations"*, In: Phys. Rev. Lett. 50:1395-1398, 1983

[3] X-G Wen, F. Wilczek, and A. Zee, *"Chiral spin states and superconductivity"*, In: Phys. Rev. B, 39:11413, 1989

[4] X-G Wen, *"Vacuum degeneracy of chiral spin state in compactified spaces"*, In: Phys. Rev. B, 40:7387, 1989.

[5] X-G Wen, *"Topological order in rigid states"*, In: J.Mod.Phys. B, 4:239, 1990

[6] X. Chen, Z-C Gu, X-G Wen, *"Local unitary transformation, long-range quantum entenglement, wave function renormalization, and topological order"*, In: Phys.Rev, B 82:155138, 2010.

[7] Q. Shen,*"Topological insulators"*, Vol. 174, Springer, 2012.

[8] W. Dür, G. Vidal, J. I. Cirac *"Three qubits can be entangled in two inequivalent ways"*, In: Phys.Rev, A 62:062314, 2000.

[9] G. M. Crosswhite, D. Bacon *"Finite Automata for Caching in Matrix Product Algorithms"*, 2018.

[10] D. Tong, *"The Quantum Hall Effect"*, In: TIFR Infosys Lectures ,2016.

[11] A. Auerbach, *"Interacting Electrons and Quantum Magnetism"*, Springer-Verlag, 1994.

[12] T. Kennedy and H. Tasaki, *"Hidden Z_2xZ_2 symmetry breaking and the Haldane phase in $S = 1$ quantum spin chain"*,In: Phys. Rev. B 45 , pp. 304–307, 1992.

[13] H. M. Babujian, *"Exact solution of the one-dimensional isotropic Heisenberg chain with arbitrary spin S"*, In: Physics Letters A 90.9, 1992.

[14] M. N. Barber, M. T. Batchelor, *"Spectrum of the biquadratic spin-1 antiferromagnetic chain"*, In: Phys.Rev.B 40, pp. 4621-4626, 1989.

[15] X. Chen, Z-C Gu, X-G Wen,*"Classification of gapped symmetric phases in one-dimensional spin systems"*,In:Phys.Rev.B 83, 2011.

[16] X. Chen, Z-C Gu, X-G Wen,*"Complete classification of one-dimensional gapped quantum phases in interacting spin systems"*,In: Phys. Rev.B 84, 2011.

[17] A. Klumper, *"The spectra of q-state vertex models and related antiferromagnetic quantum spin chains"*, In: Journal of Physics A: Mathematical and General, p 809, 1990.

[18] D. Perez-Garcia et al., *"Matrix Product State Representation"*, In: Quantum Info. comput., pp 401-430, 2007.

[19] F. Pollmann and A. M. Turner, *"Detection of symmetry-protected topological phases in one dimension"*, In: Physical Review B 86, 2012.

[20] U. Schollwoeck, *"The density-matrix renormalization group in the age of matrix product state"*, In: Annals of Physics - ANN PHYS N Y 326, 2010.

[21] B. Sutherland, *"Model for a multicomponent quantum system"*, In:Phys.Rev.B 12, pp 3795-3805, 1975.

[22] L. A. Takahashi, *"The picture of low-lying excitations in the isotropic Heisenberg chain of arbitrary spins"*, In:Phys.Rev.B 12, pp 3795-3805, 1975.

[23] G. Vidal, *"Efficient Classical Simulation of Slightly Entangled Quantum Computations"*, In:Phys.Rev.Lett. 69, pp 2863-2866, 1992.

[24] A. Antini, *"Non-local order parameters in one-dimensional spin systems"*, Thesis Alma, 2018.

[25] L.Pezzè, M. Gabbrielli, L.Lepori and Augusto Smerzi *"Multipartite entanglement in topological quantum phase"*, In:Phys.Rev.Lett. 119.250401, 2017.

[26] R. Horodecki, P. Horodecki, M. Horodecki, and K. Horodecki, *"Quantum entanglement"*, In: Rev Mod Phys 81, 865, 2009.

[27] O. Guhne, G. Toth, *"Entanglement detection"*, In: Phys Rep 474, 1 2009.

[28] L. Amico, R. Fazio, A. Osterloh, and V. Vedral, *"Entanglement in many-body systems"*, In: Rev. Mod. Phys. 80, 517, 2008.

[29] T. J. Osborne and M. A. Nielsen, *"Entanglement in a simple quantum phase transition"*, In: Phys. Rev. A 66, 032110, 2002.

[30] A. Osterloh, L. Amico, G. Falci, and R. Fazio, *"Scaling of entanglement close to a quantum phase transition"*, In: Nature 416, 608, 2002.

[31] D. Vodola, L. Lepori, E. Ercolessi, A. V. Gorshkov, and G. Pupillo, *"Kitaev Chains with Long-Range Pairing"*, In: Phys. Rev. Lett. 113, 156402, 2014.

[32] L. Pezzè, A. Smerzi *"Entanglement, Nonlinear Dynamics, and the Heisenberg Limit"*, In: Phys. Rev. Lett. 102, 100402, 2009.

[33] D. Vodola, L. Lepori, E. Ercolessi and G. Pupillo, *"Longrange Ising and Kitaev Models : Phases, Correlations and Edge Modes"*, In: New J. Phys. 18, 015001, 2016.

[34] R. Movassagh and P. W. Shor, *"Supercritical entanglement in local systems : Counterexample to the area law for quantum matter"*, In: PNAS 113, 13278, 2016.

[35] O. Guhne, G. Toth and H. J. Briegel, *"Multipartite entanglement in spin chains"*, In: New J. Phys. 7, 229 2005.

[36] M. Hofmann, A. Osterloh, and O. Guhne, *"Scaling of genuine multiparticle entanglement close to a quantum phase transition"*, In: Phys. Rev. B 89, 134101, 2014 .

[37] P. Hauke, M. Heyl, L. Tagliacozzo, and Peter Zoller, *"Measuring multipartite entanglement through dynamic susceptibilities"*, In: Nat. Phys. 12, 778, 2016.

[38] W.-F. Liu, J. Ma, and X. Wang, *"Quantum Fisher Information and spin squeezing in the ground state of the XY model"*, In: J. Phys. A 46, 045302, 2013.

[39] L. Pezzè and A. Smerzi, *"Entanglement, nonlinear dynamics, and the Heisenberg limit"*, In: Phys. Rev. Lett. 102, 100401, 2009.

[40] G. Toth, *"Multipartite entanglement and high-precision metrology"*, In: Phys. Rev. A 85, 022322, 2012 .

[41] A. Y. Kitaev, *"Unpaired Majorana fermions in quantum wires"*, In: Physics-Uspekhi 44, 131, 2001.

[42] J. Alicea, *"New directions in the pursuit of Majorana fermions in solid state systems"*, In: Rep. Prog. Phys. 75, 076501, 2012.

[43] 22C. Kane, *"Topological Band Theory and the Z_2 Invariant"*, In: Contemporary Concepts of Condensed Matter Science, Vol. 6, pp. 3–34, 2013.

[44] 3J. K. Asbóth, L. Oroszlány, andA. Pályi *"Short Course on Topological Insulators"*, In: Lecture Notes in Physics 919, 2016.

[45] U. Schollwoeck, *"The density-matrix renormalization group in the age of matrix product states"*, In: Annals of Physics - ANN PHYS N Y 326, 2010.

[46] L. Jing, J. Xiao-Xing, Z. Wei, *"Quantum Fisher Information for density matrix with arbitrary rank"*, In: Commun. Theor. Phys. 61, pp 44-45, 2014.

[47] S. Boyd, L. Vandenberghe *"Convex optimizzation"*, In: Cambrige University press, 2004.

[48] G. Toth, C. Knapp, O. Guhne, H. J. Briegel *"Spin squeezing and entanglement"*, In: New J. Phys. 8, 229, 2018.

[49] V. Giovannetti, S. Lloyd, L. Maccone, *"Quantum metrology"*, In: PHys, Rev. Lett. 96, 010401, 2006.